Cardiac Consequences of Epileptic Seizures in the Tetanus Neurotoxin Model of Temporal Lobe Epilepsy

Alexander MJ Ashby-Lumsden

Wolfson College

Department of Pharmacology

Thesis Submitted for the Degree of

Master of Science By Research

ABSTRACT

Death is the most destructive outcome of epilepsy. Around 18% of deaths in those with epilepsy cannot be attributed to the disease itself; these deaths are collectively categorised as Sudden Unexplained Deaths in Epilepsy (SUDEP). Currently, the cause of SUDEP is hypothesised to involve seizure-induced respiratory or cardiac failure. Ictal (during seizure) central and obstructive apnoea, decreases in ictal oxygen saturation, changes in blood pressure, heart rate, autonomic control and cardiac conductivity in both patients and animal models have all been observed. In order to explore the effects of seizures on the autonomic control and cardiac conductivity, tetanus neurotoxin was injected into the ventral hippocampus of male Wistar rats; previously implanted with biopotential radiotelemeters.

Continuous recordings of electrocardiogram, electrocorticogram, and video were made for six to eight weeks post induction of epilepsy. The conductivity of the heart was analysed by calculating the PR, QT, corrected QT (QTc) intervals and QRS width. The central control of the heart was explored by analysing the interictal heart rate and calculating various time-based Heart rate variability measures. Statistical analysis was performed using One-Way ANOVA with Bonferroni post-hoc comparisons.

Increases in the PR interval, QRS width, RR interval, QT and QTc intervals were observed between preinduction and 150th seizure. The change in PR interval, RR interval, and QT interval persisted into the Post Seizure State. Significant differences were not observed for any of the Heart Rate Variability measures. The increase in QT and QTc intervals indicate a pathological change in the time taken for cardiac ventricular depolarisation and repolarisation to occur. The changes in PR and RR intervals and QRS width are not physiologically significant. Due to large variation between animals, meaningful conclusions about changes in central control of the heart could not be drawn. This study ultimately shows that the tetanus neurotoxin model of temporal lobe epilepsy induces changes in cardiac conductivity, and could aid in investigating the mechanisms through which SUDEP occurs.

FOR EVA

TABLE OF CONTENTS

INTRODUCTION 1

SUDDEN UNEXPLAINED DEATH IN EPILEPSY 1

TETANUS NEUROTOXIN MODEL OF TEMPORAL LOBE EPILEPSY 12

VENTRAL HIPPOCAMPUS AND THE CARDIOVASCULAR SYSTEM 14

AIMS AND HYPOTHESIS 15

METHODS 17

RADIOTELEMETER IMPLANTATION 17

INDUCTION OF EPILEPSY: TETANUS NEUROTOXIN INJECTION 20

IN VIVO RECORDING OF SEIZURES AND ELECTROCARDIOGRAM 21

DATA ANALYSIS 22

RESULTS 28

INTERICTAL ECG WAVEFORM 31

INTERICTAL RR INTERVAL AND HEART RATE 41

INTERICTAL HEART RATE VARIABILITY 43

DISCUSSION 51

ECG WAVEFORM CHANGES AND SUDEP 51

HEART RATE AND SUDEP 57

HEART RATE VARIABILITY AND SUDEP 58

THE USE OF TENT AS A MODEL FOR SUDEP 60

FURTHER EXPERIMENTAL WORK 62

CONCLUSION 65

BIBLIOGRAPHY 66

LIST OF FIGURES

FIGURE 1 16

FIGURE 2 20

FIGURE 3 21

FIGURE 4 23

FIGURE 5 25

FIGURE 6 29

FIGURE 7 33

FIGURE 8 34

FIGURE 9 36

FIGURE 10 37

FIGURE 11 39

FIGURE 12 40

FIGURE 13 42

FIGURE 14 43

FIGURE 15 46

FIGURE 16 47

FIGURE 17 49

FIGURE 18 50

LIST OF TABLES

TABLE 1 ……..30

TABLE 2 ……..32

TABLE 3 ……..44

TABLE 4 ……..45

LIST OF ABBREVIATIONS

ANOVA	Analysis of Variance
AV	Atrioventricular
CA	Cornu Ammonis
DMVN	Dorsal Motor Vagal Nucleus
ECG	Electrocardiogram
ECoG	Electrocorticogram
GTCS	Generalised Tonic Clonic Seizure
HF	High Frequency
HRV	Heart Rate Variability
I_{Kr}	Rapid delayed rectifier potassium ion current
LF	Low Frequency
LVH	Left Ventricular Hypertrophy
NAc	Nucleus Accumbens
NSAID	Non-Steroidal Anti-Inflammatory Drug
QTc	Corrected QT Interval
RMSSD	Root Mean Square of Successive Differences
SDNN	Standard Deviation of all RR intervals
SDSD	The standard deviation of successive differences between adjacent RR intervals
SMEI	Severe Myoclonic Epilepsy of Infancy
SNARE	Soluble NSF Attachment Protein Receptor
SUDEP	Sudden Unexplained Death in Epilepsy
TeNT	Tetanus Neurotoxin
TLE	Temporal Lobe Epilepsy
VAMP	Vesicle Associated Membrane Protein
VLF	Very Low Frequency

INTRODUCTION

Epilepsy is the third most prevalent chronic neurological disease, affecting around 50 million people worldwide[1,2]. Epilepsy is a disease of recurring and unprovoked seizures initiated by pathological hyperexcitability of neuronal networks in different regions of the brain. The clinical manifestations of these seizures vary depending on the brain region affected, with the International League Against Epilepsy outlining a methodical classification system[3]. The most devastating consequence of epilepsy is death, and the risk of death is two to three times higher for those with epilepsy compared to the general population[4]. A proportion of deaths in epilepsy cannot be attributed to the disease and are described as sudden and unexplained. Collectively they are categorised as sudden unexplained/unexpected death in epilepsy (SUDEP).

SUDDEN UNEXPLAINED DEATH IN EPILEPSY

SUDEP encompasses deaths in patients with epilepsy that are sudden, unexpected, non-traumatic, non-drowning, can either be witnessed or unwitnessed, with or without evidence of seizure[4] and when post-mortem examination does not reveal a cause of death[5]. Research has recently focused on identifying any underlying mechanisms that may cause these unexplained deaths in those with epilepsy[5]. Upon autopsy, deaths are either “definite SUDEP” or “probable SUDEP”, however these definitions are broad, and classifications can be erroneous due to lack of evidence or if there is another credible cause of death.

The incidence of SUDEP can vary considerably depending on the type of epilepsy population investigated. Ficker et al.[6] reported that the risk of sudden death in those

with epilepsy is 20 times higher when compared to the general population[4,5]. Incidence rates of SUDEP for a general epilepsy population ranges from 0.9 to 2.3 per 1000 patient years[7–15]. The incidence is increased for those with chronic refractory epilepsy, ranging from 1.1 to 5.9 per 1000 patient years[16–24]. Further, the incidence of SUDEP is even higher for patients who are surgery candidates (6.3 to 9.3 per 1000 patient years[25–28]) and patients that have had unsuccessful surgery[5]. Children have been found to have a lower incidence rate of SUDEP when compared with adults, however data suggests that children with Dravet Syndrome/Severe Myoclonic Epilepsy of Infancy (SMEI) have a high reported rate of SUDEP[29]. SUDEP is the leading cause of death for 10-50% of those patients with refractory epilepsy who attend epilepsy referral centres[5]; patients that could be categorised as the most at risk epilepsy patients. SUDEP is therefore a considerable risk to patients and of constant concern to them and their families.

SUDEP Risk Factors

Numerous risk factors and biomarkers for SUDEP have been identified in order to ascertain which patients are at risk of this "random" phenomenon and enable their education and monitoring[30]. Along with the gender of the patient (males have a 1.4 times higher risk of SUDEP than females[5]) a number of risk factors have been categorised as the "SUDEP-7 Risk Inventory"[15]. Patients who experience generalised tonic-clonic seizures (GTCSs) are at higher risk of SUDEP; and indeed the more GTCSs the patient experiences the greater risk they have[5,15], therefore this study will explore the cumulative stresses caused by repeated seizures. A patient who experiences over 50 GTCSs in a year has an odds ratio of 14.51 that they will experience SUDEP, compared with an odds ratio of 2.94 for those who experience less than three[5]. Increased risk of SUDEP is not limited to GTCSs, in fact having more than 50 seizures of any type over a 12 month period

significantly increases the patient's risk of SUDEP[15,31]. Additionally, patients with a greater than 30 year history of epilepsy are a higher risk[15], as well as those with a younger age of onset[4], and those with an IQ less than 70[31].

Combination antiepileptic drug therapy (polytherapy), frequent medication changes, poor compliance and certain antiepileptic drugs have all been identified as risk factors for SUDEP[4,15,31–33]. Those patients using three or more antiepileptic drugs have an eight times increased risk of SUDEP when compared to monotherapy[4,31]. This increased risk may be in fact be associated more with the severity of the epilepsy the individual experiences that requires polytherapy rather than the drugs themselves. However, Nilsson and colleagues[34] have identified that those patients using a widely used antiepileptic drug carbamazepine, a voltage-dependent sodium channel blocker that prevents repetitive neuronal firing[35], have an increased risk of SUDEP. Furthermore, patients on high doses of carbamazepine as well as polytherapy have been shown to be at an increased risk of SUDEP[5,32,34].

Possible Mechanisms of SUDEP

The exact mechanism through which SUDEP occurs is unknown. The majority of recent research has focused on cardiac dysrhythmia, autonomic dysregulation, seizure-induced hypoventilation, and pulmonary oedema[5,33] as underlying mechanisms. Currently, evidence suggests a prominent role for respiratory dysfunction[5,36–40], however SUDEP may in fact be caused by one of these mechanisms in isolation or in combination with others, and this may vary between individuals and epilepsy types[5].

Respiratory changes during seizures have been well documented, with central and obstructive apnoea, excessive bronchial and oral secretions, pulmonary oedema, and

hypoxia all observed[32,38–45]. Johnston and colleagues[40] found that in a sheep model of SUDEP, induced by intravenous bicuculline, those animals that died had a greater increase in pulmonary vascular pressure and hypoventilation than those that survived. Further, studies have shown that severe hypoventilation of central origin[39] and seizure-induced changes in pulmonary vascular pressures[38] contributed to the death of sheep, that death in audiogenic mice was prevented by placing the animals in an oxygen enriched environment[46], and that signs of neurogenic pulmonary oedema were observed in deaths in a baboon model of epilepsy[47]. Indeed, Bateman and colleagues[36,37] have demonstrated that ictal (during seizure) oxygen desaturation occurs in around a third of patients with uncontrolled/refractory epilepsy. Both human and animal studies therefore suggest that respiratory mechanisms have a role in sudden death in epilepsy and potentially SUDEP[5].

Sudden death in the general population is closely associated with cardiac arrhythmias, which is therefore a widely investigated cardiac mechanism of SUDEP[4]. Furthermore, changes in heart rate variability (HRV), blood pressure, heart rate, autonomic control and the electrocardiogram (ECG) waveform have been observed in both patients and animal models of SUDEP[5,32,33,48,49]. Moreover, arrhythmia and repolarisation abnormalities such as atrial fibrillation, supraventricular tachycardia and ventricular premature depolarisation have also been reported in up to 56% of generalised seizures in humans[48,50]. Increased systolic arterial pressure[49], mean arterial pressure[51] and abnormal blood pressure variability[52] (which indicates an impaired baroreflex function[53]) have all also been observed.

Various changes in the heart rates of patients and animals, including the direction and extent of change, are reported. Sinus rate change is observed during most epileptic

seizures, and sinus tachycardia has been reported in 50-100% of seizures[48]. Damasceno and colleagues[49] demonstrated elevated basal heart rate in an audiogenic rat model of epilepsy, with Leutmezer and colleagues[54] observing ictal tachycardia in 86.9% of seizures across 58 patients. Further, Opherk et al.[55] retrospectively analysed 102 seizures across 41 patients and observed tachycardia in 99% of those seizures; and Tigaran and colleagues[56] showed that patients with pharmacologically uncontrolled seizures experienced tachycardia. Finally, Zijlmans et al.[57] reported tachycardia in 73% of the 281 seizures analysed from 81 patients.

Whilst increases in heart rate are more commonly observed, ictal bradycardia is currently receiving attention as it could potentially progress to cardiac asystole and SUDEP[48]. Indeed, the first reported instance of ictal asystole was by AE Russell in 1906, who observed the disappearance of patients pulse during a seizure[58]. Subsequently, numerous animal and patient studies have reported episodes of asystole, bradycardia or both, however their incidence is more rare than tachycardia. Mameli et al.[59] demonstrated bradyarrhythmic episodes, which lasted up to 15 seconds during seizures induced by applying penicillin G directly to the thalamus and hypothalamus of rats. Hotta and colleagues[60] also induced a decrease in heart rate of 100 beats per minute by stimulating the vagus nerve of anesthetised rats in a manner which mimicked the patterns previously observed in seizures. Further, sinus bradycardia and asystole have been observed in human patients by various studies[44,61–63], although the actual occurrence can be as low as 2% of seizures analysed[48]. Lathers and Schraeder[64] suggest that ictal bradyarrhythmias could potentially result in complete heart block, which can lead to asystole and cardiac death. There is a lack of clinical evidence of ictal bradycardia in patients that make it difficult to ascertain its importance in SUDEP[48].

Those with epilepsy may be susceptible to developing cardiac arrhythmias due to a number of factors, including: the potential cardiac destabilisation caused by certain antiepileptic drugs, genetic predisposition, cardiac channelopathies and long-term cardiac structural abnormalities[4]. The interventions made to help control the patient's seizure may in fact be involved in the mechanism of SUDEP, through an additional adverse cardiac and autonomic effect[48]. As mentioned above, patients taking high doses of carbamazepine have an increased risk of SUDEP[34]. The precise mechanism through which carbamazepine increases risk is unknown, however a number of key observations have been made. Firstly, carbamazepine has been shown to induce cardiac arrhythmia in a dose related manner, although these events are rare and observed mainly in the elderly and predisposed patients[65]. Carbamazepine has also been shown to adversely affect autonomic cardiac control by reducing heart rate variability (HRV) in patients with epilepsy[66,67] and could therefore make patients more vulnerable to a fatal event[34]. Moreover, another antiepileptic drug lamotrigine has been shown to inhibit the cardiac rapid delayed rectifier potassium ion current (I_{Kr}), which has been associated with prolonged QT interval[4,68], and it has been hypothesised that metabolic acidosis induced by seizures coupled with this reduced I_{Kr} could result in a fatal arrhythmia[68].

Familial history of sudden cardiac death in SUDEP cases has not been found[32,69,70]. Nonetheless, the similarities between SUDEP and sudden death in the general population have led to many to postulate the potential relationship between genes that predispose to cardiac arrhythmias and SUDEP, with Glasscock providing a thorough review[71]. A prominent theory involves Long-QT Syndrome, an autosomal recessive disease that can cause torsades de pointes, ventricular tachycardia, syncope and sudden death and is caused by altered ion channel function (discussed below) that results in prolonged cardiac

action potentials[32]. The QT interval can be increased by prolonging the initial phase of the cardiac action potential, by increasing the sodium current, or by delaying the repolarisation phase, by reducing the potassium current[32]. The products of a number of genes have been identified that cause Long-QT Syndrome, including those that drive the repolarisation phase and the initial inward sodium current of the cardiac action potential. For example, the LQT2 gene – a loss of function mutation of the hERG gene – encodes a voltage gated K^+ α subunit and results in a reduction of the repolarising current[32]. Further potassium channel genes involved in Long-QT Syndrome are LQT7, through a loss of function mutation; LQT1, which encodes the α subunit of the potassium channel responsible for the I_{Ks} component of the delayed-rectifier current, and LQT6, which encodes the β subunit of K_V channels[32]. Additionally, gain of function mutations of SCN1A and SCN5A result in prolonged membrane depolarisation and delayed ventricular repolarisation respectively[32]. Abnormalities in the expression of these genes could potentially be involved in SUDEP.

The brain expresses a number of the genes involved in Long-QT Syndrome and therefore it is hypothesised that they could be involved in SUDEP. Indeed, Severe Myoclonic Epilepsy of Infancy (SMEI), caused by mutations in SCN1A, has a poor prognosis, high mortality rate and a high incidence of SUDEP[29]. Other neurocardiac genes are associated with SUDEP, with a number causing both epileptic seizures and arrhythmias, including KCNA1[72–74], SCN8A[75,76], HCN2[77], PRRT2[78] and SCN1A[79–81]. KCNA1 gene deletions in mice have been shown to result severe tonic-clonic seizures, a 75% mortality by 10 weeks, ictal bradycardia and atrioventricular block[72–74]. Further, SCN8A mutations have been linked to epilepsy in mice and one human pedigree, with one case of SUDEP linked to a gain of function phenotype of SCN8A[76]. A mutation of the cation

channel encoding HCN2 gene has also been associated with SUDEP although it has a low expression in cardiac tissue[77]. Finally, PRRT2 is the newest of the potential genomic causes of SUDEP, which has a high expression in the brain and low to undetectable expression in the heart[71]. PRRT2 is a presynaptic transmembrane protein that is involved in vesicle fusion and a truncation of this gene was observed in a single case of SUDEP in a 14-year old male was found post mortem[78]. As with many of the gene mutations mentioned above, there is a lack of evidence linking PRRT2 and these cardiac inherited genes and SUDEP[32,48,71,82]. However, the expression of the products of these genes could play a role in the mechanisms underlying SUDEP.

SUDEP and ECG Waveform Changes

As mentioned above, sudden cardiac death in the general population has been widely investigated and a structural cause of death has not been identified in SUDEP[82]. Seizure induced ECG abnormalities and ECG waveform changes are observed in many human and animal studies. Prolongation of the QT Interval (Figure 5C), as well as QRS width prolongation, and ST elevation are reported in a number of studies. Prolongation of the QRS width is clinically important as it signifies that the electrical conduction through the ventricular myocardium is slower than normal, and a increased QRS width is observed in 14 to 47% of heart failure patients[83]. Indeed, QRS width lengthens as left ventricular function deteriorates, meaning its presence can be an indicator of poor prognosis.

Damasceno and colleagues[49] found an increase in both the QT Interval and the QRS width in rats genetically predisposed to experiencing audiogenic seizures. In human studies, increased QT Interval has been observed by Opherk et al.[55], Moseley and

colleagues[84]; whilst Tavernor and colleagues[85] observed a modest increase in the QT interval. This increase can cause potentially fatal events such as torsades de pointes, ventricular tachycardia, and syncope[32]. Further ST elevation, where the S wave to T wave segment of the ECG is elevated above the normal isoelectric line and is often observed in acute myocardial infarction[86], has been reported by many studies[55–57].

Ultimately, analysing three time differences within the ECG waveform can identify the speed of cardiac conductivity. The length of time between the start of the P wave and the start of the QRS complex (the PR Interval; Figure 5C) indicates the time taken for the electrical signal to pass from the sinoatrial node, through the atrioventricular (AV) node and to the Bundle of His. The length of time between the Q wave and the S wave (QRS width; Figure 5C) indicates the time taken for the ventricular myocardium to depolarise fully. Finally, as mentioned, the length of time between the Q and the T wave (QT Interval; Figure 5C) indicates the time take for the ventricles to depolarise and repolarise; or if the QRS width is consistent can identify how quickly the ventricles repolarise. The QT Interval, however, is dependent on heart rate and therefore an appropriate correction needs to be employed in order to adjust for the varying heart rate[87,88]. Numerous formulae have been proposed to generate a corrected QT Interval (QTc) that is independent of rate, allows prediction of QT duration at other heart rates other than that measured, and is simple enough for daily use[87,88]. In the laboratory, species differences result in the use of inappropriate correction methods designed for humans and therefore potentially flawed conclusions. This study will employ the method devised by Kmecova and Klimas[87] that endeavours to adjust the QT Interval to the rat heart rate.

SUDEP AND HEART RATE VARIABILITY CHANGES

Heart rate variability (HRV) is a quantitative measure of autonomic modulation of the sino-atrial node, and at its simplest is a measure of beat-to-beat variability[82,89]. In the general population, reduced HRV has been associated with atrial fibrillation, cardiovascular disease, poor outcomes in those patients with heart failure, and sudden cardiac death[82,89]. Therefore, various HRV measures have been employed to assess autonomic changes in patients with epilepsy. There are two main categories of HRV measures: time domain methods and frequency domain methods. Time domain methods can range from calculating the difference between the longest and the shortest R-to-R interval to more complicated equations like the Root Mean Square of Successive Differences (RMSSD)[89]. Further explanation of these HRV measures used in this study can be found in the *Methods: Data Analysis* section. Frequency domain methods are more complex. They are primarily concerned with examining various spectral components of a Fast Fourier Transform. In short-term recordings, two to five minutes in length, three main spectral components can be distinguished[i]: very low frequency (≤ 0.04 Hz; VLF), low frequency (0.04-0.15 Hz; LF) and high frequency (0.15-0.4 Hz; HF)[89]. The HF component corresponds to parasympathetic activity, sympathetic activity is the major contributor to the LF component, and that the LF/HF ratio indicates the level of sympathetic cardiac control[89]; although recent studies have refuted this[90,91].

Changes in HRV have been observed in patients with epilepsy. For example those refractory epilepsy patients who score highly on the SUDEP-7 inventory[30] have low RMSSD measures[31]. Indeed, a decrease in either autonomic activity or HRV has been

[i]The frequency ranges for low and high frequency components varies from those values stated above in rats. LF ranges from 0.04-1.0 Hz, and HF ranges from 1.0-3.0 Hz[186].

observed in many studies. Ansakorpi and colleagues[92] reported a decrease in HRV, using the time-based SDNN measure (Standard Deviation of all RR intervals), in patients with temporal lobe epilepsy when compared to controls. Further, Ansakorpi et al.[93] observed lower HRV in patients exposed to a table tilt test. Autonomic over-activity has been seen in animal models, with a 10-fold increase in parasympathetic activity – recorded via the vagus nerve – observed by Sakamoto et al.[94], who induced status epilepticus with systemic kainic acid injections. Conversely, Evrengül et al.[95] showed higher HRV in male patients who had generalised tonic clonic seizures compared to controls when using standard time-based methods and showed a large increase in the LF component of the power spectrum, indicating a potential increased sympathetic activity in these patients. Another study found no association between SUDEP and any HRV measures[96], however this study only involved 7 patients with epilepsy and is therefore potentially statistically underpowered, especially when considering that inter-patient variability in HRV measures is often large[67,97]. Some patients that ultimately die of SUDEP have also been observed to have progressive changes in HRV. Rauscher and colleagues[98] observed a progressive deterioration in RMSSD and the HF component over an eight-month period prior to the patient's death. Further, Lacuey et al.[99] reported a decrease in a number of time-based HRV parameters in two patients over a three or five-year period that also died of SUDEP.

The current literature investigating the possible mechanisms contributing to SUDEP is clearly diverse, with evidence indicating a role for both respiratory and cardiac based influences. Autonomic dysfunction has been attributed as the cause of a number of the cardiovascular changes induced by seizure, and thus investigation into changes in

the ECG waveform and heart rate variability could help to explore this autonomic dysfunction further.

TETANUS NEUROTOXIN MODEL OF TEMPORAL LOBE EPILEPSY

TEMPORAL LOBE EPILEPSY AND THE HIPPOCAMPUS

Temporal lobe epilepsy (TLE) is the most common focal epilepsy whereby pathological discharges are generated by an epileptic focus within the hippocampus or related structures such as the amygdala[100]. In physiological tissue, three hippocampal sub-regions (the dentate gyrus, CA3 and CA1) receive input from the entorhinal cortex and output to the subiculum. Each sub-region communicates with the others using excitatory projections, and the dentate gyrus and CA3 sub-regions contain recurrent excitatory connections that allow normal tissue to locally generate epileptiform activity[101]. The interactions between hippocampal sub-regions exhibit activity-dependent plasticity, are involved in learning and memory, and are temporally modulated by inhibitory interneurons[102]. Due to its plastic nature, the hippocampus is susceptible to the development of aberrant excitatory loops and subsequently spontaneous seizure generation[103].

Various animal models of TLE are currently employed either using chemical means, such as pilocarpine[104–106], kainic acid[94,107–109] and tetanus neurotoxin[110–114], and physical means such as electrical kindling[51,115]. Each of these chronic models have advantages and disadvantages, but each are considered to be a good model of human epilepsy as each is capable of generating spontaneous seizures.

Tetanus Neurotoxin

Tetanus neurotoxin (TeNT) is derived from the *Clostridium tetani* bacteria and is a zinc metalloprotease that exclusively targets neurons[116,117]. The neurotoxin contains both light and heavy chains, with the heavy chain comprised of two domains. These domains confer neuronal specificity and give the ability to internalise into neurons. Once internalised, the light chain is activated by cleavage of a disulphide bond, and is then able to carry out its proteolytic activity on its target: the Vesicle Associated Membrane Protein (VAMP)[113,117]. VAMP is part of the SNARE complex that is responsible for presynaptic neurotransmitter release, and therefore TeNT prevents synaptic transmission.

Peripherally, this disruption of synaptic transmission results in spastic paralysis[118], whilst centrally TeNT has an impact on both excitatory and inhibitory transmission, however the decrease in inhibitory transmission has been shown to have a higher impact. Further, it has been demonstrated that this affect on inhibitory transmission in the hippocampus is eliminated 8 to 16 days post neurotoxin injection[113].

The TeNT Model of Temporal Lobe Epilepsy

When injected centrally, TeNT causes epileptic seizures[119], with the type of epilepsy modelled dependent on the location of the injection, as this determines the focus. For example, the neocortex[120,121], motor cortex[122,123], visual cortex[124,125] and hippocampus[112–114,126–128] have all been previously targeted. Intrahippocampal injections of TeNT result in spontaneous seizures occurring one week post injection[114], but have also been shown four days post injection[129]. Low dose intracranial injections induce minimal cell loss, no morphological changes[112,130] nor do they result in cell death, hippocampal sclerosis or status epilepticus at any stage[110,112,114,131].

The TeNT model of TLE induces spontaneous seizures that can be categorised as complex partial with secondary generalisation, with behavioural manifestations and pathological brain activity similar to that seen in human patients[119]. At their peak, seizures can occur up to 30 times a day, rarely exceed two minutes in duration, and animals often gain seizure remission six to eight weeks post onset[112,131]. Furthermore, the model has been well characterised and is reliable: seizures are initiated with behavioural arrest and vibrissal twitching and continue to forelimb clonus and subsequently rearing and falling[114,131,132]. As stated above, there are many different methods of inducing epilepsy in animal models, and the correct model should be used to answer your question. As such, this study will use the tetanus neurotoxin model as it induces spontaneous seizures, without status epilepticus. Moreover, as animals often enter into seizure remission, this will permit the long-term cumulative effect of epileptic seizures and identify whether or not any effect persists after seizure activity has ceased.

VENTRAL HIPPOCAMPUS AND THE CARDIOVASCULAR SYSTEM

The rodent hippocampi have dorsal and ventral sections that are joined at the hippocampal commissure. Previously, TeNT has been injected into both the dorsal[112–114] and ventral[119,128] hippocampus to induce epileptic seizures as described above. In order to explore the effect of epileptic seizures on the cardiovascular system the ventral hippocampus, due to its electrical connections to the brainstem and the autonomic nervous system, was injected with TeNT. Briefly, the hippocampus is connected to the hypothalamus via efferent connections in the fornix[133] (FIGURE 1). The hypothalamus in turn has efferent connections to the brainstem via the mammillotegmental tract[134], and synapses with the nucleus ambiguus and the dorsal motor vagal nucleus in the midbrain

and the intermediolateral nucleus/stellate ganglion in the spinal cord[135]. These nuclei are involved in the regulation of the cardiovascular system via parasympathetic (nucleus ambiguus and dorsal motor vagal nucleus) and sympathetic (intermediolateral nucleus/stellate ganglion) efferents contained in the vagal nerve and the glutamatergic bulbospinal pathway respectively[136] (FIGURE 1). It is therefore envisaged that inducing epileptic seizures in the ventral hippocampus, will replicate the autonomic disturbances observed in human studies.

AIMS AND HYPOTHESIS

This study aimed to explore the effects of epileptic seizures on cardiac function. Firstly, it aimed to explore the effect of epileptic seizures, identified via electrocorticogram (ECoG) recordings, on the conduction through the heart by measuring the PR and QT intervals and QRS width over the course of the disease. We hypothesised that there would be a progressive deterioration in the conduction of the heart; similar to that seen in human patients and other animal studies, namely where the QT interval would increase. We aimed to establish the changes in the autonomic nervous system over the course of the disease, by calculating various measures of heart rate variability and analysing heart rate. The hypothesis was that there would be a progressive deterioration in the central control of the heart. This would be similar to that observed in human studies and other animal studies and would indicate an imbalance between the sympathetic and parasympathetic arms of the autonomic nervous system. Finally, this study aimed to establish whether the TeNT model of temporal lobe epilepsy is a reliable and accurate model of SUDEP, and to identify cardiac measurements that could possibly be used to help those patients with higher risk.

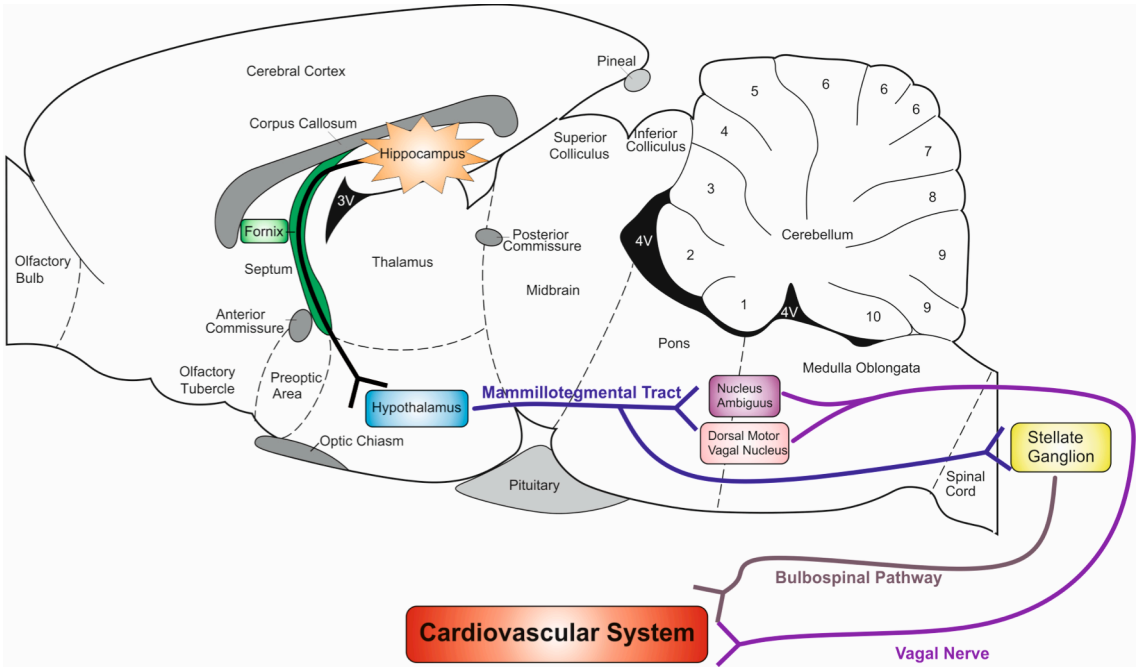

Figure 1 *(adapted from [139]) A diagrammatic representation of the electrical connections between the hippocampus and hypothalamus, via the fornix, and the hypothalamus and the autonomic nervous system. The hypothalamus has efferent connections to the Stellate Ganglion and the Nucleus Ambiguus and Dorsal Motor Vagal Nucleus via the mammillotegmental tract. The NAc and DMVN influence the cardiovascular system via the Vagal nerve, whereas the Stellate Ganglion has glutamatergic efferents housed within the bulbospinal pathway. It is envisaged that injecting TeNT into the ventral hippocampus will induce autonomic disturbances similar to those seen in humans and other animal models.*

METHODS

This study was performed in accordance with all local and Home Office Regulations set out by Animals (Scientific Procedures) Act 1986. Five male Wistar rats (Harlan, UK) were used in this study. Animals were housed either in the Biomedical Services (BMS) unit at the University of Oxford or at the University of Birmingham's Biomedical Services Unit (BMSU) on a 12 hour light to dark cycle (0700 to 1900). Food and water was available *ad libitum* at all times. Each experimental animal was housed with a naïve companion rat in custom made Perspex cages (dimensions 40 cm x 27 cm x 30 cm), was monitored daily for epileptic activity, and recorded, via webcam, for seizure categorisation using the Racine Scale[132,137]. The animals were killed 6-8 weeks post induction, with the brain and heart perfused fixed with 4% paraformaldehyde for examination at a later date.

RADIOTELEMETER IMPLANTATION

Buprenorphine (Vetergesic, 0.05 mg kg^{-1}) and meloxicam (Metacam, 1 mg kg^{-1}) were injected subcutaneously 30 minutes prior to the start of the surgery in order for the plasma concentration to be at its optimal prior to the first incision. The animal was anaesthetised with 4% isoflurane in oxygen at 1 litre min^{-1} and subsequently maintained at 1-3% isoflurane in oxygen, monitoring respiration rate and pedal reflex at regular intervals and adjusting anaesthesia levels as appropriate. Body temperature was monitored throughout the procedure and maintained at 37°C using a homeothermic blanket and rectal probe (Harvard Apparatus, United States). Aseptic technique was adhered to throughout the procedure.

After stable anaesthesia was achieved, Amoxicillin Trihydrate and Clavulanic Acid (Synulox, 20 mg kg^{-1}) and glucose saline (10 mL kg^{-1}) were administered subcutaneously, Lacri-Lube eye ointment (Allergan, United States) was applied to the eyes and a prilocaine and lidocaine cream (EMLA Cream) was applied to the ear canal using a cotton bud. Subsequent glucose saline doses were administered every 60 minutes until the completion of the procedure. The animal's fur was shaved on the dorsal surface of the head, extending from between the eyes and the back of the skull. The ventral aspect of the abdomen and the chest were also shaved. Shaved areas were then cleaned of any remaining fur using chlorhexidine gluconate (Hibiscrub, Mölnlycke Health Care, United Kingdom). The final stage of preparation was to sterilise the surgical sites using 2% chlorhexidine gluconate and 70% isopropyl alcohol in a sterile applicator (Chloraprep, CareFusion, United Kingdom).

Each animal was implanted with a Telemetry Research radiotelemeter (TR50BB, Millar Instruments, United States) and an indwelling cranial cannula was inserted over the ventral hippocampus. Firstly, the radiotelemeter was implanted into the abdominal cavity and secured in place by suturing it to the abdominal wall, lateral to the incision, using non-absorbable 5-0 Prolene sutures (Ethicon, United States). The wires were subsequently tunnelled through the abdominal wall using a small bore trocar, with the ECG wires exiting laterally to the right of the incision and the electrocorticogram (ECoG) wires laterally to the left. The abdominal wall was then repaired using 5-0 Prolene sutures.

To implant the wires to record the ECG, they were tunnelled to two sites on the rat's ribcage, as described by Kramer et al[138]. Using a trocar, the negative electrode was tunnelled to a small (2-3 mm) incision over the right rostral portion of the ribcage, and

the positive electrode tunnelled to a small incision over the left caudal portion of the ribcage. Both electrodes were secured in place using non-absorbable 5-0 Prolene sutures. The signal of the ECG was then confirmed and the electrode placement readjusted if necessary. The ECG incisions were then repaired using absorbable 4-0 Vicryl sutures (Ethicon, United States).

The dorsal aspect of the upper cervical region was sterilised with Chloroprep and a small incision was made to enable the subcutaneous tunnelling of the ECoG wires from the abdomen to the cervical site using a trocar. The abdominal incision was then repaired using absorbable 4-0 Vicryl sutures. The animal was subsequently transferred to a stereotaxic frame (Stoelting, United States), the surgical site sterilised with Chloroprep, and an incision made to expose the skull. To ensure accuracy, the heights of bregma and lambda were ensured to be within 0.2 mm of each other. Burr holes were then drilled using a micro-drill (230 VAC Drill, Microtorque II; Circuit Medic, United States) over the ventral hippocampus (Anterior-Posterior - 4.3 mm, Medial-Lateral - 4.4 mm [139]; Figure 3) for the indwelling cannula, for the ECoG electrodes (above the dorsal hippocampus), and finally a further two to three holes for anchoring screws (Figure 2). The cannula was stereotaxically placed into the correct burr hole, and secured in place using light cured dental cement (NX3 Nexus, Kerr Dental, UK) along with the anchoring screws. Finally, the ECoG wires were bent into a U shape (Figure 3), placed into the burr holes above the hippocampus, and secured in place using cement, creating a cement head cap. The head wound was the closed with 4-0 Vicryl sutures so that the wound margin was closely opposed to the head cap. The animal recovered in a warm cage with appropriate bedding (Alpha-dri) and appetising food. Opiate and NSAID analgesia was given for 3-5 days post-operatively, and to prevent infection subcutaneous injections of antibiotics were given for five days post-operation.

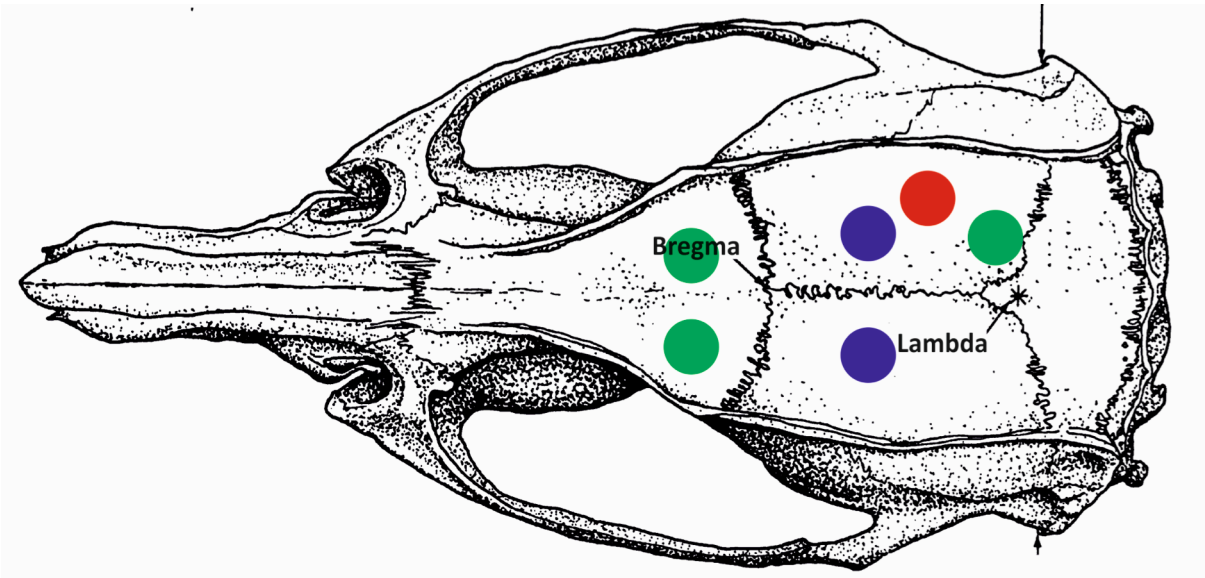

FIGURE 2 *(adapted from [139]) The approximate locations of the anchoring screws (green), electrodes (blue) and guide cannula (red). The guide cannula was immediately above the Ventral hippocampus (Anterior-Posterior - 4.3 mm, Medial-Lateral - 4.4 mm). The electrodes were placed into the cortex above the dorsal hippocampus, in the approximate positions shown in blue.*

INDUCTION OF EPILEPSY: TETANUS NEUROTOXIN INJECTION

When the animal was fully recovered from the implantation surgery, with its weight exceeding its preoperative weight and no signs of continued pain or distress evident, epilepsy was induced. This was approximately two weeks after the implantation of the radiotelemeter.

Each animal was anaesthetised and placed into a stereotaxic frame. 2.5 ng TeNT (List Biological Laboratories Inc., United States) in 1 µL of 2% bovine serum albumin in phosphate buffered saline was injected through the guide cannula, at 200 nL min^{-1} using a Hamilton Syringe (25G, 7001 KH, Hamilton Company, United States) and a microinjection pump (WZ-74905-02, Cole-Parmer, United Kingdom). The target site was 7.5 mm below the cortical surface (Figure 3). The syringe was left *in situ* for five minutes after the end of

the injection to limit backflow up the needle tract. The animal was recovered and housed with a naïve companion animal.

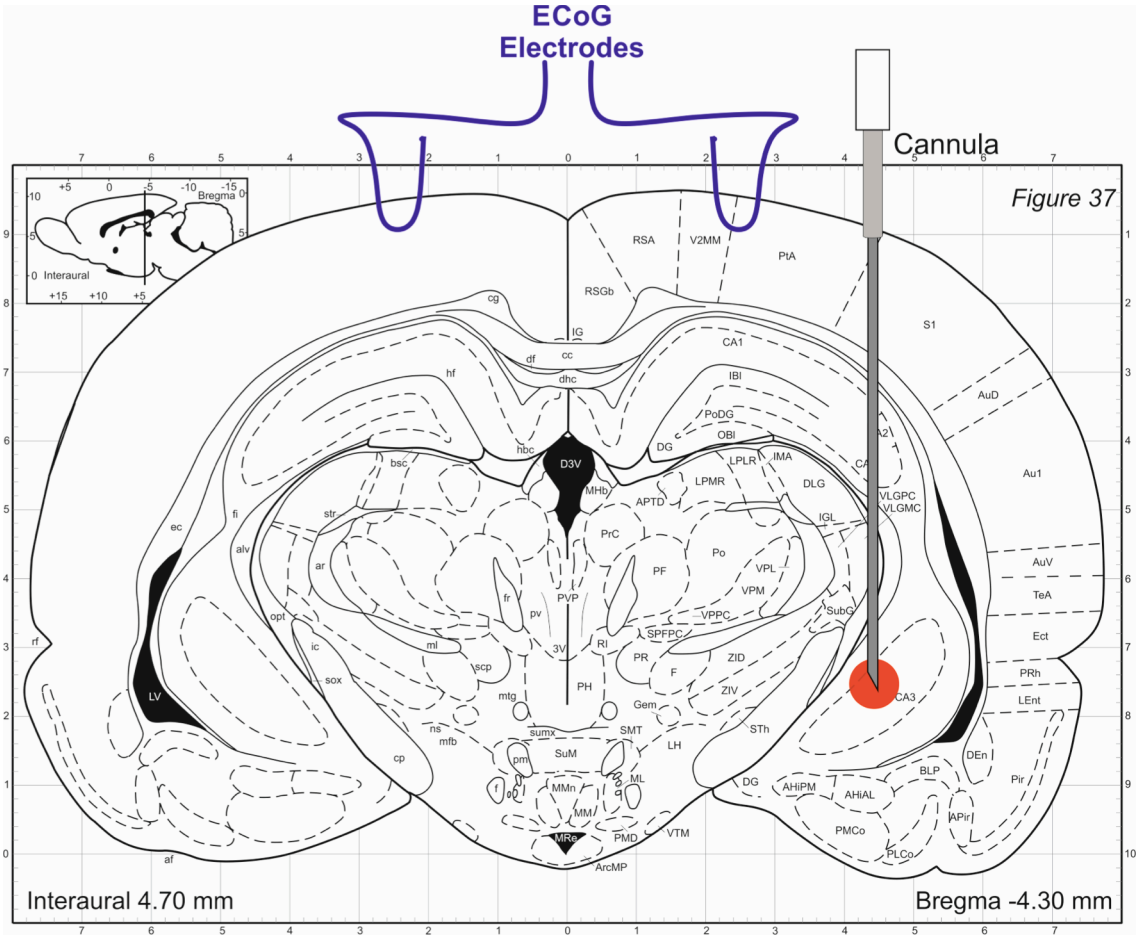

FIGURE 3 *(adapted from [139]) The target location (red circle) for the TeNT injection in the ventral hippocampus: Anterior-Posterior -4.3 mm, Medial-Lateral -4.4 mm, Ventral Depth -7.5 mm, the approximate location of the two ECoG electrodes and the positioning of the guide cannula. Also shown for representation purposes is a needle.*

IN VIVO RECORDING OF SEIZURES AND ELECTROCARDIOGRAM

The ECoG and ECG were recorded continuously, along with video. Each cage was placed on a SmartPad (TR180; Millar Instruments, United States) which powered the radiotelemeter and acquired each signal at 2 kHz sampling frequency. Recordings were digitised by a Power1401 (Cambridge Electronic Design Ltd., United Kingdom) and stored in Spike2 format (Cambridge Electronic Design Ltd., UK) for later analysis. Video files

were analysed and seizures were scored using the Racine scale[132,137] which classifies the seizures depending on their motor manifestations. Briefly, Scale 1 - absence of movement and/or purposeless chewing; Scale 2 - abnormal head bobbing; Scale 3 - forelimb clonus; Scale 4 - postural rearing; and Scale 5 - postural rearing and falling. This video analysis also allowed verification of the seizure initiation and termination, when compared with the ECoG signal.

DATA ANALYSIS

Seizures were differentiated from normal activity by using both ECoG data and the onset and termination of motor outputs, captured by the video recording. Briefly, seizures had periods of rhythmic electrical activity that exceeded 0.5 mV in amplitude and an increase in power in the 10-300 Hz band. Seizures were identified by identifying periods of high power within the 10-300 Hz frequency band of the raw ECoG, and then manually assessing the ECoG signal and accompanying video to verify seizure activity. Example of different types of seizures can be seen in Figure 4, with large increases in the ECoG amplitude clearly observed, coupled with rhythmic activity. Previous work[129] has shown that the post ictal changes in heart rate can persist for 45 to 60 minutes post seizure termination; therefore Interictal periods were defined as being 45 minutes prior to seizure onset and at least 45 to 60 minutes from the previous seizure's termination.

R-WAVE DETECTION

In order to process changes in ECG waveform or HRV, a sophisticated method of R-wave detection was used to avoid contamination from movement artefacts. This noise rendered simple methods such as "thresholding" impractical as the real R-wave signal could often not be discriminated from noise by amplitude alone (see Figure 5B for an

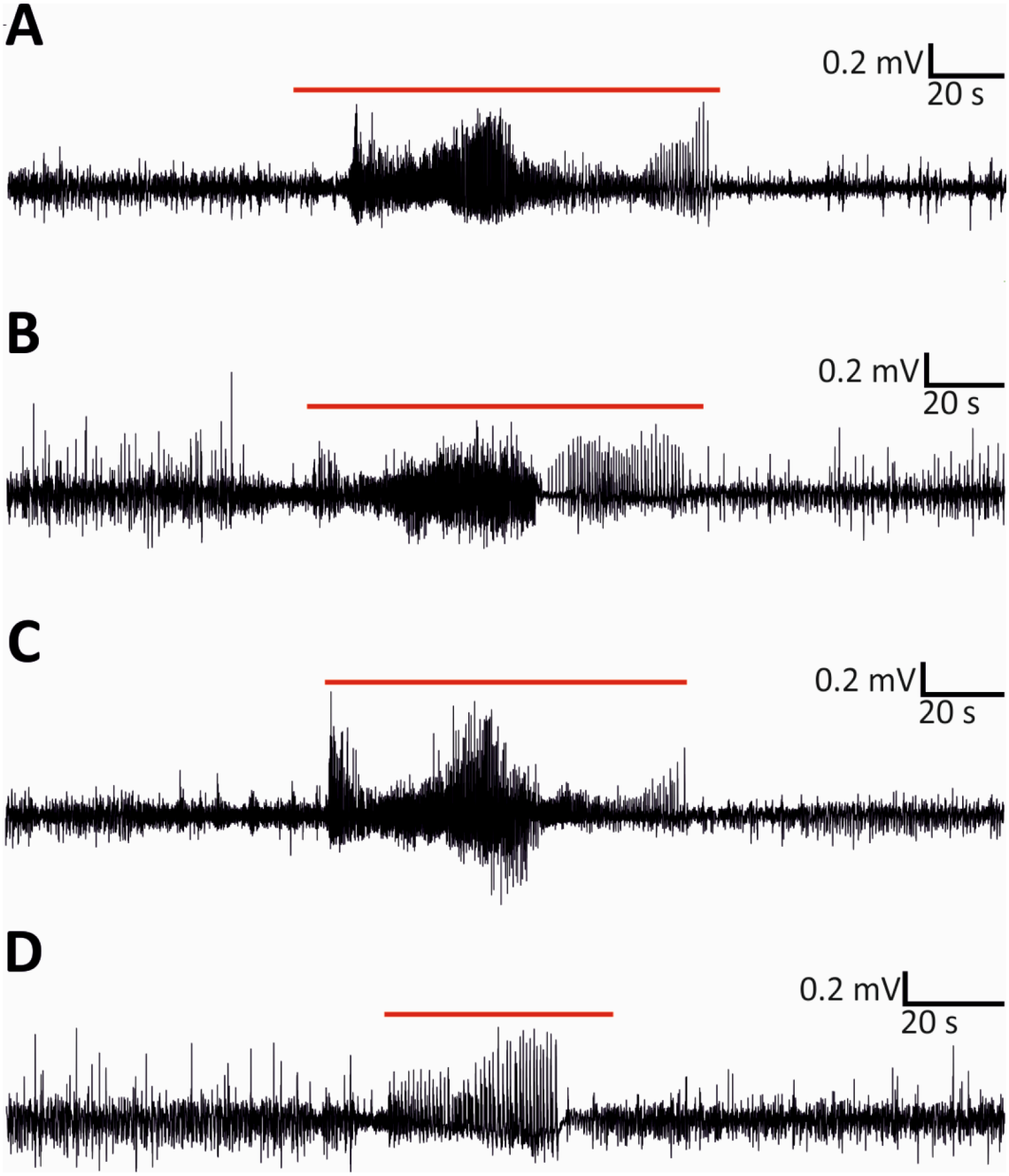

FIGURE 4 *Examples of seizures with different morphologies, amplitudes, and durations taken from AAL131104, with seizure activity – determined by motor output and ECoG activity – denoted by the red line.* ***A*** *The first seizure experienced by animal AAL131104, which lasted 105 seconds, was categorised as Racine Scale 2 and occurred 2.5 days post intrahippocampal TeNT injection.* ***B*** *The 112th seizure experienced, lasted 100 seconds, was categorised as Scale 3 and occurred 9.7 days post injection.* ***C*** *The 14th seizure, which lasted 86 seconds, categorised as Scale 4 and occurred 5.0 days post injection.* ***D*** *The 55th seizure, which lasted 45 seconds, was categorised as Scale 5 and occurred 8.5 days post intrahippocampal injection.*

example of noise). Therefore, the author created a custom-made Spike2 script in order to perform R-wave detection (see Appendix B) based upon the Pan-Tompkins Algorithm[140]. Firstly, a bandpass Finite Infinite Response filter at 42 to 61 Hz was applied to the raw ECG signal and the resulting signal differentiated at a 0.004 second time constant. The resulting waveform was squared and subsequently integrated by applying the Spike2 *Smooth* function at a 25 ms time constant. Finally, the peak of the resulting square waveform was detected and a marker placed at that time point. The script then evaluated the original raw ECG waveform to ensure that the marker corresponded with the exact time point of the R-wave and moved the marker if required. The ECG waveform, heart rate, and heart rate variability were then evaluated using these time-points.

ECG Waveform Analysis

The ECG waveform can be analysed in a number of ways to reveal information about the conductivity through the heart. Using the time-point markers of each R wave and the inbuilt functionality of Spike2, the ECG waveform was analysed in five second epochs, sampled every 30 seconds during a 10 to 15 minute interictal period. The inbuilt *Waveform Average* function of Spike2, using the R-wave time points as a reference, created the average ECG waveform for each five-second epoch, within a 100 ms window of each marker. Markers were then placed on different landmarks of the averaged waveform in order to calculate the PR Interval, QRS width, and QT Interval (see Figure 5). The corrected QT interval (QT_c) was calculated using the modified Bazett formula created by Kmecova and Klinas[87], where the RR interval of the rat was used to calculate the QT interval independent of changes in RR Interval.

$$\mathrm{QTC} = \frac{\mathrm{QT}}{(\mathrm{RR}/\mathrm{f})^2} \qquad (\mathrm{f} = 150\ \mathrm{ms})$$

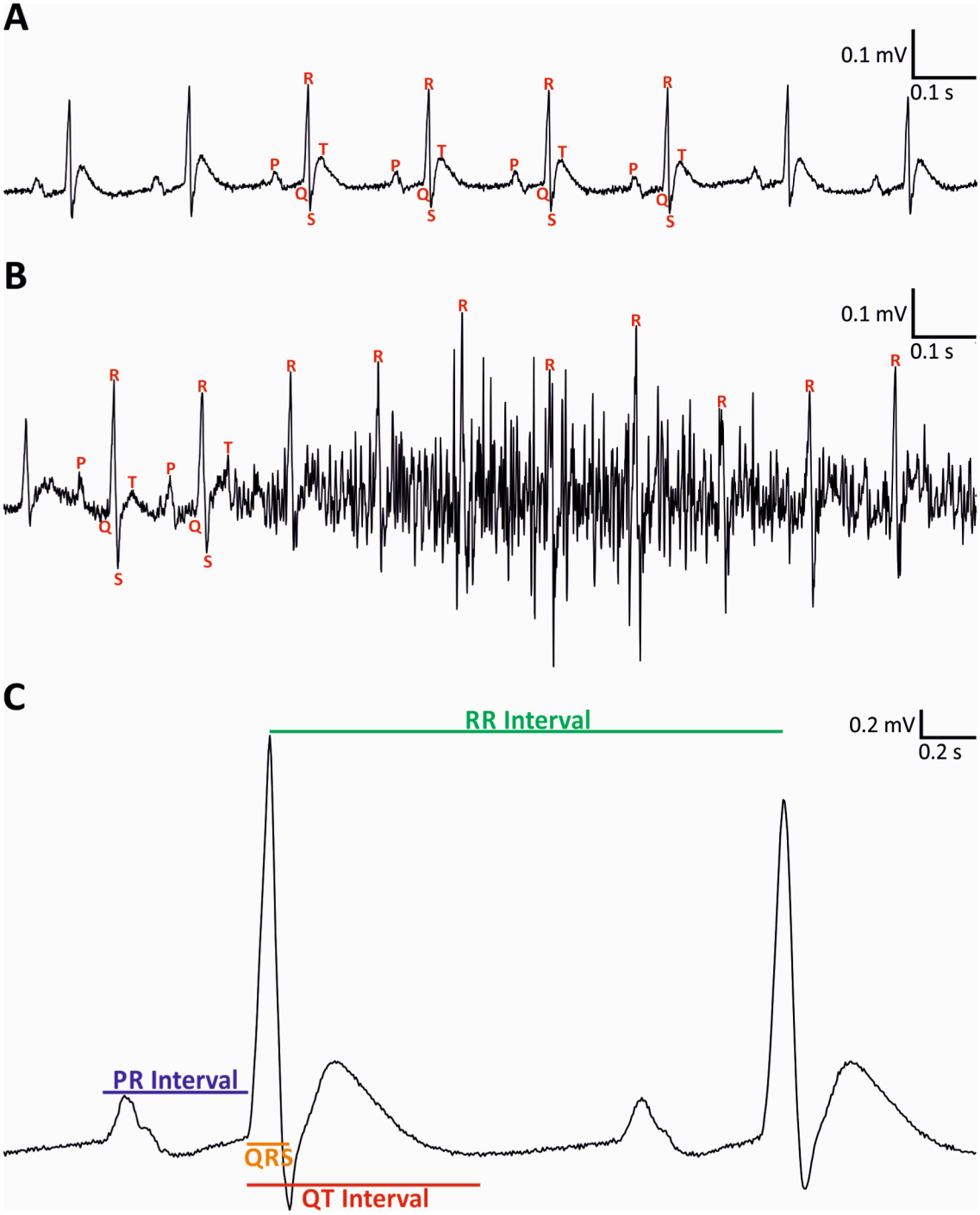

FIGURE 5 ***A*** *Example ECG with the characteristic P-wave, QRS complex and T-wave.* ***B*** *The problem of noise artefacts on the ECG channel necessitated a sophisticated method of discriminating the R-wave. It can clearly be seen that the noise prevents adequate discrimination of the R-wave, but also the associated P, Q, S and T waves.* ***C*** *An example average waveform analysis, showing how the PR, RR and QT intervals and the QRS complex width were measured. The relative heights of the two R waves were also analysed, with any relationship below 40% indicating that the heart rate varies too much over the 5-second epoch to generate reliable results.*

The amplitude of the second R wave was compared to the first to ensure that the RR interval during the 5-second epoch was stable for comparison. Consequently, any epoch with an R wave relationship below 40% was rejected from the analysis.

Heart Rate Variability Analysis

There are two methods of analysing HRV: time and frequency based analysis. This study analysed time based methods using a custom made MatLab script created in house (see Appendix C) that used the time points of each R-wave within the 10-minute interictal epoch. Briefly, the script analysed the differences between neighbouring R-waves and processed them according to the mathematical formula required for time-based methods. The different equations are discussed below.

- RMSSD – The root mean square of successive differences between RR intervals, a measure of vagus-mediated heart rate variability and autonomic regulation of the heart[31].

$$\mathbf{RMSSD} = \sqrt{\frac{\mathbf{1}}{\mathbf{N-1}}\sum_{\mathbf{j=1}}^{\mathbf{N-1}}(\mathbf{RR_{j+1}} - \mathbf{RR_j})^{\mathbf{2}}}$$

- SDNN - The standard deviation of all RR intervals, indicating the total variability across the epoch and provides a general measurement the autonomic nervous system's balance[89,95].

$$\mathbf{SDNN} = \sqrt{\frac{\mathbf{1}}{\mathbf{N-1}}\sum_{\mathbf{j=1}}^{\mathbf{N}}(\mathbf{RR_j} - \overline{\mathbf{RR}})^{\mathbf{2}}}$$

- SDSD – The standard deviation of successive differences between adjacent RR intervals and representing short-term variation[141].

$$\mathbf{SDSD} = \sqrt{\mathbf{E}\{\Delta\mathbf{RR}_\mathbf{j}^\mathbf{2}\} - \mathbf{E}\{\Delta\mathbf{RR}_\mathbf{j}\}^\mathbf{2}}$$

- SD Ratio – This is the ratio between the SD1 and SD2 values. The SD1 represents short-term heart rate variability 11whilst SD2 represents long-term heart rate variability[142].

$$\mathbf{SD1} = \sqrt{\frac{\mathbf{SDSD^2}}{\mathbf{2}}}$$

$$\mathbf{SD2} = \sqrt{\mathbf{2}\left(\mathbf{SDNN^2}\right) - \frac{\mathbf{SDSD^2}}{\mathbf{2}}}$$

Statistical Analysis

All data was expressed as mean ± standard deviation. One-way analysis of variance (ANOVA) with post-hoc Bonferroni comparisons was performed using SPSS (IBM, United States). Data was analysed at various time points throughout the course of the disease: the interictal period immediately before the 1st, 50th, 100th, 150th, 200th, 250th, 250th and 300th seizures, as well as Preinduction and the Post Seizure State. The Preinduction data was obtained from the day immediately prior to induction, and the Post Seizure State was obtained immediately before the end of the experiment.

RESULTS

Seizure activity began in all animals around 2 to 7 days post intrahippocampal TeNT injection, however the number and the severity of the seizures induced varied across subject animals. Table 1 presents data for each animal in this study, the number of seizures detected, the average length of these seizures, the range of seizure lengths, and the modal Racine seizure score. As video recording was not possible for JJ130513 and JJ130521, the modal seizure scores for these animals are absent.

Between 43 and 382 seizures were experiences by the subject. Seizure profiles (Figure 6) were created using each seizure's length and the time the seizure initiated, in order to show each animal's seizure progression over the course of the experiment. As can be seen from the seizure profiles, all animals, except JJ140924, experienced seizures in clusters with an initial cluster followed by a one to two day period of apparent quiescence. As the ECoG electrodes were located in the cortex, it is possible that during these apparent periods of quiescence the animal experienced focal or partial seizures that were not detectable and that seizure manifestations were not obvious on the video recording. Further, a number of seizures could not be classified (yellow marker) due a number of factors, such as the camera's view being obscured by the companion animal and cage furniture, or because the cage was moved away from the camera momentarily.

The length of seizures the animals experienced followed the same general pattern (Figure 6), whereby the length increased to a maximum, and then decreased to a more consistent length of around 50 to 100 seconds. The mean seizure length and mean number of seizures per day was inconsistent across all five animals. As can be seen from Figure 6 and Table 1, the mean seizure length varied from 74 ± 5 seconds to 95 ± 5

seconds. Furthermore, the maximum seizure length experienced ranged from 130 seconds to 317 seconds.

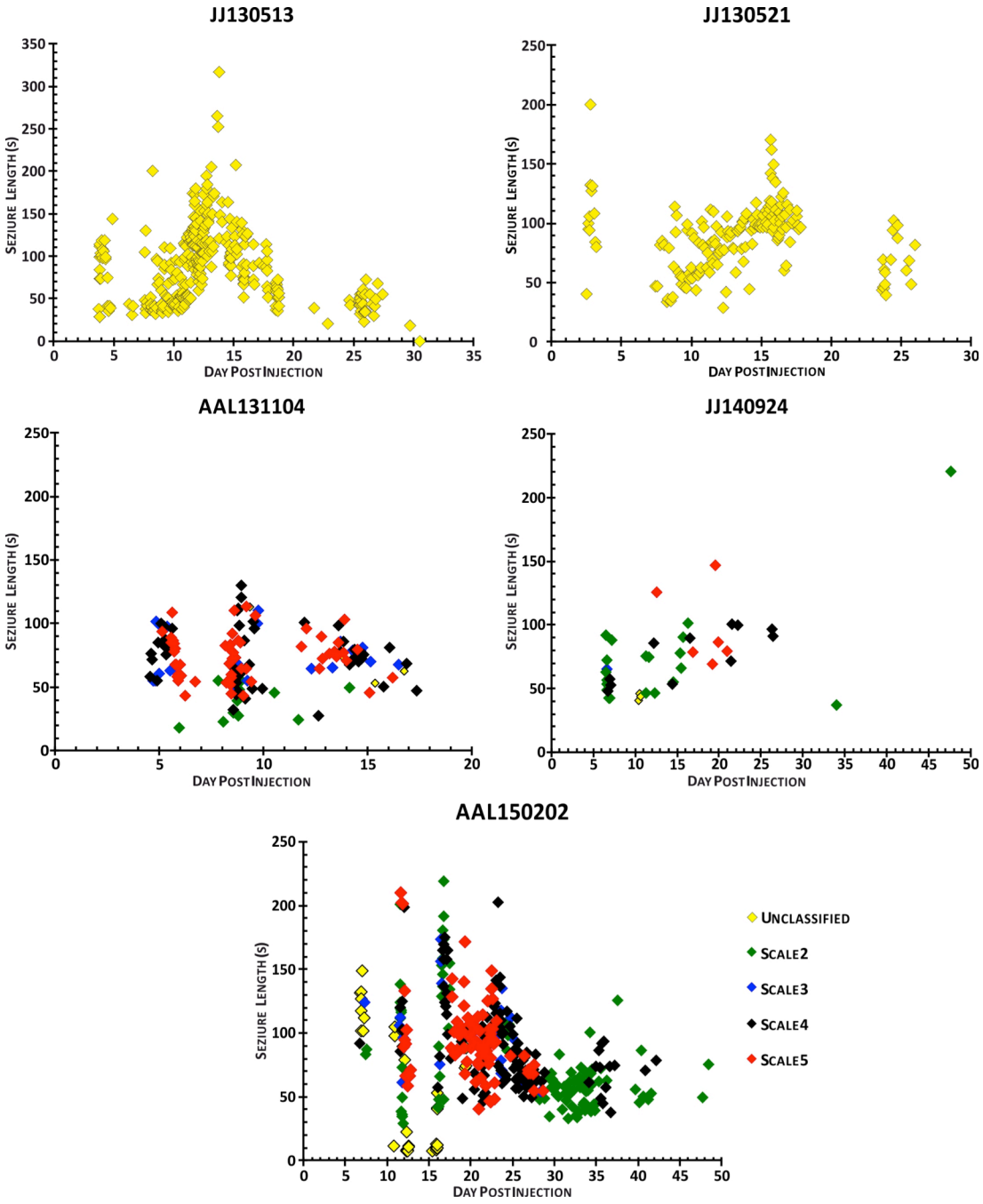

FIGURE 6 *The seizure profiles generated for each experimental animal, with seizure length in seconds plotted against the day post injection. Seizures were classified using the Racine Scale, where Scale 2 (green) corresponds to abnormal head bobbing; Scale 3 (blue) to forelimb clonus; Scale 4 (black) to postural rearing; and Scale 5 (red) to postural rearing and falling. Unclassified (yellow) seizures were those that could not be scored as the view of the animal was obscured or due to technical issues.*

Finally, the seizure frequency varied between the subject animals, with JJ130513 and AAL131104 experiencing 16 and 13 seizures per day respectively, whereas JJ140924 only experienced one seizure per day over the course of the experiment.

JJ140924 is considered an outlier and was therefore excluded from further analysis. As can be seen from Figure 6, it experienced a comparatively low number of seizures, 43, dispersed over a period of 48 days, a mean seizure length of 74 ± 5 seconds, and the modal seizure score of 2 – behavioural arrest with vibrissal twitching. This study aimed to explore the effect of cumulative seizure insult on the cardiovascular system, and due to the lack of clustered generalised seizures (Figure 6), the data from JJ140924 was deemed not comparable to the others.

TABLE 1

ANIMAL ID	LATENCY TO FIRST SEIZURE (DAYS)	TOTAL NUMBER OF SEIZURES	MEAN SEIZURES PER DAY	MEAN SEIZURE LENGTH (SEC)	MAX SEIZURE LENGTH (SEC)	MINIMUM SEIZURE LENGTH (SEC)	MODAL SEIZURE SCORE
JJ130513	3.7	275	16	95 ± 5	317	28	-
JJ130521	2.5	168	6	88 ± 2	200	28	-
AAL131104	2.5	159	13	75 ± 3	130	18	5
JJ140924	6.5	43	1	74 ± 5	220	37	2
AAL150202	6.7	382	7	83 ± 2	219	7	4

A summary of each of the animals used in this study, showing the latency from induction to the first seizure, the total number of seizures detected and the mean seizure length. Animals JJ13013 and JJ130521 did not have video recording so seizure classification using the Racine scale was not possible.

INTERICTAL ECG WAVEFORM

PR INTERVAL

The PR interval was relatively stable across the course of the disease for each animal (Figure 7). The interictal PR interval (Figure 11A) for the experimental population at nine time points - Preinduction, 1st, 50th, 100th, 150th, 200th, 250th, 300th Seizure and Post Seizure State - showed a significant increase (One Way ANOVA, $\alpha = 0.05$). Of particular note, there was a significant increase in the PR interval from Preinduction (44.1 ± 1.9 ms) to the interictal period immediately before the 1st Seizure (46.9 ± 2.3 ms). The PR interval also significantly increased between the 1st and 150th Seizure (46.9 ± 2.3 ms to 49.5 ± 2.6 ms). Further, there was a significant increase in the PR interval from Preinduction to the Post Seizure State (44.1 ± 1.9 ms to 47.7 ± 3.5 ms). Appendix A shows a complete table of the statistical comparisons between the different time points.

The four animals' preinduction values (42.4 ± 1.3 ms; 46.3 ± 1.0 ms; 44.5 ± 1.7 ms; 44.6 ± 1.1 ms) varied from one another and therefore the data for each animal was normalised to the Preinduction value for that animal (see Figure 12A). When normalised, the PR interval significantly increased from Preinduction to the 1st Seizure by 6.1 ± 3.4%, a 6% increase. There was a 8.7 ± 4.4% significant increase in normalised PR interval by the 150th Seizure, and there was a 6.9 ± 0.7% increase from Preinduction to the Post Seizure State.

TABLE 2

	JJ130513	JJ130521	AAL131104	AAL150202
PR INTERVAL				
ALL DATA (MS)	44.4 ± 2.6	45.5 ± 2.6	48.1 ± 2.8	43.8 ± 2.8
RANGE (MS)	35.0 to 53.5	35.5 to 52.0	27.5 to 56.0	31.4 to 49.5
PREINDUCTION (MS)	44.5 ± 1.7	44.7 ± 1.1	46.3 ± 1.0	42.4 ±1.3
POST SEIZURE STATE (MS)	51.1 ± 1.5	46.7 ± 2.1	49.4 ± 3.3	44.4 ± 2.7
QRS WIDTH				
ALL DATA (MS)	10.7 ± 1.2	12.8 ± 1.8	14.7 ± 1.5	15.0 ± 2.0
RANGE (MS)	8.5 to 14.5	10.0 to 20.1	11.0 to 19.4	10.5 to 22.3
PREINDUCTION (MS)	10.7 ± 0.8	11.6 ± 1.3	14.2 ± 1.4	14.3 ± 1.8
POST SEIZURE STATE (MS)	12.0 ± 1.4	12.5 ± 1.6	13.9 ± 1.6	14.0 ± 1.4
QT INTERVAL				
ALL DATA (MS)	71.1 ± 5.1	79.7 ± 6.9	71.3 ± 5.9	71.0 ± 8.5
RANGE (MS)	58.5 to 87.4	40.9 to 97.6	48.8 to 89.9	48.0 to 89.4
PREINDUCTION (MS)	69.0 ± 5.5	72.3 ± 4.7	64.2 ± 4.7	61.0 ± 4.6
POST SEIZURE STATE (MS)	80.2 ± 3.9	85.7 ± 6.2	67.7 ± 3.0	65.6 ± 8.2
QTC INTERVAL				
ALL DATA (MS)	75.7 ± 5.3	78.8 ± 5.5	70.1 ± 7.2	65.9 ± 9.6
RANGE (MS)	60.0 to 90.9	41.4 to 96.2	46.5 to 91.0	40.9 to 90.5
PREINDUCTION (MS)	74.9 ± 6.0	76.7 ± 3.5	64.7 ± 7.4	58.6 ± 4.3
POST SEIZURE STATE (MS)	73.7 ± 3.7	81.8 ± 5.7	61.4 ± 4.5	60.7 ± 12.0
RR INTERVAL				
ALL DATA (MS)	133.3 ± 16.4	155.0 ± 24.3	156.9 ± 18.4	177.0 ± 25.5
RANGE (MS)	94.5 to 199.0	104.0 to 216.0	118.5 to 215.0	145.5 to 233.4
PREINDUCTION (MS)	127.8 ± 9.6	134.6 ± 22.5	139.6 ± 41.3	162.8 ± 13.8
POST SEIZURE STATE (MS)	178.0 ± 11.9	167.2 ± 28.1	183.8 ± 18.4	181.0 ± 28.7

A summary of the mean, ranges, preinduction and post seizure state values for the PR, QT, QTc, RR intervals and QRS width for JJ130513, JJ130521, AAL131104, and AAL150202. Where possible data is reported as mean ± standard deviation. All Data is the mean of all data points collected for each animal over the course of the disease, with the range showing the minimum and maximum value of all data points. The Preinduction and Post Seizure State values are immediately before the animal was injected with TeNT and immediately before the end of the experiment respectively.

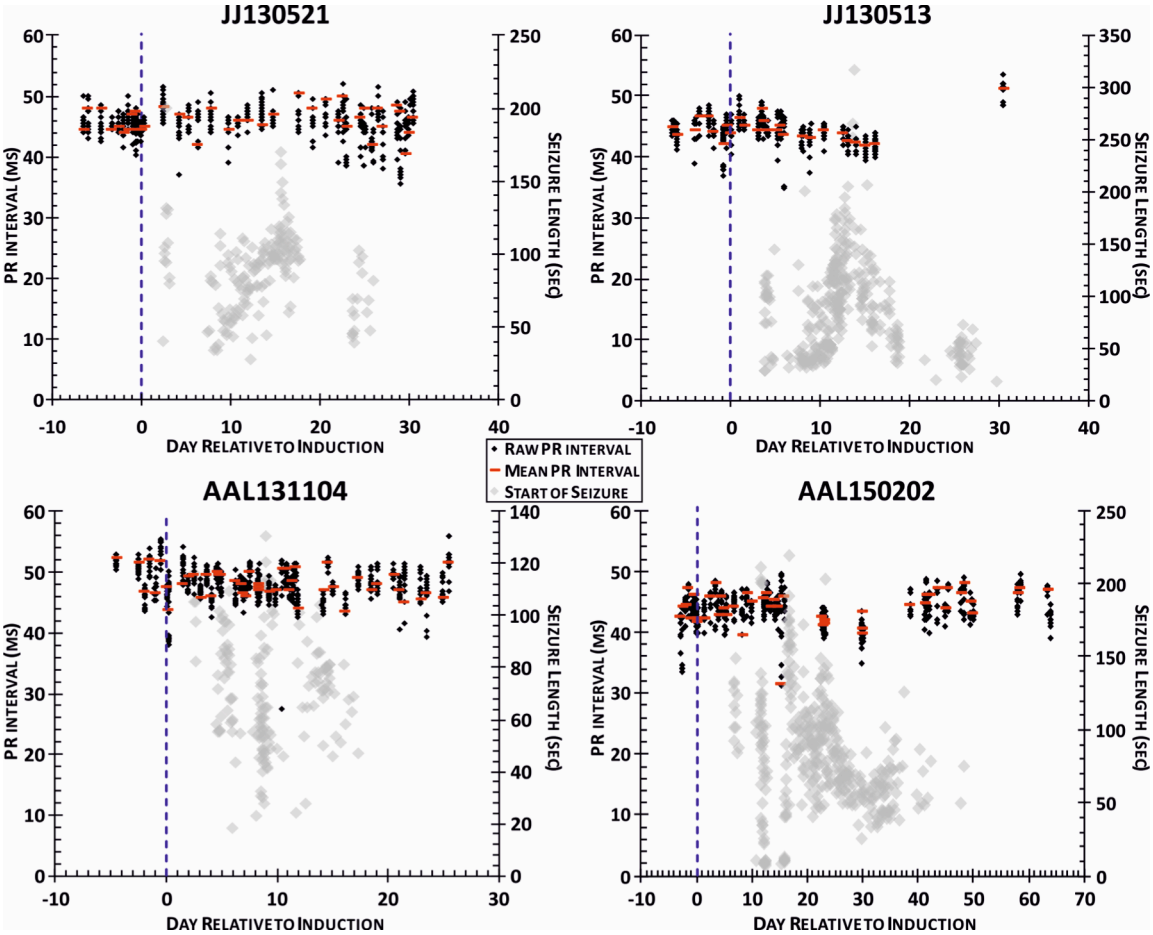

FIGURE 7 *The changes in PR interval over the course of the syndrome. Each data point (◆) denotes the PR interval of a 5-second epoch with the mean of all data points from that time point denoted by a red line (–). This data is superimposed upon the seizure profile for each animal (◆).*

QRS WIDTH

The QRS width was relatively stable across the course of the disease for each individual animal. An isolated trend can be seen in JJ130521, where the QRS width could be separated into two groups localised around 11 and 14 ms.

The combined QRS widths (see Figure 11B) statistically increased from Preinduction (12.6 ± 2.1 ms) to the 50th Seizure (14.2 ± 2.8 ms) and to the 150th Seizure (14.9 ± 2.1 ms). Furthermore, there was a significant decrease in QRS width between the 150th Seizure and Post Seizure State (13.2 ± 1.7 ms). The Post Seizure State was not significantly different from the Preinduction value (12.6 ± 2.1 ms vs. 13.2 ± 1.7 ms).

The Preinduction QRS width for each animal varied significantly from each other and therefore the data for each animal was normalised to its Preinduction value (see Figure 12B). There was a significant increase of 15.4 ± 13.1% in normalised QRS width from the Preinduction to the 150th Seizure. The normalised QRS width then significantly decreased from 150th Seizure to the Post Seizure State, 1.15 ± 0.13 vs. 1.03 ± 0.13 (normalised units).

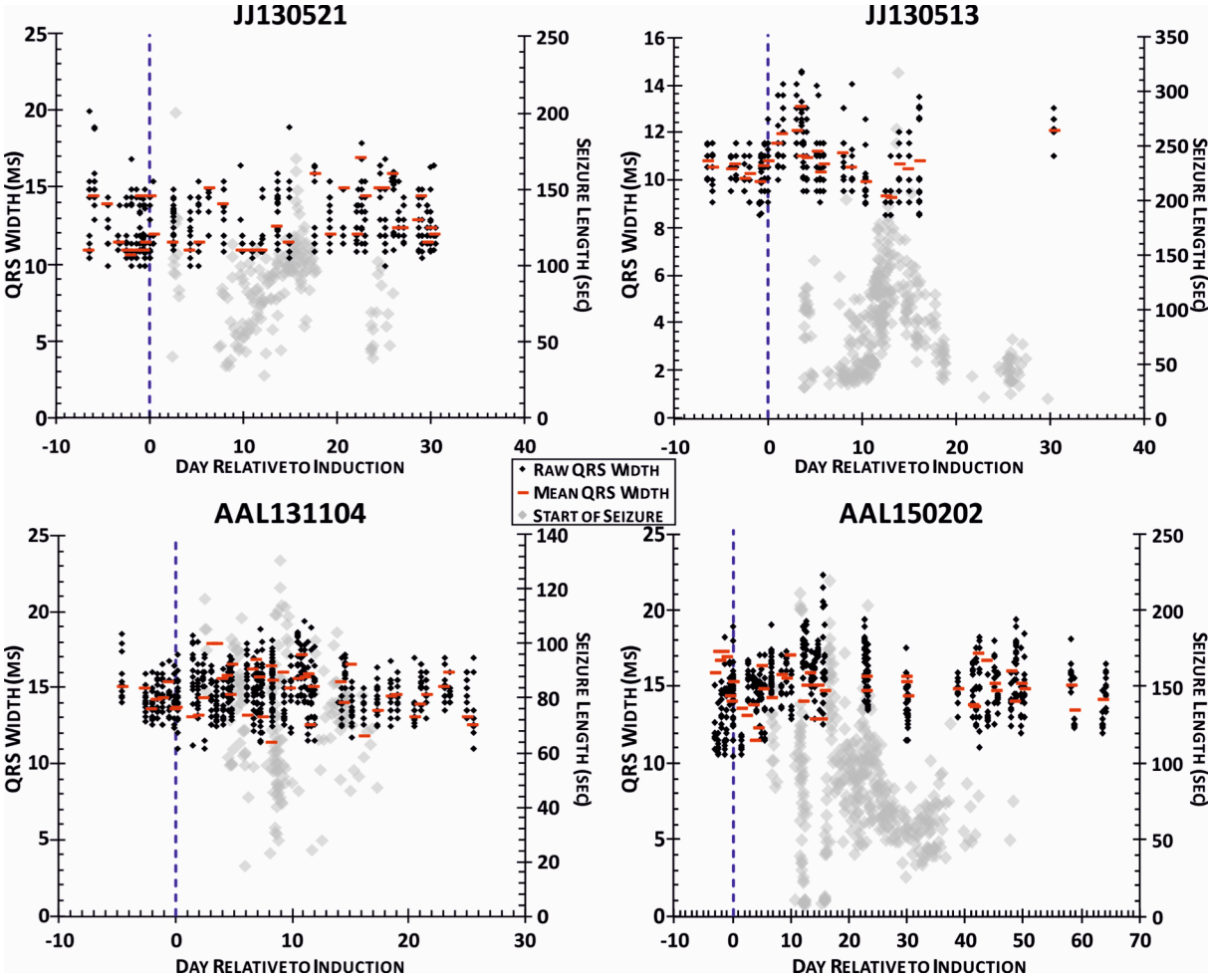

FIGURE 8 *The changes in QRS width over the course of the syndrome. Each data point (◆) denotes the QRS width of a 5-second epoch with the mean average of all data points from that time point denoted by a red line (–). This data is superimposed upon the seizure profile for each animal (◆).*

QT INTERVAL

The QT interval for each animal changed over the course of the disease (see Figure 9). The QT interval increased over the course of the disease for all four animals, however the increase in QT interval for JJ130513 and JJ130521 was larger than that of the other two animals (Table 2).

The QT interval for the population increased over the course of the disease (Figure 11C). The QT interval significantly increased from Preinduction (65.5 ± 6.7 ms) to the 1st Seizure (70.9 ± 4.4 ms). The QT interval significantly increased to the interictal period immediately before the 150th Seizure (82.7 ± 6.3 ms). Furthermore, the QT interval remained significantly elevated from the Preinduction length for the whole time course of the disease, with the QT interval during the Post Seizure State was 74.7 ± 10.4 ms. Interestingly, the QT interval significantly increased between Seizure 100 and Seizure 150 (77.0 ± 4.7 ms to 82.7 ± 6.3 ms). As can be seen from Figure 9, each animal experiences a large cluster of seizures, and in each case Seizure 150 occurs in the centre of this cluster, and this clustering of a large number of seizures could be the cause for this increase in QT interval. A full summary of the statistical significant comparisons between the different time points can be seen in Appendix A.

When normalised to the Preinduction QT interval, there is a significant 21.3 ± 3.4% increase between the Preinduction to the 150th Seizure. The increase in normalised QT interval after induction of epilepsy is maintained throughout the time course of the disease state and into the Post Seizure State, and further significant comparisons can be seen in Appendix A.

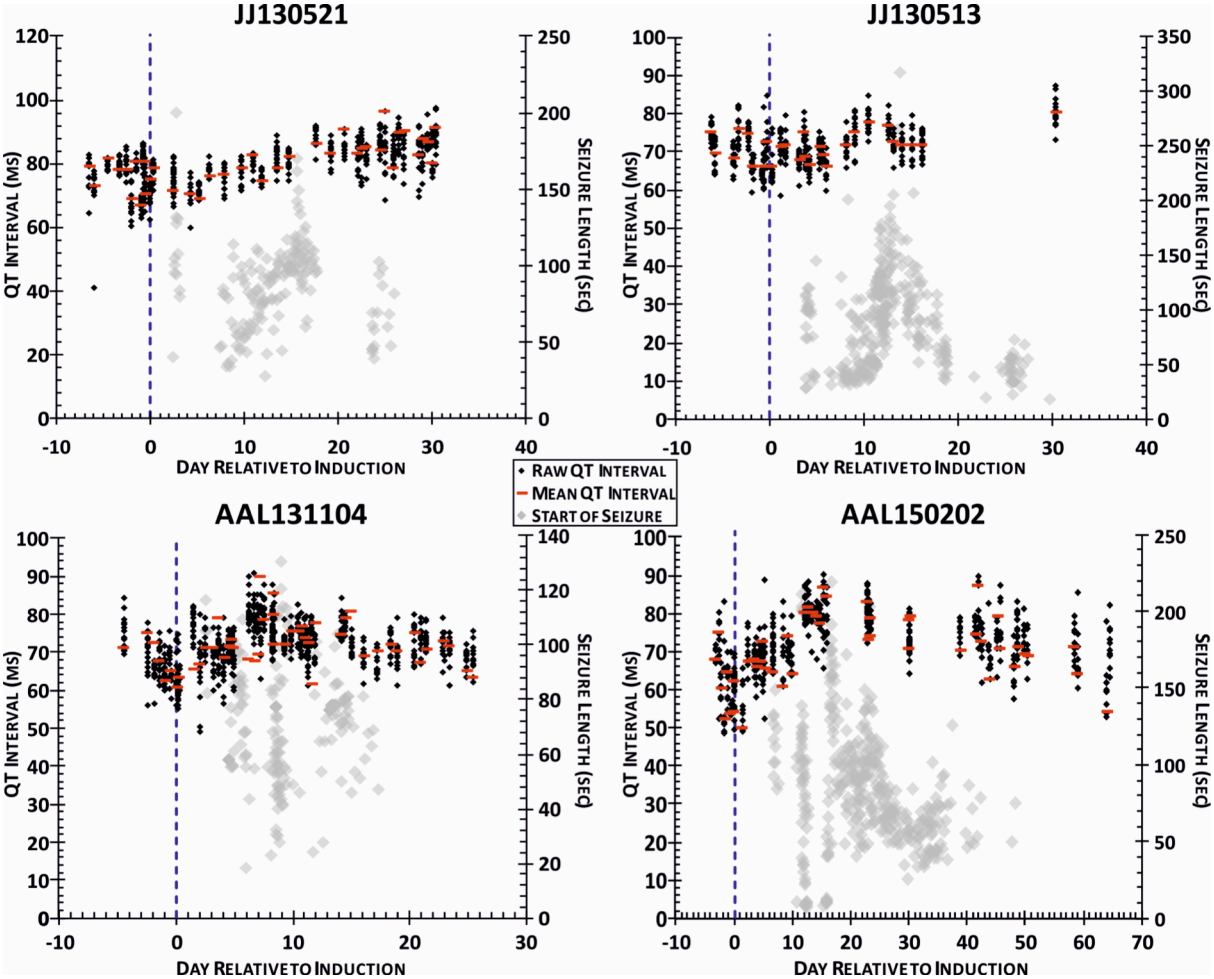

FIGURE 9 *The changes in QT interval over the course of the syndrome. Each data point (◆) denotes the QT interval of a 5-second epoch with the mean average of all data points from that time point denoted by a red line (–). This data is superimposed upon the seizure profile for each animal (◆).*

QTc INTERVAL

The QT interval was corrected to account for the variance of the RR interval using the Kmecova method[87]. AAL150202's QTc interval increases over the course of the disease increasing from 60.1 ms to a maximum of 82.4 ms 23 days post induction. The QTc interval increases from 65.6 ms preinduction to a maximum of 89.3 ms, 6 days post induction for animal AAL131104. Further, the QTc interval for JJ130513 increases from 72.8 ms to a maximum of 82.9 ms approximately 12.5 days post induction. Lastly, the

QTc interval increases to a maximum of 95.8 ms, 25 days post induction, from a preinduction length of 78.0 ms, for JJ130521.

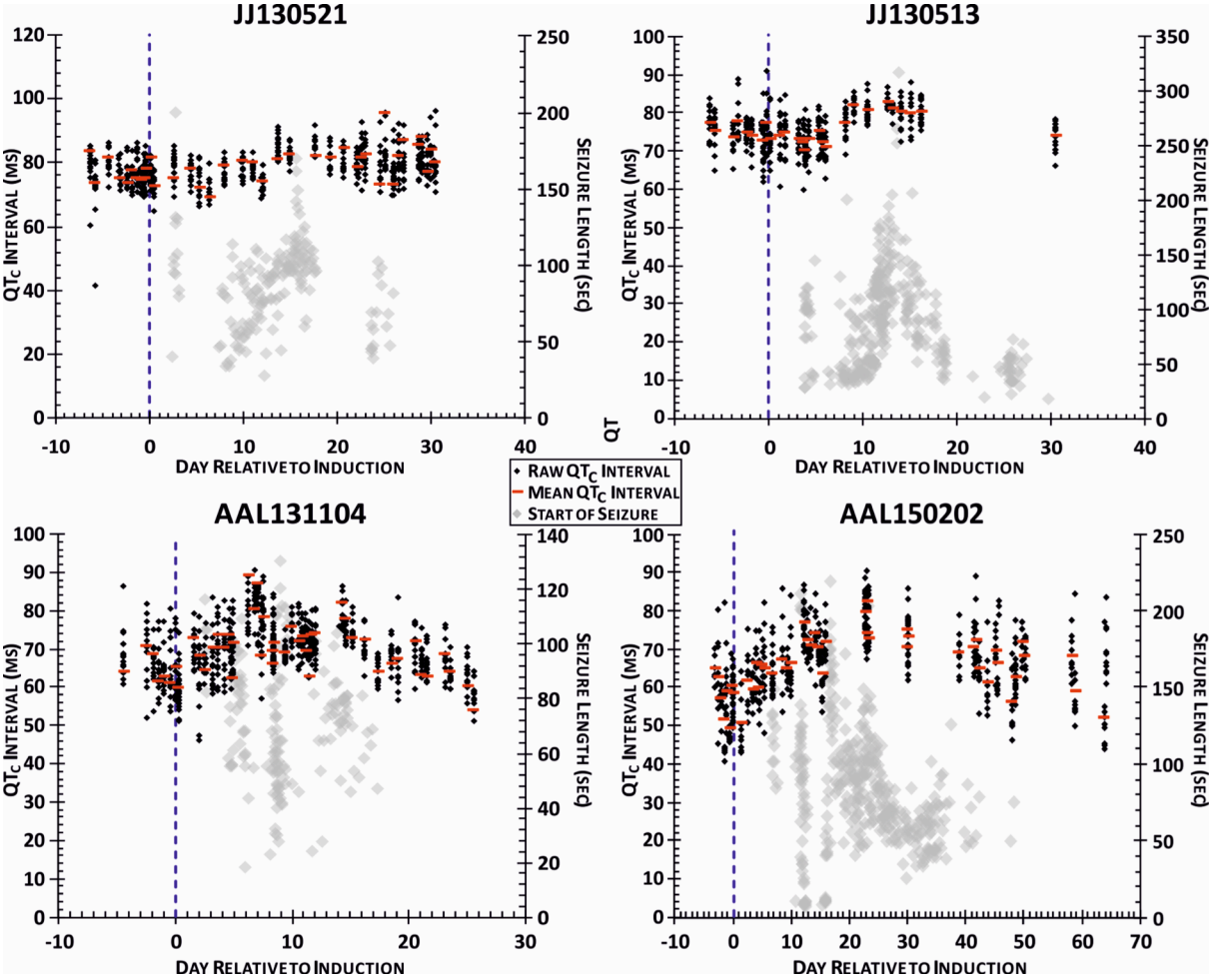

FIGURE 10 *The changes in QTC interval over the course of the syndrome. Each data point (◆) denotes the QTc interval of a 5-second epoch with the mean of all data points from that time point denoted by a red line (–). This data is superimposed upon the seizure profile for each animal (◆).*

When combined, the QTc interval significantly increases from 68.5 ± 9.4 ms Preinduction, to 80.2 ± 5.8 ms by the 150th Seizure (see Figure 11). This increase is maintained for the time course of the disease, however the Post Seizure State is not significantly different from Preinduction. When normalised (see Figure 12), the QTc interval significantly increases to 1.14 ± 0.05 and 1.17 ± 0.17 (normalised units) prior to

the 150th and 250th Seizures respectively. The Post Seizure State is not significantly different from the Preinduction QTc interval. The full extent of the comparisons between the different time points can be seen in Appendix A.

FIGURE 11 ***(NEXT PAGE)*** *The changes in PR interval (**A**), QRS width (**B**), QT interval (**C**), and QTc interval (**D**) over the time course of the syndrome, categorised by seizure number. Each data point (◆) denotes the mean ± SD for each time point and is superimposed upon all data for each animal (◆). Significance (α = 0.05) was determined using a One-Way ANOVA and is denoted by (*), however for clarity not all of the statistical differences have been identified. This information can be found in Appendix A.*

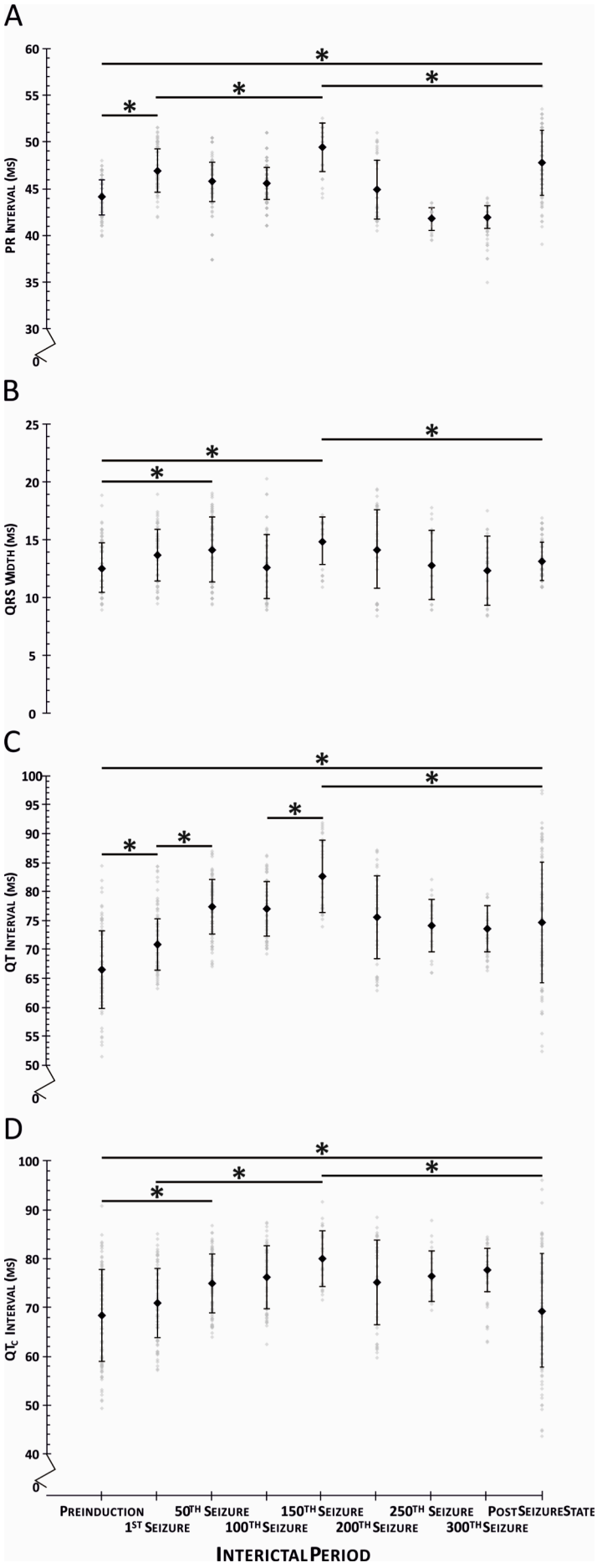
A
PR Interval (ms)
B
QRS Width (ms)
C
QT Interval (ms)
D
QTc Interval (ms)
Preinduction
1st Seizure
50th Seizure
100th Seizure
150th Seizure
200th Seizure
250th Seizure
300th Seizure
Post Seizure State
Interictal Period

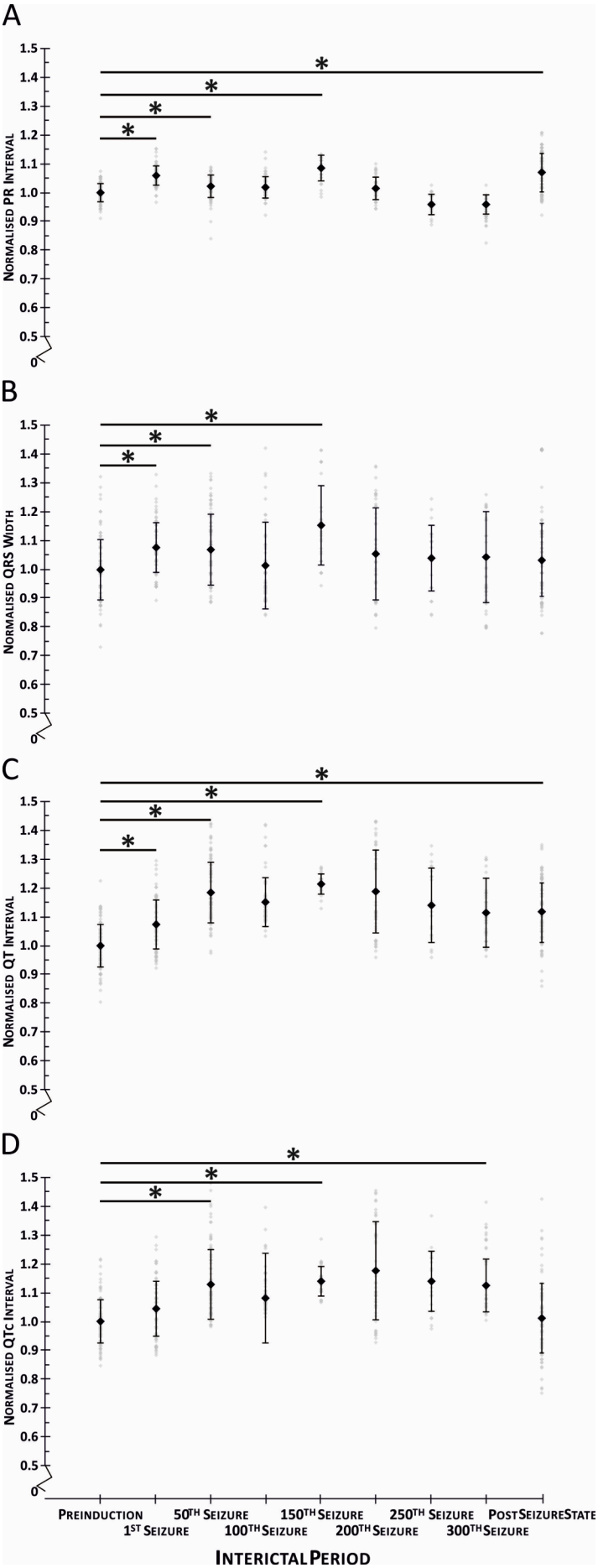
A
B
C
D
Normalised PR Interval
Normalised QRS Width
Normalised QT Interval
Normalised QTc Interval
1.5
1.4
1.3
1.2
1.1
1.0
0.9
0.8
0.7
0.6
0.5
0
*
Preinduction
1st Seizure
50th Seizure
100th Seizure
150th Seizure
200th Seizure
250th Seizure
300th Seizure
Post Seizure State
Interictal Period

FIGURE 12 (PREVIOUS PAGE) *The changes in Normalised PR interval (A), QRS width (B), QT interval (C), and QTc interval (D) over the time course of the syndrome, categorised by seizure number. Each data point (u) denotes the mean ± SD for each time point and is superimposed upon all data for each animal (u). Significance (α = 0.05) was determined using a One-Way ANOVA and is denoted by (*), however for clarity not all of the statistical differences have been identified. This information can be found in Appendix A.*

INTERICTAL RR INTERVAL AND HEART RATE

The interictal RR interval, and therefore heart rate, changed over the time course of the disease (Figure 13A). The RR interval statistically increased from Preinduction to the interictal period immediately before the 150th Seizure (142.9 ± 25.7 ms to 159.6 ± 11.1 ms). The RR interval is statistically increased ($P<0.01$) in the Post Seizure State from Preinduction (142.9 ± 25.7 ms to 177.2 ± 24.2 ms). This equates to the interictal heart rate decreasing from 420 bpm, to 376 bpm and then 339 bpm. Normalising the RR interval (Figure 13B) resulted in a statistically significant increase ($P<0.01$) from Preinduction, to the 50th, 100th, 150th Seizures and Post Seizure State. There was a 16.4 ± 9.0% increase in normalised RR interval by the 150th Seizure and 26.1 ± 18.7% during the Post Seizure State. Over the course of the disease (Figure 13C), the heart rate decreased from 425 ± 63 bpm at Preinduction, to 378 ± 29 bpm immediately before the 150th Seizure. The heart rate further decreased to 345 ± 51 bpm during the Post Seizure State.

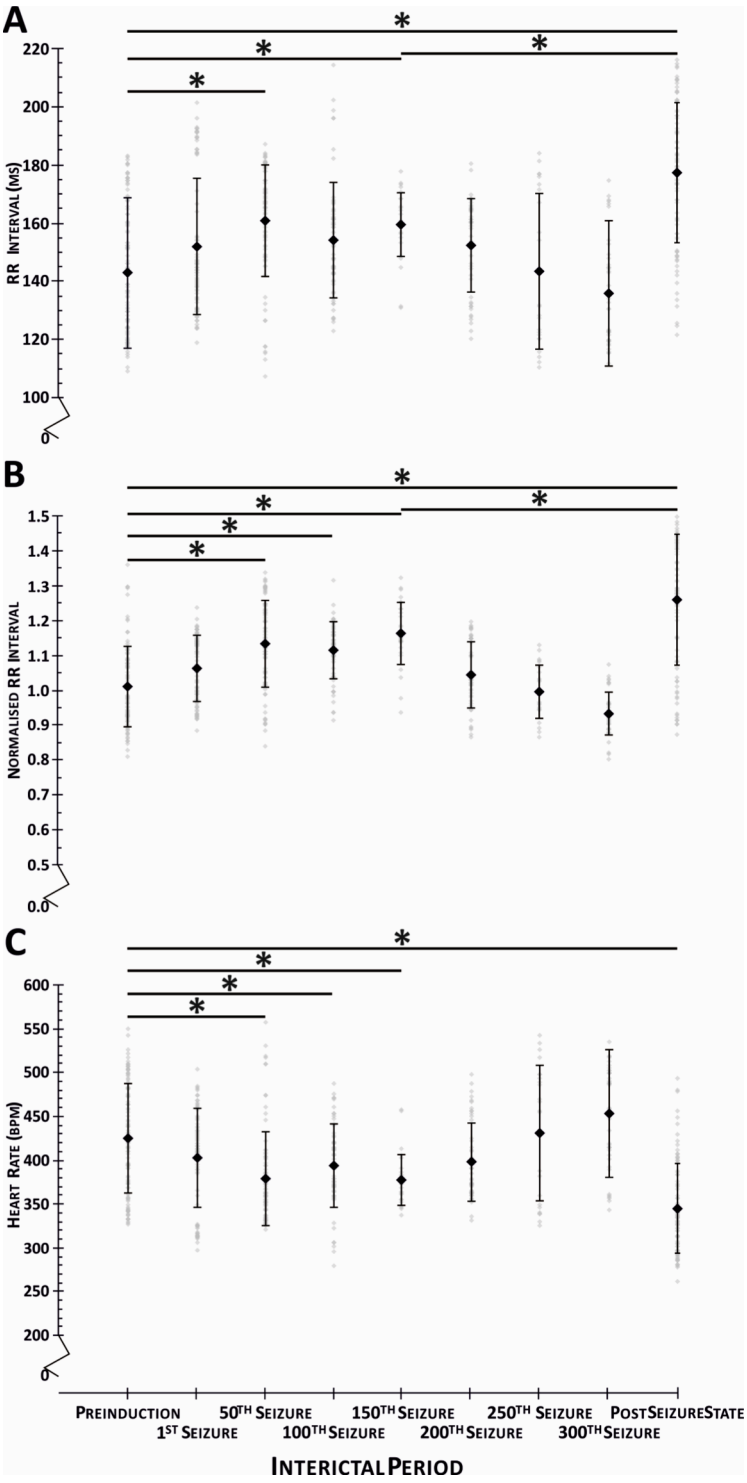

FIGURE 13 *The changes in RR Interval (**A**), Normalised RR Interval (**B**) and Heart Rate (**C**) over the course of the syndrome. The mean RR interval (denoted by ◆) is shown with the standard deviation and all date points (denoted by ◆). There was a significant (denoted by *) increase in RR interval, Normalised RR interval and decrease in Heart Rate between the Preinduction time point and the 150th Seizure. This change in RR interval, Normalised RR interval, and Heart Rate persisted into the Post Seizure State; however these values are within normal reported values for male Wistar Rats.*

INTERICTAL HEART RATE VARIABILITY

RMSSD

The RMSSD, the root mean square of successive differences between RR intervals, a measure of vagus-mediated heart rate variability and autonomic regulation of the heart[31], was calculated using the MatLab script in Appendix C. The change in RMSSD for each animal over the course of the disease is shown in Figure 14.

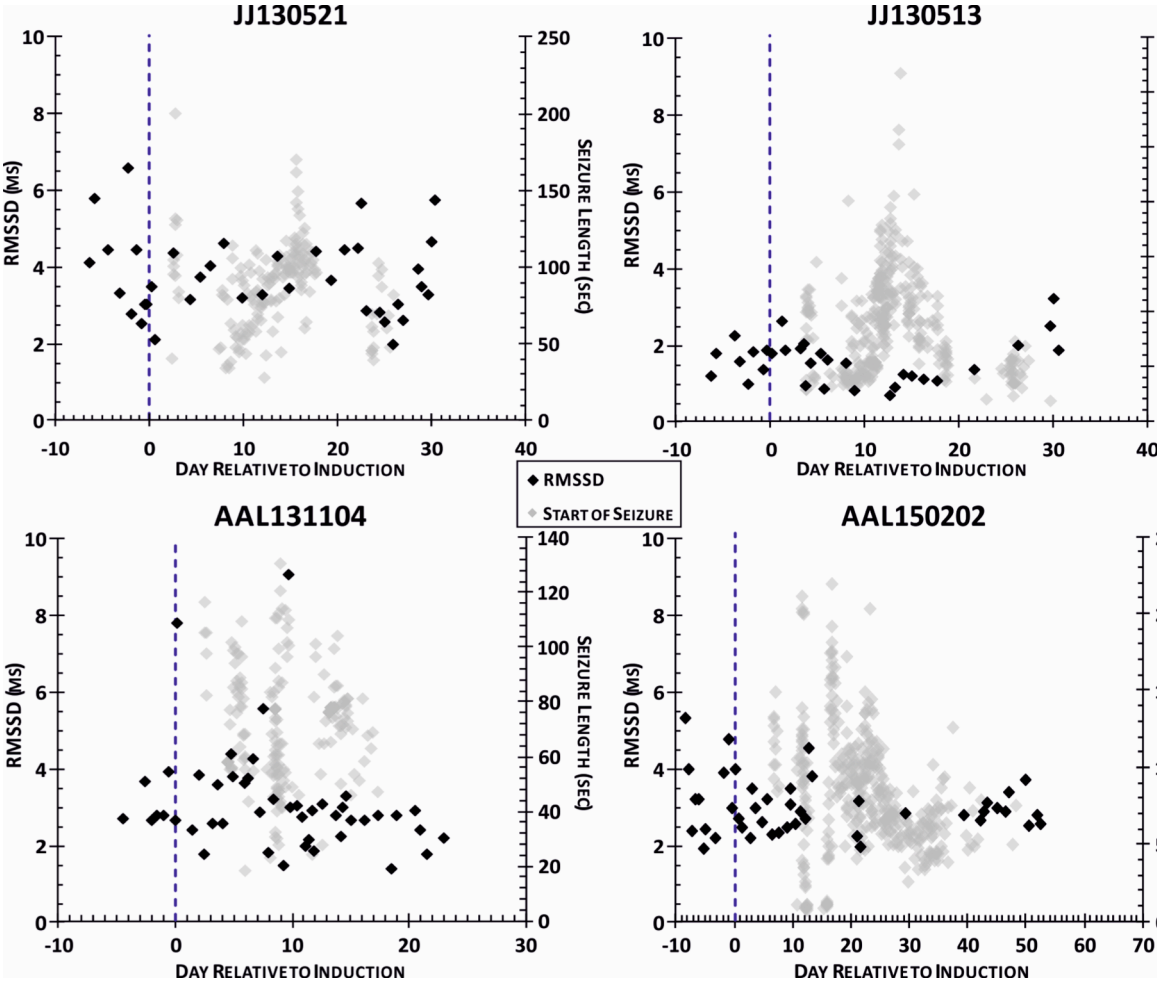

FIGURE 14 *The changes in RMSSD over the course of the syndrome. Each data point (◆) denotes the RMSSD calculated for a 10-minute interictal period. This data is superimposed upon the seizure profile for each animal (◆). There was a slight negative trend in RMSSD over the course of the disease for AAL131104 and AAL150202, whereas there is an upward trend at the end of the disease for JJ130513. The RMSSD varies across the time course of the disease for JJ130521, but there is a no trend.*

TABLE 3

	JJ130513	JJ130521	AAL131104	AAL150202
RMSSD				
ALL DATA (MS)	1.55 ± 0.56	3.74 ± 1.07	3.14 ± 1.57	2.95 ± 0.73
RANGE (MS)	0.67 to 3.17	1.98 to 6.60	1.35 to 9.03	1.91 to 5.32
PREINDUCTION (MS)	1.7	2.1	7.8	2.4
POST SEIZURE STATE (MS)	0.9	4.4	1.7	2.2
SDNN				
ALL DATA (MS)	5.63 ± 2.05	9.63 ± 3.39	8.67 ± 2.97	9.98 ± 3.29
RANGE (MS)	2.31 to 10.23	3.97 to 17.89	3.54 to 16.06	3.46 to 18.99
PREINDUCTION (MS)	6.0	7.26	8.66	12.71
POST SEIZURE STATE (MS)	2.3	12.65	3.73	8.81
SDSD				
ALL DATA (MS)	2.56 ± 0.56	3.77 ± 1.08	3.39 ± 2.27	2.96 ± 0.73
RANGE (MS)	0.67 ± 3.22	1.98 to 6.62	1.36 to 14.85	1.91 to 5.34
PREINDUCTION (MS)	1.75	2.13	2.65	2.42
POST SEIZURE STATE (MS)	1.86	5.81	8.31	2.67
SD RATIO				
ALL DATA (MS)	0.22 ± 0.09	0.15 ± 0.05	0.21 ± 0.13	0.17 ± 0.07
RANGE (MS)	0.11 to 0.54	0.07 ± 0.25	0.09 to 0.76	0.07 to 0.40
PREINDUCTION (MS)	0.15	0.15	0.15	0.10
POST SEIZURE STATE (MS)	0.11	0.20	0.49	0.14

A summary of the mean, ranges, preinduction and post seizure state values for the RMSSD, SDNN, SDSD and SD Ratio for JJ130513, JJ130521, AAL131104, and AAL150202. Where possible data is reported as mean ± standard deviation. "All Data" is the mean of all data points collected for each animal over the course of the disease, with the range showing the minimum and maximum value of all data points. The Preinduction and Post Seizure State values are immediately before the animal was injected with TeNT and immediately before the end of the experiment respectively.

Combined data from all rats (Figure 18A) shows that there was no significant difference across the course of the disease. The large variability and small number of data points have contributed to the lack of significance. This lack of significance between

the different time points is maintained when the data is normalised to Preinduction. A summary of this data is shown in Table 4.

SDNN

SDNN, the standard deviation of all RR intervals, indicates the total variability and provides a general measurement the autonomic nervous system's balance[89,95]. Over the course of the disease, the SDNN was not consistent between the four animals (Figure 15)**.** The SDNN decreased over the course of the disease in JJ130513, AAL131104, and AAL150202 and increased in JJ130521 (Table 3). The SDNN for J130521, JJ130513, AAL131104, and AAL150202 decreased during their peak seizure periods (Figure 6), to 3.96 ms 2.94 ms, 3.54 ms, and 4.12 ms respectively.

TABLE 4

	NORMALISED DATA TO PREINDUCTION (MEAN ± SD)			
	RMSSD	**SDNN**	**SDSD**	**SD RATIO**
PREINDUCTION	1	1	1	1
1ST SEIZURE	1.04 ± 0.69	0.81 ± 0.63	1.04 ± 0.71	1.4 ± 0.15
50TH SEIZURE	0.83 ± 0.32	0.76 ± 0.21	0.83 ± 0.32	1.2 ± 0.73
100TH SEIZURE	1.09 ± 0.58	0.83 ± 0.22	1.09 ± 0.58	1.3 ± 0.57
150TH SEIZURE	0.87 ± 0.18	0.83 ± 0.60	1.54 ± 0.77	2.1 ± 0.64
200TH SEIZURE	0.82 ± 0.30	0.69 ± 0.28	0.82 ± 0.29	1.2 ± 0.50
250TH SEIZURE	0.74 ± 0.10	0.54 ± 0.13	0.72 ± 0.13	1.4 ± 0.58
300TH SEIZURE	0.97 ± 0.29	0.98 ± 0.33	0.97 ± 0.30	1.1 ± 0.69
POST SEIZURE STATE	2.00 ± 1.08	1.32 ± 0.55	2.01 ± 1.08	1.7 ± 1.05

The normalised RMSSD, SDNN, SDSD and SD Ratio. This data removes the variability in the preinduction values, and shows any significant differences (*) between the different Time Points and the Preinduction state (α = 0.05; One-way ANOVA).

When combined (Figure 18B), the large variability between the different animals' SDNN has resulted in a lack of significant changes. When normalised (see Table 4), the changes in SDNN were not significant.

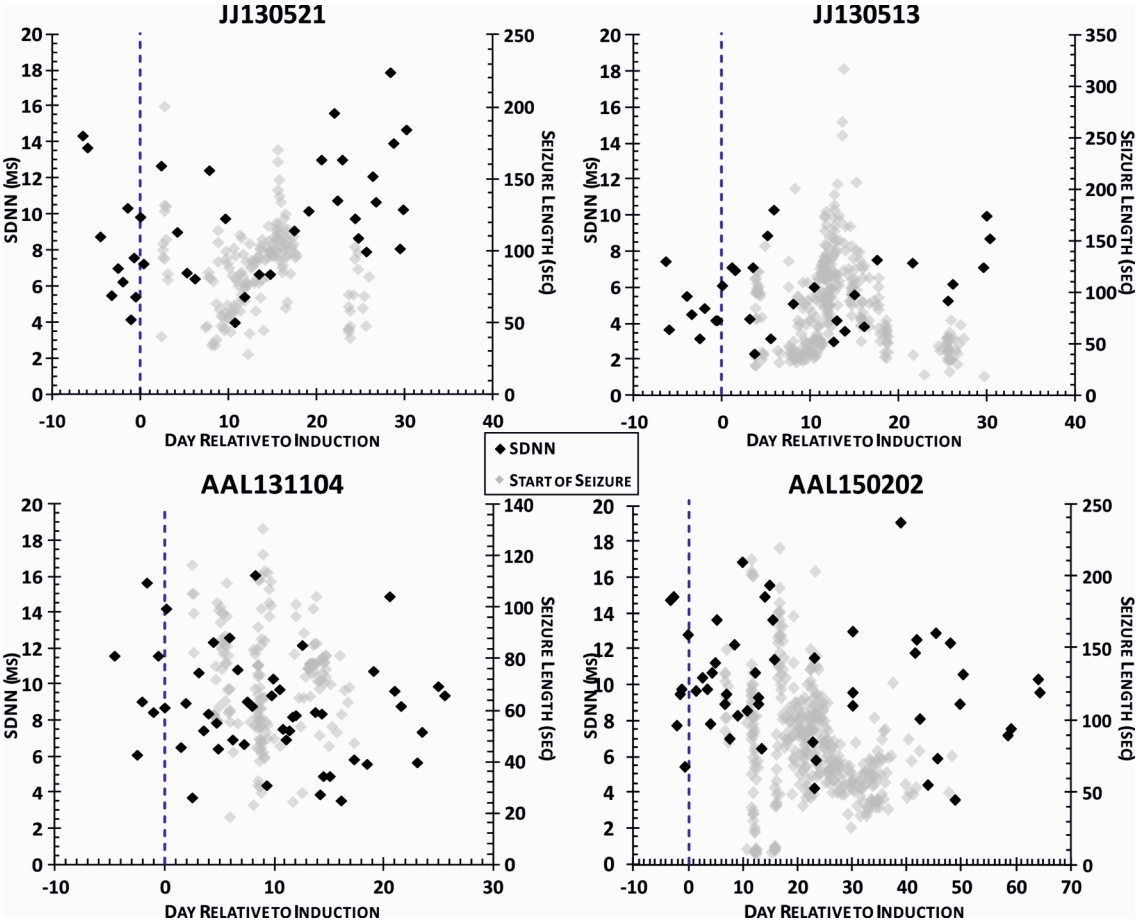

FIGURE 15 *The changes in SDNN over the course of the syndrome. Each data point (◆) denotes the SDNN of a 5-second epoch. This data is superimposed upon the seizure profile for each animal (◆). There is a slight negative trend in SDNN over the course of the disease for AAL131104 and AAL150202, and a slight positive trend for JJ130513 and JJ130521.*

SDSD

The observed change in SDSD over the time course of the disease varies slightly between animals (Figure 16). The SDSD is the standard deviation of successive differences between adjacent RR intervals and represents short-term variation in HRV. A

negative trend was observed in AAl131104, AAL150202 and JJ130513, and no discernable change in JJ130521 (Figure 16, Table 3). The SDSD for JJ130513 increased slightly towards the end of the disease and experiment.

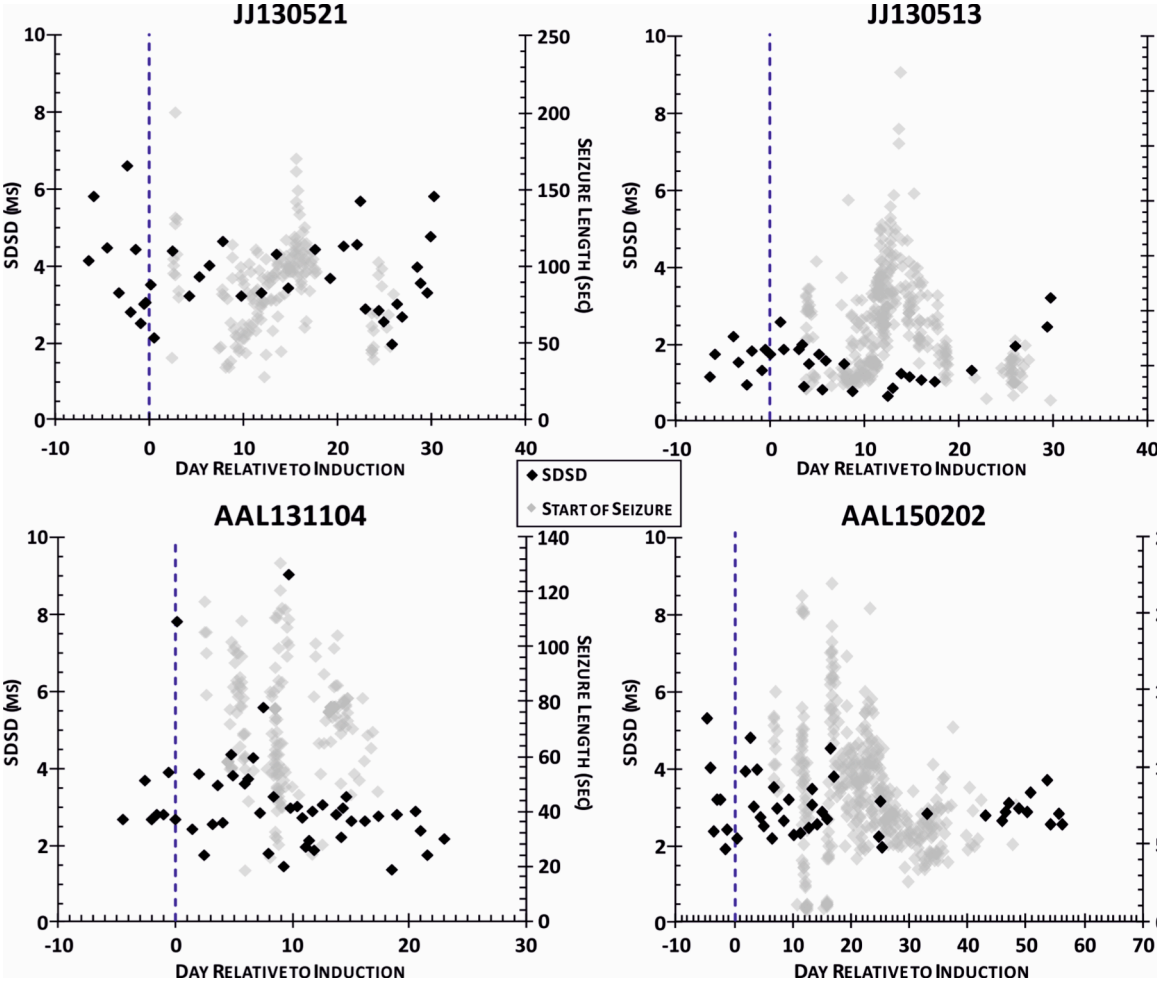

FIGURE 16 *The changes in SDSD over the course of the syndrome. Each data point (◆) denotes the SDSD of a 5-second epoch. This data is superimposed upon the seizure profile for each animal (◆). The SDSD for JJ130521 remains constant over the course of the disease, whereas a negative trend can be observed in JJ130513, AAL131104 and AAL150202. Further, the SDSD for JJ130513 increased towards the end of the experiment.*

When combined (Figure 18C), the SDSD did not change over the course of the disease. When normalised (Table 4), there was no significant difference over the course of the disease.

SD Ratio

The SD Ratio is calculated by dividing the SD1 by the SD2 value, with a decreasing ratio indicating a higher sympathetic tone. A decrease in SD Ratio was observed in JJ130521 and JJ130513 over the course of the disease (Figure 17, Table 3). JJ130513 decreased from a Preinduction ratio of 0.15 to 0.11 during the Post Seizure State, and JJ130521 decreased from 0.15 to 0.11, 28 days post induction. The SD Ratio for both AAL150202 and AAL131104 remain relatively stable throughout the experiment. When combined, the SD Ratio increased from 0.14 ± 0.04 to 0.33 ± 0.11 (Figure 18D) during the interictal period immediately before the 150th Seizure and then decreased to 0.15 ± 0.05 during the Post Seizure State (Figure 18D). None of these differences are significant. This pattern is maintained when the data is normalised (Table 4), where the normalised SD Ratio increased to 2.1 ± 0.64 during the 150th Seizure and then decreased to 0.9 ± 0.68.

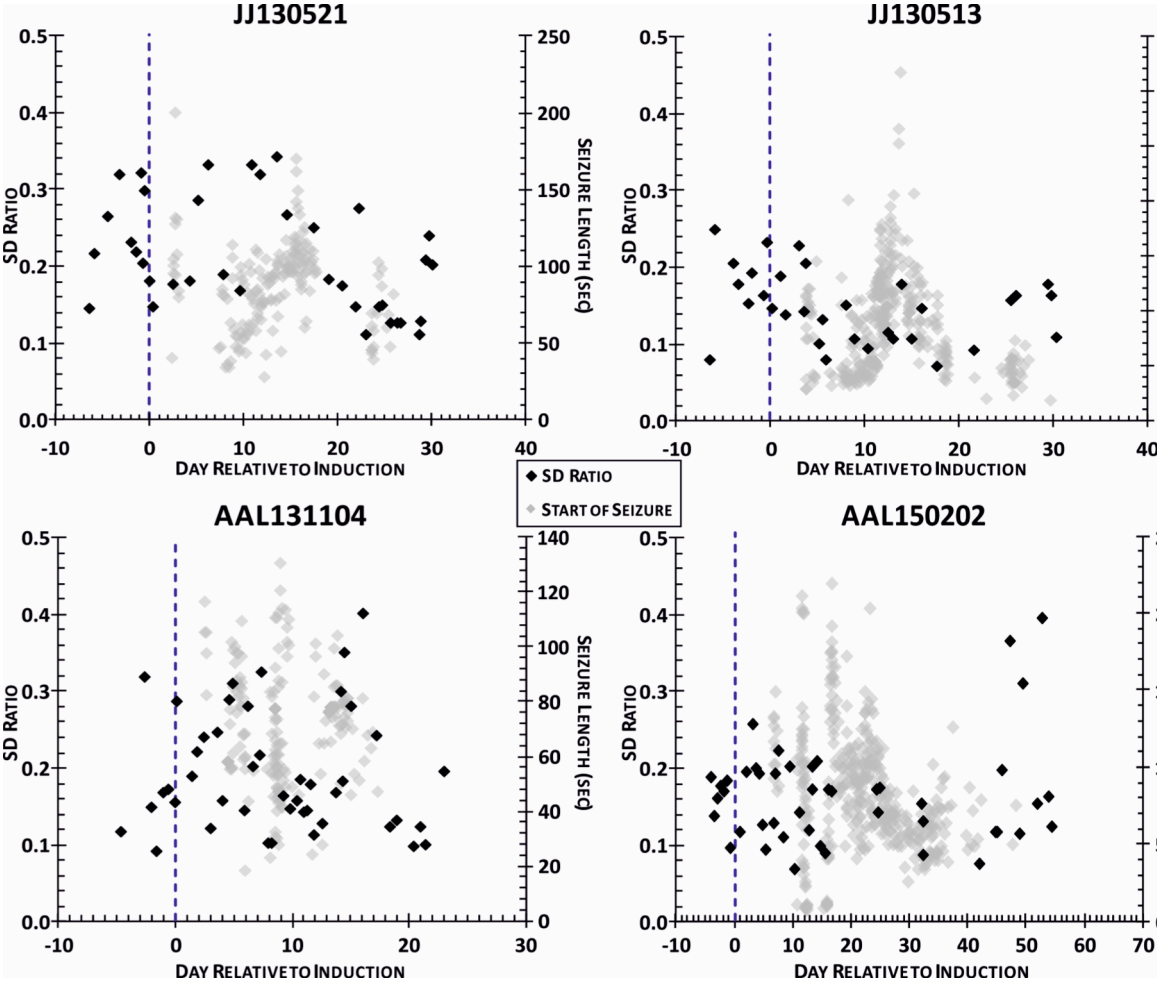

FIGURE 17 *The changes in SD Ratio over the course of the syndrome. Each data point (◆) denotes the SD Ratio of a 5-second epoch. This data is superimposed upon the seizure profile for each animal (◆).*

FIGURE 18 (NEXT PAGE) *The changes in RMSSD (**A**), SDNN (**B**), SDSD (**C**), and SD Ratio (**D**) over the time course of the syndrome categorised by seizure number. Each data point (◆) denotes the mean ± SD for each time point and is superimposed upon all data for each animal (◆). Significance is denoted by (*).*

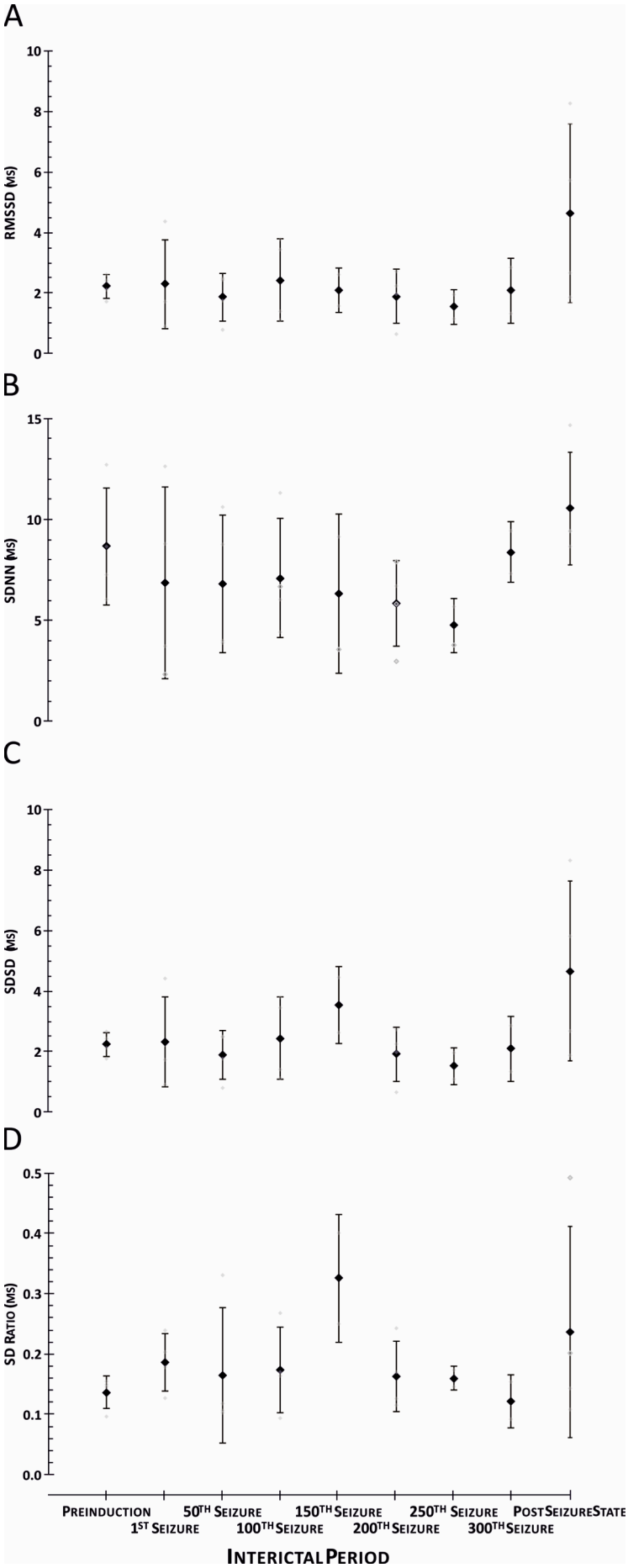
A
RMSSD (ms)
10
8
6
4
2
0
B
SDNN (ms)
15
10
5
0
C
SDSD (ms)
10
8
6
4
2
0
D
SD Ratio (ms)
0.5
0.4
0.3
0.2
0.1
0.0
Preinduction
1st Seizure
50th Seizure
100th Seizure
150th Seizure
200th Seizure
250th Seizure
300th Seizure
Post Seizure State
Interictal Period

DISCUSSION

This study provides new evidence on the effect of epileptic seizures, induced by the tetanus neurotoxin model of temporal lobe epilepsy, on the heart's conductivity. Intrahippocampal injections of TeNT successfully induced seizures in all five animals injected; however, one animal had to be excluded due to a significantly decreased number and frequency of seizures compared to the other animals. After induction, the rats experienced spontaneous seizures, and as ECoG and ECG data was recorded via radiotelemetry continuously, it was possible to assess the long-term effects of epileptic seizures on the conductivity of the heart and its central control. To the author's knowledge, this is the first study to use the tetanus neurotoxin model of epilepsy in freely moving rats implanted with radiotelemeters to assess changes in cardiovascular conductivity in epilepsy.

ECG WAVEFORM CHANGES AND SUDEP

The major finding of this study is the progressive changes in the ECG waveform over the course of the disease, indicating a progressive change in the conductivity of the heart. Firstly, the PR interval increased over the course of the disease, and remained elevated during the Post-Seizure State (Figure 11A). The maximum increase in PR interval observed in this study was 5.4 ms, between the Preinduction and 150th Seizure; a 12% increase. The PR interval is the time taken for the electrical signal to propagate from the sinoatrial (SA) node, through the right atrium, and into the left atrium via Bachmann's bundle, via the atrioventricular (AV) node and into the Bundle of His. The AV node acts to delay electrical conduction, preventing the atria and ventricles from contracting simultaneously. An increase in the PR interval, and therefore delayed conductivity from

the atria to the ventricles, indicates first-degree heart block. First degree heart block is commonly the result of AV node conductivity dysfunction as opposed to dysfunction in the atrium or His-Purkinje system; although more than one source of conductivity delay is often encountered[143]. First-degree heart block has traditionally been thought of as benign, acting as a precursor for more severe degrees of conduction block[143]. However, a prolonged PR interval could be indicative of other changes in the cardiovascular system, including both autonomic and structural cardiac abnormalities[143].

The AV node is sensitive to changes in autonomic tone, and vagal stimulation can slow AV conduction, prolonging the PR interval[144]. Parasympathetic activation decreases the slope the initial phase (Phase 0) the nodal action potential, leading to slower depolarisation, and reduction conduction velocity through the AV node[145]. Indeed, excessive vagal activation can cause AV block[144]. The increase in PR interval in this study could be a result of an increase in parasympathetic drive, however this would need to be verified with robust heart rate variability results.

Alternatively, a prolonged PR interval could be the result of hypokalaemia. A decline in serum potassium levels results in a decrease in the transmembrane gradient, a subsequent increase in the resting membrane potential, and a prolongation of the action potential[146]. This can ultimately result in prolongation of the PR interval. This electrolyte imbalance is also associated with other changes in the ECG waveform, such as a decrease in the T-wave amplitude, ST segment depression, and T wave inversion[146]. The measurements of these changes in the ECG waveform were outside the scope of this study as there was not a discernable transition point between the T-wave and the S-wave (Figure 5C). ST segment changes have been observed in a number of other studies[55–57]. Presence or absence of these markers could help elucidate whether or not an imbalance

in serum potassium levels caused the prolonged PR interval seen in this study. Therefore, a more advanced method of waveform analysis than that used in this study would need to be performed to be able to analyse the ST segment.

The observed increase in PR interval is not independent of the RR interval. The RR interval also progressively increases over the course of the disease, and as such, the PR to RR ratio remains constant at 0.3 throughout. This indicates that the increase in PR interval observed may be a result of the increase in RR interval, and not a pathological change in the AV node, atrium, His-Purkinje system, or hypokalaemia. Further experiments using isolated hearts will be outlined below (see Further Experimental Work) to explore the cause of the increase in PR interval.

The QRS width is a measure of the time taken for the electrical signal propagated from the AV node to travel through the Purkinje fibres and then the ventricular myocardium. As with the PR interval, an increase in the QRS width, as seen in this study (Figure 11B), is indicative of a slowing of the conduction through the heart. The maximum increase in QRS width observed, 2.3 ms (or an 18 % increase from Preinduction) during the interictal period immediately before the 150th Seizure (Figure 11), is modest, and whilst statistically significant, may not be physiologically significant. This result echoes Damasceno and colleagues[49], who reported an increase QRS width in rats with audiogenic seizures compared with naïve controls. An increase in QRS width can be the result of a number of processes involving both the conduction system and the myocardium, individually or in concert[144]. For example, QRS prolongation may indicate the presence of hypertrophic diseases such as left ventricular hypertrophy (LVH)[147]. LVH is a physiological adaptation to increased workload in healthy individuals involved in physical training, however it is often a pathophysiological condition caused by an extrinsic

stimulus such as hypertension[147]. Hypertension can cause LVH by increasing the left ventricular wall stress and subsequently stimulating myocyte hypertrophy, collagen formation and ultimately myocardial remodelling with a disproportionate percentage of fibrous, non-myocyte, tissue[147]. The development of LVH also has a number of non-haemodynamic influences, including α1 adrenergic agonist activity by noradrenaline, with studies suggesting that an increased cardiac sympathetic neurotransmission has a role in left ventricular mass in hypertension[147,148]. Therefore, the increase in QRS width seen in this study could be indicative of a structural change in the left ventricle, caused by hypertension or another non-haemodynamic cause.

The presence of LVH is a risk factor for cardiac mortality, and indeed the risk of sudden cardiac death in the normal population is increased in those with LVH. Therefore, even the modest 18% increase in QRS width observed would need to be investigated further due to its link with sudden death (see Further Experimental Work). However, the QRS width is at its maximum during the interictal period immediately before the 150th Seizure, and then declines back to the Preinduction width during the Post-Seizure State (Figure 11). It can therefore be concluded that the likely cause of the increase in QRS width is not through left ventricular hypertrophy, but through changes in conduction through the Purkinje fibres and the ventricular myocardium. For example, bundle branch block could be the result of ischaemia[149] or a rate dependent aberrancy[150,151], which could be explain the return to baseline observed in this study, Further experiments will need to be performed in order to isolate the true cause of the widened QRS width observed in this study.

The corrected and uncorrected QT interval (QTc and QT interval, respectively) both increase over the course of the disease (Figure 11C and D), with the QT interval

remaining elevated during the Post-Seizure State. The QT interval increases from 66.5 ± 6.7 ms to 82.7 ± 6.3 ms during the 150th Seizure, a 25% increase; and remains 12% higher during Post Seizure state. The QTc interval increases from Preinduction to 150th Seizure, by 17% (68.5 ± 9.4 ms to 80.2 ± 5.8 ms), however decreases back to 69.4 ± 11.7 ms during the Post Seizure State. The correction applied to the QT interval to generate the QTc interval removes the RR interval's influence on the QT interval and therefore the QTc is the more accurate measurement. Both QT interval measurements represent the time taken for the ventricular depolarisation and repolarisation to occur. The prolongation of the QT interval (as observed in Long QT Syndrome) is used primarily as a biomarker for the potential formation of torsades de pointes, ventricular tachycardia, and sudden death[32]. Increases in QTc values were observed during epileptiform discharges by Tavernor and colleagues[85] in a group of patients whose deaths were classified as SUDEP. Further, numerous studies have observed increases in QT and QTc intervals, including Opherk et al.[55], Moseley and colleagues[84], and Damasceno et al.[49].

A prolonged QT interval is the result of augmented depolarisation or delayed repolarisation of myocardial cells[32,49] and has long been associated with a number of cardiac ion channels that can cause Long QT Syndrome. A prolonged QT interval can result from an increase in the sodium current through gain of function of channels responsible for initial phase of the cardiac action potential (SCN1A and SCN5A), or through delaying the repolarisation phase by reducing the potassium current through loss of function of the I_{Kr} (HERG, LQT2, LQT6), I_{Ks} (LQT1, LQT5) and I_{K1} (LQT7) currents[32,152]. Indeed, Hindocha et al.[153] reported two cases of SUDEP in individuals, who although they were not genotyped themselves, had family members who possessed a SCN1A mutation. Furthermore, Tu and colleagues[154] discovered mutations of SCN5A and LQT2 (KCNH2) in six of 68 SUDEP cases.

The TeNT model of TLE is not a genetic model, and therefore mutations in these channels are not the cause of the prolonged QT interval observed in this study. However, changes in the level of expression of the genes previously associated with Long QT Syndrome could be induced by numerous mechanisms. For example, it has been shown that the sympathetic nervous system regulates the expression of various ion channels through noradrenaline and neuropeptide-Y[155,156]. The exact specificity of this control is unknown; whether or not there is simply a chronic and unregulated sympathetic influence on ion channels or a more targeted feedback mechanism that results in homeostatic plasticity. Furthermore, other signaling molecules have been identified that exert changes in ion channel expression, including angiotensin-II, endothelin-I, glucocorticoids and thyroid hormones[157]. It is therefore possible that the prolonged QT interval observed in this study is the result of a change in cardiac ion channel expression secondary to another mechanism. To identify if the prolongation of the QT interval observed in this study is a product of altered cardiac ion channel expression, further experiments into the ion channels associated with Long QT Syndrome can be easily performed (see Further Experimental Work).

Further to the above ion channel expression changes associated with Long QT Syndrome, it has been suggested that an imbalance in the sympathetic nervous system can cause a prolonged QT interval[49]. The removal of the right stellate ganglion impairs cardiac stability, and has been shown to increase the QT interval in dogs[158], cats[159], and humans[160]. The stellate ganglion is located in the sympathetic chain around C7 to T1 of the spinal cord, is formed from the fusion of the inferior cervical ganglion (C7 and C8) and the first thoracic ganglion, and its postganglionic afferents innervate the heart, along with the lungs and bronchi[161]. Indeed, left stellectomy reduces QT interval[162] and has been used as a treatment for those with refractory Long QT Syndrome[160,163–165]. The heart

receives autonomic innervation from both sympathetic and parasympathetic fibres, with the ventricles solely innervated by sympathetic neurons[163]. Therefore, the prolonged QT interval observed in this study could be the result of autonomic dysfunction, caused by a loss of sympathetic control of the ventricles. Ultimately, the cause of the prolonged QT interval observed in this study could be elucidated using isolated Langendorff hearts (see Further Experimental Work). This study set out to explore the nature of this autonomic dysfunction through RR Interval and heart rate variability analysis, which is explored in the following sections.

HEART RATE AND SUDEP

The balance between the sympathetic and parasympathetic nervous systems can be derived from the RR interval and the heart rate. An increased in the sympathetic tone results in an increase in heart rate, mediated through noradrenaline and circulating adrenaline. Conversely, an increase in parasympathetic tone leads to a decrease in heart rate, mediated via acetylcholine. This study observed an increase in interictal RR interval, corresponding to a decrease in interictal heart rate, over the course of the disease model (Figure 13). This change in RR interval was most apparent during the interictal period immediately before the 150th Seizure and during the Post Seizure State (159.6 ± 11.1 ms and 177.2 ± 24.2 ms, respectively). Around the 150th Seizure, the slower heart rate indicates a shift in autonomic tone towards the parasympathetic, with a further shift during the Post Seizure State. This increase in parasympathetic tone mirrors that observed by Mameli et al.[59] and Hotta and colleagues[60], although it is in contradiction to the elevated basal heart rate observed by Damasceno et al.[49]

It is important to note that the interictal RR intervals, and therefore interictal heart rates, observed in this study are within the normal range for adult male Wistar rats,

320 to 490 bpm[166]. The change in interictal heart rate observed in this study is indicative of a change in autonomic tone, but not a pathophysiologically significant one. A previous unpublished study[129], using the same model and techniques, observed ictal bradycardia (mean decrease of 266 ± 12 bpm) during 89% of seizures, and post ictal tachycardia (mean increase of 129 ± 7 bpm) in 93% of seizures. Therefore, the changes in interictal rate and RR interval could be the result of the autonomic disturbances observed during seizures. The changes observed in this study could be secondary to an increase in blood pressure, or indeed an increase in intracranial pressure[167,168] – a common observation in epilepsy[169,170]. Therefore, further experiments exploring changes in blood pressure would provide evidence as to the origin of the interictal heart rate decrease observed in this study.

HEART RATE VARIABILITY AND SUDEP

Heart rate variability is a non-invasive method of determining the balance between the sympathetic and parasympathetic autonomic nervous systems at a given point. The parasympathetic nervous system influences the heart rate and rhythm through the vagus nerve and acetylcholine, while the sympathetic nervous system releases noradrenaline and adrenaline to influence the heart. Under resting conditions, variations in heart rate are largely dependent on the modulation of the prevailing vagal tone[89] by the sympathetic nervous system. A reduction in HRV is associated with increased mortality and sudden death in heart failure and myocardial infarction patients[171–174], which may reflect a decrease in vagal tone and therefore sympathetic prominence[89]. Reduced HRV has also been observed in numerous animal models and in patients with epilepsy. Ansakorpi and colleagues[92] and Mukherjee et al.[175] have both demonstrated that patients with poorly controlled epilepsy have significantly lower HRV

measures when compared with those with well-controlled epilepsy. Further, DeGiorgio et al.[31] reported the association between RMSSD and the SUDEP-7 Inventory indicating poor vagus-mediated control, and Rauscher and colleagues[98] demonstrated a progressive deterioration in HRV measures over a 8-month period prior to the patient's death. This observed decrease in HRV measures prior to death is further supported by Lacuey et al.[99] who observed the same change in two patients. Conversely, Evrengül and colleagues[95] reported higher HRV measures in males with generalised tonic clonic seizures, indicating an increase in sympathetic activity.

This study showed an apparent decrease in RMSSD, SDNN, and SDSD over the course of the disease, and the SD Ratio increases during the interictal period immediately before the 150th Seizure (Figure 18). A decrease in RMSSD indicates poor vagus-mediated control[31] of the heart; a decreased SDNN indicates that both arms of the autonomic nervous system are suppressed and not functioning correctly[53]; and a decrease in SDSD indicates an increase in sympathetic activity[141]. Conversely, an increase in SD Ratio indicates less sympathetic tone[176]. The results reported in this study are not statistically conclusive (Figure 18), and therefore conclusions about the nature of the autonomic control during interictal periods cannot be drawn.

Ordinarily, the SD Ratio is used in conjunction with the shape of the Poincaré Plot to interpret the state of the autonomic nervous system. A Poincaré Plot is a geometric representation of RR_n and RR_{n+1}, with the SD1 width reflecting the parasympathetic activity and the SD2 length indicating the sympathetic modulation[176]. An elongated, torpedo shaped Poincaré Plot, coupled with a decrease in the SD Ratio is correlated with a increase in sympathetic activity; whereas a more oval shaped Poincaré Plot, coupled with a increase in the SD Ratio, is associated with less sympathetic modulation[176].

Therefore, the changes in SD Ratio observed in this study would ideally need to be assessed with their corresponding Poincaré Plots to obtain results that are more meaningful.

Definitive conclusions about the changes in HRV cannot be drawn because the study is underpowered for HRV analysis as each 10-minute epoch produces one value, as opposed to the waveform analysis that had 15 to 20 data points per interictal period. By increasing the number of animals used in this study it is envisaged that concrete conclusions could be able to be drawn as outliers and anomalous results would be easily identified. Furthermore, the use of SDNN over a 10-minute epoch must be interpreted with care. The guidelines for HRV analysis introduced by the *Task Force of The European Society of Cardiology and The North American Society of Pacing and Electrophysiology*[89] suggest analysing SDNN over a 24-hour period, however the practicality of this would be prohibitive. The R-wave detection script (see Appendix B) used in this study requires the user to visually ensure that the script has functioned correctly, a task which would not be feasible with more than the 10-minute epoch per time point used in this study. Increasing this to a 24-hour period would require the user to visually verify over 500,000 R-waves (assuming a heart rate of 350 bpm). Therefore, refinement of this R-wave detection script would allow the user greater certainty and remove the need for visual verification. Further, and most importantly, the animals in this study rarely experienced a 24-hour period free from seizure and therefore *interictal* SDNN analysis would not be possible.

THE USE OF TENT AS A MODEL FOR SUDEP

Numerous animal models of epilepsy have been used to investigate SUDEP as many of the studies using patients have a number of restrictions to their conclusions due

to the heterogeneity of the human subjects. Animal models can therefore provide key insights into the mechanisms of SUDEP. Models involving the use of chemicals to induce seizures are well established, including kainic acid[94,107,109], penicillin-G[59], and pilocarpine[104,106]. Other methods routinely used include electrical kindling[51,177], and genetic strains prone to seizures such as Wistar Audiogenic Rats[49,178], DBA/2 mice[179,180] and Genetically Epilepsy-Prone Rat (GEPR)[181,182]. Therefore, with a plethora of other models, does the tetanus neurotoxin model of temporal lobe epilepsy have any advantage over the others? The technology used in this study, two channel biopotential radiotelemeters, can only be used in rats due to their size. Therefore, it would be difficult to record the ECoG and ECG of freely moving DBA/2 mice for example; however, future advances in technology could permit this. Furthermore, the TeNT model of temporal lobe epilepsy is non-lesional and well characterised. The TeNT model is well targeted with intrahippocampal injections, and accurately reflects a TLE focus, and has less off-target effects than systemic kainic acid or pilocarpine.

As stated above, the use of animal models is the lack of heterogeneity of the subject. It can be seen from the results of this study that there was large variability between each animal's seizure experience. With a larger study, a more homogenous experimental group could be produced, allowing the results to be compared with more certainty.

The changes in QT interval, QRS width and PR interval observed in this study, coupled with unpublished work[129] by the author that reported ictal bradycardia and post ictal tachycardia, mirror changes observed in other human and animal studies. TeNT could therefore be used to explore the mechanisms that underpin SUDEP, however its use as a model of SUDEP per se is questionable. To be an effective model of SUDEP,

death must ultimately be observed. The TeNT model is very useful for dissecting the complex effects of an epileptogenic injury[183], as it can induce seizures at multiple sites within the brain[131], with targeted results. Indeed, the intrahippocampal injections used in this study have been shown to induce seizures without major morphological changes[114,119,130] and independent of status epilepticus[110,111,114]. Death, however, is not commonly observed in TeNT[131] as opposed to the kainic acid[94] and pilocarpine models[104] where it is. Accordingly, TeNT *could* be considered a poor model for the exploration of SUDEP, as death is necessary for the full exploration of SUDEP.

Due to its sensitivity and ability to model multiple foci, coupled with the lack of hippocampal sclerosis, status epilepticus, and morphological changes observed in the TeNT model of TLE, it does have a place In SUDEP research. Furthermore, the cardiac changes observed in this study and pervious work demonstrate that the TeNT model of TLE mirror that observed in humans, and therefore could be a useful tool for dissecting the mechanisms involved in SUDEP. The changes in QTc and QRS observed during the progression of the disease model return to the Preinduction baseline during the Post Seizure State, indicating that the causes of these changes may not be permanent and therefore indicate autonomic disturbances as a potential mechanism for SUDEP. In order for causes of the changes observed and for these mechanisms to be explored, further experiments need to be performed.

FURTHER EXPERIMENTAL WORK

Several limitations of this study have prevented concrete conclusions being drawn onto the effect of epileptic seizures, induced by TeNT, on the heart. This study was not able to determine the origin of the waveform changes observed. There could be a number of causes for these changes including autonomic dysfunction, changes in

electrical conduction through cardiac myocytes, and changes in cardiac ion channel expression.

To fully explore the autonomic dysfunction, a number of other methods could be employed. As well as extending the study to identify the full extent of the HRV changes induced by epileptic seizures, this study could be also be expanded to record blood pressure simultaneously with ECG and ECoG, providing further valuable information on the autonomic control during epilepsy. Unfortunately, the technology currently does not exist to perform such measurements simultaneously via radiotelemetry in the freely moving animal. Further, autonomic activity could be determined by implanting electrodes into various structures or nerves. As mentioned above, the stellate ganglion and vagus nerve are both involved in the sympathetic and parasympathetic control of the heart, and therefore recording their activity via implanted electrodes could provide information as to whether or not these structures exhibit is autonomic dysfunction. Moreover, peripheral nerve recordings, as performed by Sakamoto et al.[94], could help provide information on autonomic activity. However, such investigations would need to be performed on anaesthetised animals, and therefore would not show the progression through the course of the disease nor the activity during a seizure as many anaesthetic agents are anticonvulsants[184]. To the author's knowledge, technology is currently being developed that would be able to produce multichannel recordings that could allow for the ECG, ECoG, blood pressure, vagal nerve and stellate ganglion activity simultaneously, allowing prolonged investigations over the course of the disease to be made. Further, more invasive, techniques could be performed under terminal anaesthesia, but without a preinduction baseline, the value of this is questionable. The possible autonomic dysfunction could be explored pharmacologically, using agents such as beta-adrenergic isoprenaline or the beta-blocker propranolol, to explore the sympathetic activity, and the

M2 agonist *Arecaidine propargyl ester tosylate* (Tocris, United Kingdom) or the M2 antagonist *Dimethindene maleate* (Tocris, United Kingdom) to explore the parasympathetic activity. Furthermore, the more invasive vagotomy or left stellectomy could help determine the cause of the autonomic dysfunction. Lastly, monophasic action potential recordings, as well as ECG recordings, could be made from isolated Langendorf hearts taken at various time points during the course of the disease model. This could help provide information as to the intrinsic activity of the heart without external autonomic modulation, and identify whether the QT interval changes observed persist without external autonomic input. If these changes were to persist, it would indicate an induced intrinsic change in cardiac conductivity, rather than a change modulated by an external force.

The waveform changes observed in this study could be the result of a change in the expression in certain cardiac ion channels, induced by a yet to be determined mechanism. The expression of certain cardiac ion channels associated with Long QT Syndrome (such as SCN1A, SCN5A, HERG, LQT2, LQT6, LQT1, LQT5, and LQT7) could be evaluated on hearts previously used for isolated heart experiments. Furthermore, any differences in the expression between the different chambers of the heart could also be assessed.

The waveform changes observed could also be secondary to a respiratory dysfunction. Seyal and colleagues[185] demonstrated QTc changes were secondary to seizure induced hyperventilation. Further, the heart rate is influenced, via secondary autonomic changes, by hypoxaemia, hypoventilation and apnoea[82]. Indeed, it has been suggested that the cardiac effects of seizures, as well as a reduction in HRV, could be the result of the autonomic nervous system responding to oxygen desaturation and apnoea[82].

It is therefore vital in future experiments to record the respiration of the animals, as well as the ECoG, ECG and blood pressure, in order to understand completely the effects of epileptic seizure. However, the technology to do this via radiotelemetry is not currently available.

CONCLUSION

This study set out to explore the effects of epileptic seizures, induced by the tetanus neurotoxin model of temporal lobe epilepsy, on the central control of the heart and the conduction through it. Seizures were successfully induced in four animals; with the ECG and ECoG recorded continuously for six to eight-weeks post induction. The first finding of this study was that the QT and QTc interval both increased significantly over the course of the disease, with the QT interval remaining elevated during the post seizure state. The QT and QTc interval peaked during an intense seizure period, indicating a role for repeated seizure insult on the length of cardiac repolarisation. Furthermore, the PR interval and QRS width both significantly increased over the course of the disease. Secondly, the RR interval significantly increases over the course of the disease, however this change was not physiologically significant. Lastly, the role of the autonomic nervous system throughout the disease model remains unclear. The cause of the cardiac changes observed is unclear, however it is likely the result of modulation to the autonomic output, with epileptic disturbances spreading to the brainstem and affecting the control of the cardiovascular system. Further study of the autonomic changes, through various measures, as well as changes in respiration and blood pressure, need to be undertaken in order to provide a clearer picture of the above documented changes in cardiovascular dysfunction and their importance in SUDEP.

BIBLIOGRAPHY

1. Banerjee PN, Filippi D and Allen Hauser W (2009). The Descriptive Epidemiology of Epilepsy-A Review. **Epilepsy Res.** 85 (1): 31–45.

2. World Health Organisation (2016 [cited 2016 Dec 6].). Epilepsy. Available from: http://www.who.int/mediacentre/factsheets/fs999/en/

3. Engel J (2001). A Proposed Diagnostic Scheme for People with Epileptic Seizures and with Epilepsy: Report of the ILAE Task Force on Classification and Terminology. **Epilepsia.** 42 (6): 796–803.

4. Donner EJ (2011). Explaining the Unexplained; Expecting the Unexpected: Where Are We with Sudden Unexpected Death in Epilepsy? **Epilepsy Curr.** 11 (2): 45–9.

5. Shorvon S and Tomson T (2011). Sudden Unexpected Death in Epilepsy. **Lancet.** 378 (9808): 2028–38.

6. Ficker DM, So EL, Shen WK, Annegers JF, O'Brien PC, Cascino GD and Belau PG (1998). Population-Based Study of the Incidence of Sudden Unexplained Death in Epilepsy. **Neurology.** 51 (5): 1270–4.

7. Jick S, Cole T, Mesher R, Tennis P and Jick H (1992). Sudden Unexplained Death in Young Persons with Primary Epilepsy. **Pharmacoepidemiol Drug Saf.** 1: 59–64.

8. Leestma JE, Kalelkar MB, Teas SS, Jay GW and Hughes JR (1984). Sudden Unexpected Death Associated with Seizures: Analysis of 66 Cases. **Epilepsia.** 25 (1): 84–8.

9. Leestma JE, Walczak T, Hughes JR, Kalelkar MB and Teas SS (1989). A Prospective Study on Sudden Unexpected Death in Epilepsy. **Ann Neurol.** 26 (2): 195–203.

10. Langan Y, Nolan N and Hutchinson M (1998). The Incidence of Sudden Unexpected Death in Epilepsy (SUDEP) in South Dublin and Wicklow. **Seizure.** 7 (5): 355–8.

11. Mohanraj R, Norrie J, Stephen LJ, Kelly K, Hitiris N and Brodie MJ (2006). Mortality in Adults with Newly Diagnosed and Chronic Epilepsy: A Retrospective Comparative Study. **Lancet Neurol.** 5 (6): 481–7.

12. Nilsson L, Farahmand B, Persson P-G, Thiblin I and Tomson T (1999). Risk Factors for Sudden Unexpected Death in Epilepsy: A Case Control Study. **Lancet.** 353

(9156): 888–93.

13. Opeskin K and Berkovic SF (2003). Risk Factors for Sudden Unexpected Death in Epilepsy: A Controlled Prospective Study Based on Coroners Cases. **Seizure.** 12 (7): 456–64.

14. Tennis P, Cole TB, Annegers JF, Leestma JE, McNutt M and Rajput A (1995). Cohort Study of Incidence of Sudden Unexplained Death in Persons with Seizure Disorder Treated with Antiepileptic Drugs in Saskatchewan, Canada. **Epilepsia.** 36 (1): 29–36.

15. Walczak TS, Leppik IE, D'Amelio M, Rarick J, So E, Ahman P, Ruggles K, Cascino GD, Annegers JF and Hauser W a (2001). Incidence and Risk Factors in Sudden Unexpected Death in Epilepsy: A Prospective Cohort Study. **Neurology.** 56 (4): 519–25.

16. Annegers JF, Coan SP, Hauser WA, Leestma J, Duffell W and Tarver B (1998). Epilepsy, Vagal Nerve Stimulation by the NCP System, Mortality, and Sudden, Unexpected, Unexplained Death. **Epilepsia.** 39 (2): 206–12.

17. Derby LE, Tennis P and Jick H (1996). Sudden Unexplained Death among Subjects with Refractory Epilepsy. **Epilepsia.** 37 (10): 931–5.

18. Klenerman P, Sander JWAS and Shorvon SD (1993). Mortality in Patients with Epilepsy : A Study of Patients in Long Term Residential Care. **J Neurol Neurosurg Psychiatry.** 88: 149–52.

19. Leestma JE, Annegers JF, Brodie MJ, Brown S, Schraeder P, Siscovick D, Wannamaker BB, Tennis PS, Cierpial MA and Earl NL (1997). Sudden Unexplained Death in Epilepsy: Observations from a Large Clinical Development Program. **Epilepsia.** 38 (1): 47–55.

20. Nashef L, Fish DR, Sander JW and Shorvon SD (1995). Incidence of Sudden Unexpected Death in an Adult Outpatient Cohort with Epilepsy at a Tertiary Referral Centre. **J Neurol Neurosurg Psychiatry.** 58 (4): 462–4.

21. Nashef L, Fish DR, Garner S, Sander JWAS and Shorvon SD (1995). Sudden Death in Epilepsy: A Study of Incidence in a Young Cohort with Epilepsy and Learning Difficulty. **Epilepsia.** 36 (12): 1187–94.

22. Racoosin JA, Feeney J, Burkhart G and Boehm G (2001). Mortality in Antiepileptic

Drug. **Neurology.** 56: 514–9.

23. Timmings PL (1993). Sudden Unexpected Death in Epilepsy: A Local Audit. **Seizure.** 2 (4): 287–90.

24. Vlooswijk MCG, Majoie HJM, De Krom MCTFM, Tan IY and Aldenkamp AP (2007). SUDEP in the Netherlands: A Retrospective Study in a Tertiary Referral Center. **Seizure.** 16 (2): 153–9.

25. Dasheiff RM (1991). Sudden Unexpected Death in Epilepsy: A Series from an Epilepsy Surgery Program and Speculation on the Relationship to Sudden Cardiac Death. **J Clin Neurophysiol.** 8 (2): 216–22.

26. Hennessy MJ, Langan Y, Elwes RD, Binnie CD, Polkey CE and Nashef L (1999). A Study of Mortality after Temporal Lobe Epilepsy Surgery. **Neurology.** 53 (6): 1276–83.

27. Nilsson L, Ahlbom A, Farahmand BY and Tomson T (2003). Mortality in a Population-Based Cohort of Epilepsy Surgery Patients. **Epilepsia.** 44 (4): 575–81.

28. Tomson T (2015). Mortality after Epilepsy Surgery. **Long-Term Outcomes Epilepsy Surg Adults Child.** 46: 125–33.

29. Tomson T, Nashef L and Ryvlin P (2008). Sudden Unexpected Death in Epilepsy: Current Knowledge and Future Directions. **Lancet Neurol.** 7 (11): 1021–31.

30. Novak JL, Miller PR, Markovic D, Meymandi SK and DeGiorgio CM (2015). Risk Assessment for Sudden Death in Epilepsy: The SUDEP-7 Inventory. **Front Neurol.** 6 (DEC): 252.

31. DeGiorgio CM, Miller P, Meymandi S, Chin A, Epps J, Gordon S, Gornbein J and Harper RM (2011). RMSSD, a Measure of Heart Rate Variability, Is Associated With Risk Factors For SUDEP: The SUDEP-7 Inventory. **Epilepsy Behav.** 19 (1): 78–81.

32. Nashef L, Hindocha N and Makoff A (2007). Risk Factors in Sudden Death in Epilepsy (SUDEP): The Quest for Mechanisms. **Epilepsia.** 48 (5): 859–71.

33. Tolstykh GP and Cavazos JE (2013). Potential Mechanisms of Sudden Unexpected Death in Epilepsy. **Epilepsy Behav.** 26 (3): 410–4.

34. Nilsson L, Bergman U, Diwan V, Farahmand BY, Persson PG and Tomson T (2001). Antiepileptic Drug Therapy and Its Management in Sudden Unexpected Death in

Epilepsy: A Case-Control Study. **Epilepsia.** 42 (5): 667–73.

35. Rang H, Dale M, Ritter J and Flower R (2005.). Antiepileptic Drugs. In: **Rang and Dale's Pharmacology. Sixth Edit.** Philadelphia: Churchill Livingstone (an imprint of Elsevier); p. 575–87.

36. Bateman LM, Spitz M and Seyal M (2010). Ictal Hypoventilation Contributes to Cardiac Arrhythmia and SUDEP: Report on Two Deaths in Video-EEG-Monitored Patients. **Epilepsia.** 51 (5): 916–20.

37. Bateman LM, Li CS and Seyal M (2008). Ictal Hypoxemia in Localization-Related Epilepsy: Analysis of Incidence, Severity and Risk Factors. **Brain.** 131 (12): 3239–45.

38. Johnston SC, Darragh TM and Simon RP (1996). Postictal Pulmonary Edema Requires Pulmonary Vascular Pressure Increases. **Epilepsia.** 37 (5): 428–32.

39. Johnston SC, Horn JK, Valente J and Simon RP (1995). The Role of Hypoventiation in a Sheep Model of Epileptic Sudden Death. **Ann Neurol.** 37: 531–7.

40. Johnston SC, Siedenberg R, Min JK, Jerome EH and Laxer KD (1997). Central Apnea and Acute Cardiac Ischemia in a Sheep Model of Epileptic Sudden Death. **Ann Neurol.** 42 (4): 588–94.

41. Nashef L, Walker F, Allen P, Sander JWAS, Shorvon SD and Fish R (1996). Apnea and Bradycardia During Epileptic Seizures - Relation To Sudden Deaths in Epilepsy. **J Neurol Neurosurg Psychiatry.** 60: 297–300.

42. Blum AS, Ives JR, Goldberger AL, Al-Aweel IC, Krishnamurthy KB, Drislane FW and Schomer DL (2000). Oxygen Desaturations Triggered by Partial Seizures: Implications for Cardiopulmonary Instability in Epilepsy. **Epilepsia.** 41 (5): 536–41.

43. Swallow RA, Hillier CEM and Smith PEM (2002). Sudden Unexplained Death in Epilepsy (SUDEP) Following Previous Seizure-Related Pulmonary Oedema: Case Report and Review of Possible Preventative Treatment. **Seizure.** 11 (7): 446–8.

44. So EL, Sam MC and Lagerlund TL (2000). Postictal Central Apnea as a Cause of SUDEP: Evidence from near-SUDEP Incident. **Epilepsia.** 41 (11): 1494–7.

45. O'Regan ME and Brown JK (2007). Abnormalities in Cardiac and Respiratory Function Observed during Seizures in Childhood. **Dev Med Child Neurol.** 47 (1): 4–9.

46. Venit EL, Shepard BD and Seyfried TN (2004). Oxygenation Prevents Sudden Death in Seizure-Prone Mice. **Epilepsia.** 45 (8): 993–6.

47. Ákos Szabó C, Knape KD, Michelle Leland M, Feldman J, McCoy KJM, Hubbard GB and Williams JT (2009). Mortality in Captive Baboons with Seizures: A New Model for SUDEP? **Epilepsia.** 50 (8): 1995–8.

48. Rugg-Gunn FJ and Holdright D (2010). Epilepsy and the Heart. **Br J Cardiol.** 17 (5): 223–9.

49. Damasceno DD, Savergnini SQ, Gomes ERM, Guatimosim S, Ferreira AJ, Doretto MC and Almeida AP (2013). Cardiac Dysfunction in Rats Prone to Audiogenic Epileptic Seizures. **Seizure.** 22 (4): 259–66.

50. Nei M, Ho RT, Abou-Khalil BW, Drislane FW, Liporace J, Romeo A and Sperling MR (2004). EEG and ECG in Sudden Unexplained Death in Epilepsy. **Epilepsia.** 45 (4): 338–45.

51. Goodman JH, Homan RW and Crawford IL (1990). Kindled Seizures Elevate Blood Pressure and Induce Cardiac Arrhythmias. **Epilepsia.** 31 (5): 489–95.

52. Devinsky O, Perrine K and Theodore WH (1994). Interictal Autonomic Nervous System Function in Patients with Epilepsy. **Epilepsia.** 35 (1): 199–204.

53. Sevcencu C and Struijk JJ (2010). Autonomic Alterations and Cardiac Changes in Epilepsy. **Epilepsia.** 51 (5): 725–37.

54. Leutmezer F, Schernthaner C, Lurger S, Pötzelberger K and Baumgartner C (2003). Electrocardiographic Changes at the Onset of Epileptic Seizures. **Epilepsia.** 44 (3): 348–54.

55. Opherk C, Coromilas J and Hirsch LJ (2002). Heart Rate and EKG Changes in 102 Seizures: Analysis of Influencing Factors. **Epilepsy Res.** 52 (2): 117–27.

56. Tigaran S, Mølgaard H, McClelland R, Dam M and Jaffe A (2003). Evidence of Cardiac Ischemia during Seizures in Drug Refractory Epilepsy Patients. **Neurology.** 60 (3): 492–5.

57. Zijlmans M, Flanagan D and Gotman J (2002). Heart Rate Changes and ECG Abnormalities during Epileptic Seizures: Prevalence and Definition of an Objective Clinical Sign. **Epilepsia.** 43 (8): 847–54.

58. Russell A (1906). Cessation of the Pulse During the Onset of Epileptic Fits, With Remarks on the Mechanism of Fits. **Lancet.** 168 (4325): 152–4.

59. Mameli O, Melis F, Giraudi D, Cualbu M, Mameli S, De Riu PL and Mameli P (1993). The Brainstem Cardioarrhythmogenic Triggers and Their Possible Role in Sudden Epileptic Death. **Epilepsy Res.** 15 (3): 171–8.

60. Hotta H, Lazar J, Orman R, Koizumi K, Shiba K, Kamran H and Stewart M (2009). Vagus Nerve Stimulation-Induced Bradyarrhythmias in Rats. **Auton Neurosci Basic Clin.** 151 (2): 98–105.

61. Chaila E, Bhangu J, Tirupathi S and Delanty N (2010). Ictal Bradycardia and Asystole Associated with Intractable Epilepsy: A Case Series. **Br J Cardiol.** 17 (5): 245–8.

62. Nei M, Ho RT and Sperling MR (2000). EKG Abnormalities During Partial Seizures in Refractory Epilepsy. **Epilepsia.** 41 (5): 542–8.

63. Rocamora R, Kurthen M, Lickfett L, Von Oertzen J and Elger CE (2003). Cardiac Asystole in Epilepsy: Clinical and Neurophysiologic Features. **Epilepsia.** 44 (2): 179–85.

64. Lathers CM and Schraeder PL (1982). Autonomic Dysfunction in Epilepsy: Characterization of Autonomic Cardiac Neural Discharge Associated with Pentylenetetrazol???Induced Epileptogenic Activity. **Epilepsia.** 23 (6): 633–47.

65. Tomson T and Kennebäck G (1997). Arrhythmia, Heart Rate Variability, and Antiepileptic Drugs. **Epilepsia.** 38 (17): S48–51.

66. Persson H, Ericson M and Tomson T (2003). Carbamazepine Affects Autonomic Cardiac Control in Patients with Newly Diagnosed Epilepsy. **Epilepsy Res.** 57 (1): 69–75.

67. Tomson T, Ericson M, Ihrman C and Lindblad LE (1998). Heart Rate Variability in Patients with Epilepsy. **Epilepsy Res.** 30 (1): 77–83.

68. Danielsson BR, Lansdell K, Patmore L and Tomson T (2005). Effects of the Antiepileptic Drugs Lamotrigine, Topiramate and Gabapentin on hERG Potassium Currents. **Epilepsy Res.** 63 (1): 17–25.

69. Langan Y, Nashef L and Sander JW (2005). Case-Control Study of SUDEP. **Neurology.** 64: 1131–3.

70. Nashef L, Garner S, Sander JW, Fish DR and Shorvon SD (1998). Circumstances of Death in Sudden Death in Epilepsy: Interviews of Bereaved Relatives. **J Neurol Neurosurg Psychiatry.** 64 (3): 349–52.

71. Glasscock E (2014). Genomic Biomarkers of SUDEP in Brain and Heart. **Epilepsy Behav.** 38: 172–9.

72. Smart SL, Lopantsev V, Zhang CL, Robbins CA, Wang H, Chiu SY, Schwartzkroin PA, Messing A and Tempel BL (1998). Deletion of the K(v)1.1 Potassium Channel Causes Epilepsy in Mice. **Neuron.** 20 (4): 809–19.

73. Glasscock E, Yoo JW, Chen TT, Klassen TL and Noebels JL (2010). Kv1.1 Potassium Channel Deficiency Reveals Brain-Driven Cardiac Dysfunction as a Candidate Mechanism for Sudden Unexplained Death in Epilepsy. **J Neurosci.** 30 (15): 5167–75.

74. Glasscock E, Qian J, Yoo JW and Noebels JL (2007). Masking Epilepsy by Combining Two Epilepsy Genes. **Nat Neurosci.** 10 (12): 1554–8.

75. Sun W, Wagnon JL, Mahaffey CL, Briese M, Ule J and Frankel WN (2013). Aberrant Sodium Channel Activity in the Complex Seizure Disorder of Celf4 Mutant Mice. **J Physiol.** 59111 (591): 241–55.

76. Veeramah KR, O'Brien JE, Meisler MH, Cheng X, Dib-Hajj SD, Waxman SG, Talwar D, Girirajan S, Eichler EE, Restifo LL, Erickson RP and Hammer MF (2012). De Novo Pathogenic SCN8A Mutation Identified by Whole-Genome Sequencing of a Family Quartet Affected by Infantile Epileptic Encephalopathy and SUDEP. **Am J Hum Genet.** 90 (3): 502–10.

77. Ludwig A, Budde T, Stieber J, Moosmang S, Wahl C, Holthoff K, Langebartels A, Wotjak C, Munsch T, Zong X, Feil S, Feil R, Lancel M, Chien KR, Konnerth A, Pape HC, Biel M and Hofmann F (2003). Absence Epilepsy and Sinus Dysrhythmia in Mice Lacking the Pacemaker Channel HCN2. **EMBO J.** 22 (2): 216–24.

78. Labate A, Tarantino P, Palamara G, Gagliardi M, Cavalcanti F, Ferlazzo E, Sturniolo M, Incorpora G, Annesi G, Aguglia U and Gambardella A (2013). Mutations in PRRT2 Result in Familial Infantile Seizures with Heterogeneous Phenotypes Including Febrile Convulsions and Probable SUDEP. **Epilepsy Res.** 104 (3): 280–4.

79. Ergul Y, Ekici B, Tatli B, Nisli K and Ozmen M (2013). QT and P Wave Dispersion and

Heart Rate Variability in Patients with Dravet Syndrome. **Acta Neurol Belg.** 113 (2): 161–6.

80. Delogu AB, Spinelli A, Battaglia D, Dravet C, De Nisco A, Saracino A, Romagnoli C, Lanza GA and Crea F (2011). Electrical and Autonomic Cardiac Function in Patients with Dravet Syndrome. **Epilepsia.** 52 (SUPPL. 2): 55–8.

81. Auerbach DS, Jones J, Clawson BC, Offord J, Lenk GM, Ogiwara I, Yamakawa K, Meisler MH, Parent JM and Isom LL (2013). Altered Cardiac Electrophysiology and SUDEP in a Model of Dravet Syndrome. **PLoS One.** 8 (10).

82. Dlouhy BJ, Gehlbach BK and Richerson GB (2016). Sudden Unexpected Death in Epilepsy: Basic Mechanisms and Clinical Implications for Prevention. **J Neurol Neurosurg Psychiatry.** 87 (4): 402–13.

83. Kashani A and Barold SS (2005). Significance of QRS Complex Duration in Patients with Heart Failure. **J Am Coll Cardiol.** 46 (12): 2183–92.

84. Moseley BD, Wirrell EC, Nickels K, Johnson JN, Ackerman MJ and Britton J (2011). Electrocardiographic and Oximetric Changes during Partial Complex and Generalized Seizures. **Epilepsy Res.** 95 (3): 237–45.

85. Tavernor SJ, Brown SW, Tavernor RME and Gifford C (1996). Electrocardiograph QT Lengthening Associated with Epileptiform EEG Discharges - A Role in Sudden Unexplained Death in Epilepsy? **Seizure.** 5 (1): 79–83.

86. Lederer WJ (2006.). 20 Cardiac Electrophysiology and the Electrocardiogram. In: Boron W, Boulpaep E, editors. **Physiology. Second Edi.** Philadelphia: Saunders Elsevier; p. 2006–2006.

87. Kmecova J and Klimas J (2010). Heart Rate Correction of the QT Duration in Rats. **Eur J Pharmacol.** 641 (2–3): 187–92.

88. Malik M (2002). The Imprecision in Heart Rate Correction May Lead to Artificial Observations of Drug Induced QT Interval Changes. **Pacing Clin Electrophysiol.** 25 (2): 209–16.

89. Task Force of The European Society of Cardiology and The North American Society of Pacing and Electrophysiology A (1996). Guidelines Heart Rate Variability. **Eur Heart J.** 17: 354–81.

90. Reyes del Paso GA, Langewitz W, Mulder LJM, van Roon A and Duschek S (2013). The Utility of Low Frequency Heart Rate Variability as an Index of Sympathetic Cardiac Tone: A Review with Emphasis on a Reanalysis of Previous Studies. **Psychophysiology.** 50 (5): 477–87.

91. Martelli D, Silvani A, McAllen RM, May CN and Ramchandra R (2014). The Low Frequency Power of Heart Rate Variability Is Neither a Measure of Cardiac Sympathetic Tone nor of Baroreflex Sensitivity. **AJP Hear Circ Physiol.** 307 (7): H1005–12.

92. Ansakorpi H, Korpelainen JT, Huikuri H V, Tolonen U, Myllylä V V and Isojärvi JIT (2002). Heart Rate Dynamics in Refractory and Well Controlled Temporal Lobe Epilepsy. **J Neurol Neurosurg Psychiatry.** 72 (1): 26–30.

93. Ansakorpi H, Korpelainen JT, Suominen K, Tolonen U, Myllyla V V and Isojarvi T (2000). Interictal Cardiovascular Autonomic Responses in Patients with Temporal Lobe Epilepsy. **Philadclphia Q Int Leag Against Epilepsy Clin Res.** 41 (1): 42–7.

94. Sakamoto K, Saito T, Orman R, Koizumi K, Lazar J, Salciccioli L and Stewart M (2008). Autonomic Consequences of Kainic Acid-Induced Limbic Cortical Seizures in Rats: Peripheral Autonomic Nerve Activity, Acute Cardiovascular Changes, and Death. **Epilepsia.** 49 (6): 982–96.

95. Evrengül H, Tanriverdi H, Dursunoglu D, Kaftan A, Kuru O, Unlu U and Kilic M (2005). Time and Frequency Domain Analyses of Heart Rate Variability in Patients with Epilepsy. **Epilepsy Res.** 63 (2): 131–9.

96. Surges R, Henneberger C, Adjei P, Scott CA, Sander JW and Walker MC (2009). Do Alterations in Inter-Ictal Heart Rate Variability Predict Sudden Unexpected Death in Epilepsy? **Epilepsy Res.** 87 (2–3): 277–80.

97. Ronkainen E (2005). Suppressed Circadian Heart Rate Dynamics in Temporal Lobe Epilepsy. **J Neurol Neurosurg Psychiatry.** 76 (10): 1382–6.

98. Rauscher G, DeGiorgio AC, Miller PR and DeGiorgio CM (2011). Sudden Unexpected Death in Epilepsy Associated with Progressive Deterioration in Heart Rate Variability. **Epilepsy Behav.** 21 (1): 103–5.

99. Lacuey N, Zonjy B, Theerannaew W, Loparo KA, Tatsuoka C, Sahadevan J and Lhatoo SD (2016). Left-Insular Damage, Autonomic Instability, and Sudden

Unexpected Death in Epilepsy. **Epilepsy Behav.** 55: 170–3.

100. Wiebe S, Blume WT, Girvin JP and Eliasziw M (2001). A Randomized, Controlled Trial of Surgery for Temporal-Lobe Epilepsy. **N Engl J Med.** 345 (5): 311–8.

101. Klausberger T and Somogyi P (2008). Neuronal Diversity and Temporal Dynamics: The Unity of Hippocampal Circuit Operations. **Science (80-).** 321 (5885): 53–7.

102. Bliss TVP and Lømo T (1973). Long-Lasting Potentiation of Synaptic Transmission in the Dentate Area of the Anaesthetized Rabbit Following Stimulation of the Perforant Path. **J Physiol.** 232 (2): 331–56.

103. Coulter DA, Yue C, Ang CW, Weissinger F, Goldberg E, Hsu F-C, Carlson GC and Takano H (2011). Hippocampal Microcircuit Dynamics Probed Using Optical Imaging Approaches. **J Physiol.** 589 (8): 1893–903.

104. Scorza FA, Arida RM, Naffah-Mazzacoratti M da G, Scerni DA, Calderazzo L and Cavalheiro EA (2009). The Pilocarpine Model of Epilepsy: What Have We Learned? **An Acad Bras Cienc.** 81 (3): 345–65.

105. Scorza FA, de Almeida ACG and Scorza CA (2016). Thiamine Deficiency to Ward off Cardiovascular Dysfunction and SUDEP: Yay or Nay? **Epilepsy Behav.** 56: 48–9.

106. Colugnati DB, Gomes PAP, Arida RM, de Albuquerque M, Cysneiros RM, Cavalheiro EA and Scorza FA (2005). Avaliação de Parâmetros Cardíacos Em Animais Com Epilepsia: Possível Causa de Morte Súbita? **Arq Neuropsiquiatr.** 63 (4): 1035–41.

107. Hotta H, Koizumi K and Stewart M (2009). Cardiac Sympathetic Nerve Activity during Kainic Acid-Induced Limbic Cortical Seizures in Rats. **Epilepsia.** 50 (4): 923–7.

108. Yu LMY, Polygalov D, Wintzer ME, Chiang M and Mchugh TJ (2016). CA3 Synaptic Silencing Attenuates Kainic Acid- Induced Seizures and Hippocampal Network. **eNeuro.** 3 (1): 1–18.

109. Zhang K, Tolstykh GP, Sanchez RM and Cavazos JE (2011). Chronic Cellular Hyperexcitability in Elderly Epileptic Rats with Spontaneous Seizures Induced by Kainic Acid Status Epilepticus While Young Adults. **Aging (Albany NY).** 2 (4): 332–8.

110. Hawkins CA and Mellanby JH (1987). Limbic Epilepsy Induced by Tetanus Toxin: A Longitudinal Electroencephalographic Study. **Epilepsia.** 28 (4): 431–44.

111. Finnerty GT and Jefferys JG (2000). 9-16 Hz Oscillation Precedes Secondary

Generalization of Seizures in the Rat Tetanus Toxin Model of Epilepsy. **J Neurophysiol.** 83 (4): 2217–26.

112. Jiruska P, Shtaya ABY, Bodansky DMS, Chang WC, Gray WP and Jefferys JGR (2013). Dentate Gyrus Progenitor Cell Proliferation after the Onset of Spontaneous Seizures in the Tetanus Toxin Model of Temporal Lobe Epilepsy. **Neurobiol Dis.** 54: 492–8.

113. Ferecskó AS, Jiruska P, Foss L, Powell AD, Chang WC, Sik A and Jefferys JGR (2015). Structural and Functional Substrates of Tetanus Toxin in an Animal Model of Temporal Lobe Epilepsy. **Brain Struct Funct.** 220 (2): 1013–29.

114. Jiruska P, Finnerty GT, Powell AD, Lofti N, Cmejla R and Jefferys JGR (2010). Epileptic High-Frequency Network Activity in a Model of Non-Lesional Temporal Lobe Epilepsy. **Brain.** 133 (5): 1380–90.

115. Loscher W (2011). Critical Review of Current Animal Models of Seizures and Epilepsy Used in the Discovery and Development of New Antiepileptic Drugs. **Seizure.** 20 (5): 359–68.

116. Farrar JJ, Yen LM, Cook T, Fairweather N, Binh N, Parry J and Parry CM (2000). Tetanus. **J Neurol Neurosurg Psychiatry.** 69: 292–301.

117. Schiavo G, Matteoli M and Montecucco C (2000). Neurotoxins Affecting Neuroexocytosis. **Physiol Rev.** 80 (2): 717–66.

118. Pellizzari R, Rossetto O, Schiavo G and Montecucco C (1999). Tetanus and Botulinum Neurotoxins: Mechanism of Action and Therapeutic Uses. **Philos Trans R Soc B Biol Sci.** 354 (1381): 259–68.

119. Mellanby J, George G, Robinson A and Thompson P (1977). Epileptiform Syndrome in Rats Produced by Injecting Tetanus Toxin into the Hippocampus. **J Neurol Neurosurg Psychiatry.** 40 (4): 404–14.

120. Brener K, Amitai Y, Jeffreys JGR and Gutnick MJ (1990). Chronic Epileptic Foci in Neocotex: In Vivo and in Vitro Efects of Tetanus Toxin. **Eur J Neurosci.** 3 (June): 47–54.

121. Empson RM, Amitai Y, Jefferys JGR and Gutnick MJ (1993). Injection of Tetanus Toxin into the Neocortex Elicits Persistent Epileptiform Activity but Only Transient

Impairment of GABA Release. **Neuroscience.** 57 (2): 235–9.

122. Nilsen KE, Walker MC and Cock HR (2005). Characterization of the Tetanus Toxin Model of Refractory Focal Neocortical Epilepsy in the Rat. **Epilepsia.** 46 (2): 179–87.

123. Louis ED, Williamson PD and Darcey TM (1990). Chronic Focal Epilepsy Induced by Microinjection of Tetanus Toxin into the Cat Motor Cortex. **Electroencephalogr Clin Neurophysiol.** 75 (6): 548–57.

124. Mainardi M, Pietrasanta M, Vannini E, Rossetto O and Caleo M (2012). Tetanus Neurotoxin-Induced Epilepsy in Mouse Visual Cortex. **Epilepsia.** 53 (7): 132–6.

125. Vannini E, Restani L, Pietrasanta M, Panarese A, Mazzoni A, Rossetto O, Middei S, Micera S and Caleo M (2016). Altered Sensory Processing and Dendritic Remodeling in Hyperexcitable Visual Cortical Networks. **Brain Struct Funct.** 221 (6): 2919–36.

126. Jefferys JG (1989). Chronic Epileptic Foci in Vitro in Hippocampal Slices from Rats with the Tetanus Toxin Epileptic Syndrome. **J Neurophysiol.** 62 (2): 458–68.

127. Vreugdenhil M, Hack SP, Draguhn A and Jefferys JGR (2002). Tetanus Toxin Induces Long-Term Changes in Excitation and Inhibition in the Rat Hippocampal CA1 Area. **Neuroscience.** 114 (4): 983–94.

128. Mellanby J, Renshaw M, Cracknell H, Rands G and Thompson P (1982). Long-Term Impairment of Learning Ability in Rats after an Experimental Hippocampal Epileptiform Syndrome. **Exp Neurol.** 75 (3): 690–9.

129. Ashby-Lumsden A (2013.). Tetanus Toxin Model of Temporal Lobe Epilepsy in the Freely Moving Rat. University of Birmingham;

130. Jefferys JGR, Evans BJ, Hughes SA and Williams SF (1992). Neuropathology of the Chronic Epileptic Syndrome Induced by Intrahippocampal Tetanus Toxin in Rat: Preservation of Pyramidal Cells and Incidence of Dark Cells. **Neuropathol Appl Neurobiol.** 18 (1): 53–70.

131. Jefferys JGR and Walker MC (2006.). Tetanus Toxin Model of Focal Epilepsy. In: Pitkanen P, Schwartzkroin P, Moshe S, editors. **Models of Seizures and Epilepsy.** Amsterdam: Elsevier Academic Press; p. 407–14.

132. Racine RJ (1972). Modification of Seizure Activity by Electrical Stimulation: II. Motor

Seizure. **Electroencephalogr Clin Neurophysiol.** 32 (3): 281–94.

133. Bear M, Connors B and Paradiso M (2007.). Memory Systems. In: **Neuroscience: Exploring the Brain. Third Edit.** Baltimore: Lippincott, Williams and Wilkins; p. 725–60.

134. Crossman A and Neary D (2005.). Hypothalamus, Limbic System and Olfactory System. In: **Neuroanatomy: An Illustrated Colour Text. Third Edit.** London: Churchill Livingstone (an imprint of Elsevier); p. 161–8.

135. Glick DB (2010.). The Autonomic Nervous System. In: **Miller's Anesthesia. 23rd Editi.** New York: McGraw Hill Medical; p. 261–304.

136. Barrett KE, Barman SM, Boitano S and Brooks H (2016.). Cardiovascular Regulatory Mechanisms. In: Barrett K, Barman S, Boitano S, Brooks H, editors. **Ganong's Review of Medical Physiology. 23rd Editi.** New York: McGraw Hill Medical; p. 555–68.

137. D'Ambrosio R and Miller JW (2010). What Is an Epileptic Seizure? Unifying Definitions in Clinical Practice and Animal Research to Develop Novel Treatments. **Epilepsy Curr.** 10 (3): 61–6.

138. Kramer K, van Acker SABE, Voss HP, Grimbergen JA, van der Vijgh WJF and Bast A (1993). Use of Telemetry to Record Electrocardiogram and Heart Rate in Freely Moving Mice. **J Pharmacol Toxicol Methods.** 30 (4): 209–15.

139. Paxinos G and Watson C (1998). The Rat Brain in Stereotaxic Coordinates. **Fourth.** In: London: Academic Press Inc.;

140. Afonso V (1993.). ECG QRS Detection. In: Tompkins W, editor. **Digital Signal Processing.** New Jersey: Prentice Hall; p. 236–64.

141. Niskanen JP, Tarvainen MP, Ranta-Aho PO and Karjalainen PA (2004). Software for Advanced HRV Analysis. **Comput Methods Programs Biomed.** 76 (1): 73–81.

142. Nayak C, Sinha S, Nagappa M, Thennarasu K and Taly AB (2015). Lack of Heart Rate Variability during Apnea in Patients with Juvenile Myoclonic Epilepsy (JME). **Sleep Breath.** 19 (4): 1175–83.

143. Cheng S, Keyes M, Larson M, McCabe E, Newton-Cheh C, Levy D, Benjamin E, Vasan R and Wang T (2009). Long-Term Outcomes in Individuals With Prolonged PR

Interval or First-Degree Atrioventricular Block. **Jama.** 301 (24): 2571–7.

144. Nada A, Gintant GA, Kleiman R, Gutstein DE, Gottfridsson C, Michelson EL, Strnadova C, Killeen M, Geiger MJ, Fiszman ML, Koplowitz LP, Carlson GF, Rodriguez I and Sager PT (2013). The Evaluation and Management of Drug Effects on Cardiac Conduction (PR and QRS Intervals) in Clinical Development. **Am Heart J.** 165 (4): 489–500.

145. Amin AS, Tan HL and Wilde AAM (2010). Cardiac Ion Channels in Health and Disease. **Hear Rhythm.** 7 (1): 117–26.

146. Diercks DB, Shumaik GM, Harrigan RA, Brady WJ and Chan TC (2004). Electrocardiographic Manifestations: Electrolyte Abnormalities. **J Emerg Med.** 27 (2): 153–60.

147. Kahan T (2005). Left Ventricular Hypertrophy in Hypertension: Its Arrhythmogenic Potential. **Heart.** 91 (2): 250–6.

148. Schlaich MP, Kaye DM, Lambert E, Sommerville M, Socratous F and Esler MD (2003). Relation between Cardiac Sympathetic Activity and Hypertensive Left Ventricular Hypertrophy. **Circulation.** 108 (5): 560–5.

149. Channer K and Morris F (2002). Myocardial Ischaemia. **BMJ Br Med J.** 324 (7344): 1023–6.

150. F[isch C, zipes DP and McHenry PL (1973). Rate Dependent Aberrancy. **Circulation.** 48 (4): 714–24.

151. Chilson DA, Zipes DP, Heger JJ, Browne KF and Prystowsky EN (1984). Functional Bundle Branch Block: Discordant Response of Right and Left Bundle Branches to Changes in Heart Rate. **Am J Cardiol.** 54 (3): 313–6.

152. Antzelevitch C (2002). Sympathetic Modulation of the Long QT Syndrome. **Eur Heart J.** 23 (16): 1246–52.

153. Hindocha N, Nashef L, Elmslie F, Birch R, Zuberi S, Al-Chalabi A, Crotti L, Schwartz PJ and Makoff A (2008). Two Cases of Sudden Unexpected Death in Epilepsy in a GEFS+ Family with an SCN1A Mutation [1]. **Epilepsia.** 49 (2): 360–5.

154. Tu E, Bagnall RD, Duflou J and Semsarian C (2011). Post-Mortem Review and Genetic Analysis of Sudden Unexpected Death in Epilepsy (SUDEP) Cases. **Brain**

Pathol. 21 (2): 201–8.

155. Bru-Mercier G, Deroubaix E, Capuano V, Ruchon Y, Rücker-Martin C, Coulombe A and Renaud JF (2003). Expression of Heart K+ Channels in Adrenalectomized and Catecholamine-Depleted Reserpine-Treated Rats. **J Mol Cell Cardiol.** 35 (2): 153–63.

156. Protas L, Barbuti A, Qu J, Rybin VO, Palmiter RD, Steinberg SF and Robinson RB (2003). Neuropeptide Y Is an Essential In Vivo Developmental Regulator of Cardiac ICa,L. **Circ Res.** 93 (10): 972–9.

157. Rosati B and McKinnon D (2004). Regulation of Ion Channel Expression. **Circ Res.** 94 (7): 874–83.

158. Yanowitz F, Preston JB and Abildskov JA (1966). Functional Distribution of Right and Left Stellate Innervation to the Ventricles: PRODUCTION OF NEUROGENIC ELECTROCARDIOGRAPHS CHANGES BY UNILATERAL ALTERATION OF SYMPATHETIC TONE. **Circ Res.** 18 (4): 416–28.

159. Schwartz PJ (1978). Experimental Reproduction of the Long Q-T Syndrome. **Am J Cardiol.** 41 (2): 374.

160. Austoni P, Rosati R, Gregorini L, Bianchi E, Bortolani E, Fox U and Schwartz P (1977). Effects of Stellectomy on Exercise-Induced Q-T Changes in Man. **Circulation.** 56 (4): 184–184.

161. Richerson GB (2009.). Chapter 14 - The Autonomic Nervous System. In: Boron W, Boulpaep E, editors. **Medical Physiology: A Cellular and Molecular Approach. Second Edi.** Philadelphia: Saunders Elsevier; p. 351–70.

162. Schlack W, Schäfer S and Thämer V (1994). Left Stellate Ganglion Block Impairs Left Ventricular Function. **Anesth Analg.** 79 (6): 1082–8.

163. Coyer BH, Pryor R, Kirsch WM and Blount SG (2017). Left Stellectomy in the Long QT Syndrome. **Metall Ital.** 109 (1): 5–10.

164. Hwang SW, Thomas JG, Whitehead WE, Curry DJ, Dauser RC, Kim ES, Luerssen TG and Jea A (2011). Left Thoracopic Sympathectomy for Refractory Long QT Syndrome in Children. **J Neurosurg Pediatr.** 8 (5): 455–9.

165. Wang L (2003). Left Cardiac Sympathectomy Prevents Exercise-Induced QTc

Prolongation in Congenital Long QT Syndrome. **Exp Clin Cardiol.** 8 (1): 31–2.

166. Pass D and Freeth G (1999). The Rat. **ANZCCART News.** 6 (4): Insert.

167. Mangrum JM and DiMarco JP (2000). The Evaluation and Management of Bradycardia. **N Engl J Med.** 342 (10): 703–9.

168. Fodstad H, Kelly PJ and Buchfelder M (2006). History of the Cushing Reflex. **Neurosurgery.** 59 (5): 1132–7.

169. Gabor AJ, Brooks AG, Scobey RP and Parsons GH (1984). Intracranial Pressure during Epileptic Seizures. **Electroencephalogr Clin Neurophysiol.** 57 (6): 497–506.

170. Minns RA and Brown JK (1978). Intracranial Pressure Changes Associated with Childhood Seizures. **Dev Med Child Neurol.** 20 (5): 561–9.

171. So EL (2008). What Is Known about the Mechanisms Underlying SUDEP? **Epilepsia.** 49 (SUPPL. 9): 93–8.

172. Kleiger RE, Miller JP, Bigger JT and Moss AJ (1987). Decreased Heart Rate Variability and Its Association with Increased Mortality after Acute Myocardial Infarction. **Am J Cardiol.** 59 (4): 256–62.

173. Takase B, Kurita A, Noritake M, Uehata A, Maruyama T, Nagayoshi H, Nishioka T, Mizuno K and Nakamura H (1992). Heart Rate Variability in Patients with Diabetes Mellitus, Ischemic Heart Disease, and Congestive Heart Failure. **J Electrocardiol.** 25 (2): 79–88.

174. Bigger JT, Fleiss JL, Rolnitzky LM and Steinman RC (1993). Frequency Domain Measures of Heart Period Variability to Assess Risk Late after Myocardial Infarction. **J Am Coll Cardiol.** 21 (3): 729–36.

175. Mukherjee S, Tripathi M, Chandra PS, Yadav R, Choudhary N, Sagar R, Bhore R, Pandey RM and Deepak KK (2009). Cardiovascular Autonomic Functions in Well-Controlled and Intractable Partial Epilepsies. **Epilepsy Res.** 85 (2–3): 261–9.

176. Hsu CH, Tsai MY, Huang GS, Lin TC, Chen KP, Ho ST, Shyu LY and Li CY (2012). Poincaré Plot Indexes of Heart Rate Variability Detect Dynamic Autonomic Modulation during General Anesthesia Induction. **Acta Anaesthesiol Taiwanica.** 50 (1): 12–8.

177. Pansani AP, Colugnati DB, Sonoda EYF, Arida RM, Cravo SL, Schoorlemmer GHM,

Cavalheiro EA and Scorza FA (2010). Tachycardias and Sudden Unexpected Death in Epilepsy: A Gold Rush by an Experimental Route. **Epilepsy Behav.** 19 (3): 546–7.

178. Fazan R, de Oliveira M, Oliveira JAC, Salgado HC and Garcia-Cairasco N (2011). Changes in Autonomic Control of the Cardiovascular System in the Wistar Audiogenic Rat (WAR) Strain. **Epilepsy Behav.** 22 (4): 666–70.

179. Ross KC and Coleman JR (2000). Developmental and Genetic Audiogenic Seizure Models: Behavior and Biological Substrates. **Neurosci Biobehav Rev.** 24 (6): 639–53.

180. De Sarro G, Russo E, Citraro R and Meldrum BS (2015). Genetically Epilepsy-Prone Rats (GEPRs) and DBA/2 Mice: Two Animal Models of Audiogenic Reflex Epilepsy for the Evaluation of New Generation AEDs. **Epilepsy Behav.**

181. Reigel CE, Jobe PC, Dailey JW and Savage DD (1989). Ontogeny of Sound-Induced Seizures in the Genetically Epilepsy-Prone Rat. **Epilepsy Res.** 4 (1): 63–71.

182. Faingold CL (1995). The Genetically Epilepsy-Prone Rat. **Gen Pharmacol.** 16 (1–2): 91–9.

183. Buckmaster PS (2004). Laboratory Animal Models of Temporal Lobe Epilepsy. **Comp Med.** 54 (5): 473–85.

184. Perks A, Cheema S and Mohanraj R (2012). Anaesthesia and Epilepsy. **Br J Anaethesia.** 108 (4): 562–71.

185. Seyal M, Pascual F, Lee CYM, Li CS and Bateman LM (2011). Seizure-Related Cardiac Repolarization Abnormalities Are Associated with Ictal Hypoxemia. **Epilepsia.** 52 (11): 2105–11.

186. Kuwahara M, Yayou K, Ishii K, Hashimoto S, Tsubone H and Sugano S (1994). Power Spectral Analysis of Heart Rate Variability as a New Method for Assessing Autonomic Activity in the Rat. **J Electrocardiol.** 27 (4): 333–7.

Appendix A

One-way ANOVA with Post-Hoc Bonferroni Comparisons for Raw Waveform Data

PR Interval

Comparisons		Mean Difference	Significance
Preinduction State	1st	-2.8410631*	***.000***
	50th	-1.6475770*	***.000***
	100th	-1.4950786*	***.005***
	150th	-5.3837955*	***.000***
	200th	-.8093603	1.000
	250th	2.3085345*	***.002***
	300th	3.0529225*	***.000***
	Post Seizure State	-3.6528051*	***.000***
1st Seizure	Pre	2.8410631*	***.000***
	50th	1.19348611	.061
	100th	1.3459845*	***.039***
	150th	-2.5427324*	***.000***
	200th	2.0317028*	***.000***
	250th	5.1495976*	***.000***
	300th	5.8939856*	***.000***
	Post Seizure State	-.8117420	1.000
50th Seizure	Pre	1.6475770*	***.000***
	1st	-1.193486117	.061
	100th	.1524984	1.000
	150th	-3.7362185*	***.000***
	200th	.8382167	1.000
	250th	3.9561115*	***.000***
	300th	4.7004995*	***.000***
	Post Seizure State	-2.0052281*	***.000***
100th Seizure	Pre	1.4950786*	***.005***
	1st	-1.3459845*	***.039***
	50th	-.1524984	1.000
	150th	-3.8887169*	***.000***
	200th	.6857182	1.000
	250th	3.8036131*	***.000***
	300th	4.5480011*	***.000***

QRS Width

Comparisons		Mean Difference	Significance
Preinduction State	1st	-1	.106
	50th	-1.6038138*	***.000***
	100th	-.0873786	1.000
	150th	-2.3049708*	***.000***
	200th	-1.6054761*	***.007***
	250th	-0.2320154	1.000
	300th	0.243077436	1.000
	Post Seizure State	-0.5889775	1.000
1st Seizure	Pre	1.087614052	.106
	50th	-0.51619970	1.000
	100th	1.000235427	.564
	150th	-1.2173568	.780
	200th	-0.51786205	1.000
	250th	0.855598589	1.000
	300th	1.330691488	.181
	Post Seizure State	.4986365	1.000
50th Seizure	Pre	1.6038138*	***.000***
	1st	0.516199709	1.000
	100th	1.5164351*	***.008***
	150th	-0.701157063	1.000
	200th	-.0016623	1.000
	250th	1.371798298	.619
	300th	1.8468912*	***.003***
	Post Seizure State	1.014836235	.222
100th Seizure	Pre	.0873786	1.000
	1st	-1.000235427	.564
	50th	-1.5164351*	***.008***
	150th	-2.2175922*	***.002***
	200th	-1.5180975*	***.046***
	250th	-0.144636838	1.000
	300th	0.33045606	1.000

	Post Seizure State	-2.1577265*	.000		Post Seizure State	-0.501598901	1.000
150th Seizure	Pre	5.3837955*	.000	150th Seizure	Pre	2.3049708*	.000
	1st	2.5427324*	.000		1st	1.2173568	.780
	50th	3.7362185*	.000		50th	0.701157063	1.000
	100th	3.8887169*	.000		100th	2.2175922*	.002
	200th	4.5744351*	.000		200th	0.699494714	1.000
	250th	7.6923300*	.000		250th	2.072955361	.088
	300th	8.4367180*	.000		300th	2.5480483*	.001
	Post Seizure State	1.7309904*	.031		Post Seizure State	1.7159933*	.037
200th Seizure	Pre	.8093603	1.000	200th Seizure	Pre	1.6054761*	.007
	1st	-2.0317028*	.000		1st	0.517862058	1.000
	50th	-.8382167	1.000		50th	.0016623	1.000
	100th	-.6857182	1.000		100th	1.5180975*	.046
	150th	-4.5744351*	.000		150th	-0.699494714	1.000
	250th	3.1178948*	.000		250th	1.373460647	.964
	300th	3.8622828*	.000		300th	1.8485535*	.016
	Post Seizure State	-2.8434447*	.000		Post Seizure State	1.016498585	.714
250th Seizure	Pre	-2.3085345*	.002	250th Seizure	Pre	0.232015463	1.000
	1st	-5.1495976*	.000		1st	-0.855598589	1.000
	50th	-3.9561115*	.000		50th	-1.371798298	.619
	100th	-3.8036131*	.000		100th	0.144636838	1.000
	150th	-7.6923300*	.000		150th	-2.072955361	.088
	200th	-3.1178948*	.000		200th	-1.373460647	.964
	300th	.7443880	1.000		300th	.4750929	1.000
	Post Seizure State	-5.9613396*	.000		Post Seizure State	-0.356962062	1.000
300th Seizure	Pre	-3.0529225*	.000	300th Seizure	Pre	-0.243077436	1.000
	1st	-5.8939856*	.000		1st	-1.330691488	.181
	50th	-4.7004995*	.000		50th	-1.8468912*	.003
	100th	-4.5480011*	.000		100th	-0.33045606	1.000
	150th	-8.4367180*	.000		150th	-2.5480483*	.001
	200th	-3.8622828*	.000		200th	-1.8485535*	.016
	250th	-.7443880	1.000		250th	-.4750929	1.000
	Post Seizure State	-6.7057276*	.000		Post Seizure State	-0.832054961	1.000
Post Seizure State	Pre	3.6528051*	.000	Post Seizure State	Pre	0.588977525	1.000
	1st	.8117420	1.000		1st	-.4986365	1.000
	50th	2.0052281*	.000		50th	-1.014836235	.222
	100th	2.1577265*	.000		100th	0.501598901	1.000
	150th	-1.7309904*	.031		150th	-1.7159933*	.037
	200th	2.8434447*	.000		200th	-1.016498585	.714
	250th	5.9613396*	.000		250th	0.356962062	1.000
	300th	6.7057276*	.000		300th	0.832054961	1.000

QT Interval

Comparisons		Mean Difference	Significance
Preinduction State	1st	-4.3631841*	***.000***
	50th	-10.8145914*	***.000***
	100th	-10.4911165*	***.000***
	150th	-16.1321121*	***.000***
	200th	-9.0781143*	***.000***
	250th	-7.6684607*	***.000***
	300th	-5.5005875*	***.000***
	Post Seizure State	-8.1755078*	***.000***
1st Seizure	Pre	4.3631841*	***.000***
	50th	-6.4514074*	***.000***
	100th	-6.1279324*	***.000***
	150th	-11.7689281*	***.000***
	200th	-4.7149303*	***.003***
	250th	-3.305276656	1.000
	300th	-1.13740347	1.000
	Post Seizure State	-3.8123238*	***.006***
50th Seizure	Pre	10.8145914*	***.000***
	1st	6.4514074*	***.000***
	100th	.3234749	1.000
	150th	-5.3175207*	***.006***
	200th	1.7364771	1.000
	250th	3.146130722	1.000
	300th	5.3140039*	***.001***
	Post Seizure State	2.639083619	.282
100th Seizure	Pre	10.4911165*	***.000***
	1st	6.1279324*	***.000***
	50th	-.3234749	1.000
	150th	-5.6409956*	***.005***
	200th	1.4130022	1.000
	250th	2.822655783	1.000
	300th	4.9905290*	***.007***
	Post Seizure State	2.31560868	1.000
150th Seizure	Pre	16.1321121*	***.000***
	1st	11.7689281*	***.000***
	50th	5.3175207*	***.006***
	100th	5.6409956*	***.005***
	200th	7.0539978*	***.000***
	250th	8.4636514*	***.000***

QTc Interval

Comparisons		Mean Difference	Significance
Preinduction State	1st	-3	1.000
	50th	-6.5058790*	***.000***
	100th	-7.8147670*	***.000***
	150th	-11.6844598*	***.000***
	200th	-6.8291644*	***.000***
	250th	-7.9918512*	***.001***
	300th	-7.7318659*	***.000***
	Post Seizure State	-0.883669984	1.000
1st Seizure	Pre	2.506742522	1.000
	50th	-3.999136498	.070
	100th	-5.3080245*	***.005***
	150th	-9.1777172*	***.000***
	200th	-4.322421865	.150
	250th	-5.485108667	.180
	300th	-5.2251234*	***.040***
	Post Seizure State	1.6230725	1.000
50th Seizure	Pre	6.5058790*	***.000***
	1st	3.999136498	.070
	100th	-1.3088880	1.000
	150th	-5.178580746	.130
	200th	-.3232854	1.000
	250th	-1.485972169	1.000
	300th	-1.225986869	1.000
	Post Seizure State	5.6222090*	***.000***
100th Seizure	Pre	7.8147670*	***.000***
	1st	5.3080245*	***.005***
	50th	1.3088880	1.000
	150th	-3.869692721	1.000
	200th	.9856027	1.000
	250th	-0.177084143	1.000
	300th	0.082901156	1.000
	Post Seizure State	6.9310971*	***.000***
150th Seizure	Pre	11.6844598*	***.000***
	1st	9.1777172*	***.000***
	50th	5.178580746	.130
	100th	3.869692721	1.000
	200th	4.855295379	.446
	250th	3.692608577	1.000

	300TH	10.6315246*	*.000*
	POST SEIZURE STATE	7.9566043*	*.000*
200TH SEIZURE	PRE	9.0781143*	*.000*
	1ST	4.7149303*	*.003*
	50TH	-1.7364771	1.000
	100TH	-1.4130022	1.000
	150TH	-7.0539978*	*.000*
	250TH	1.4096536	1.000
	300TH	3.577526786	.389
	POST SEIZURE STATE	0.902606496	1.000
250TH SEIZURE	PRE	7.6684607*	*.000*
	1ST	3.305276656	1.000
	50TH	-3.146130722	1.000
	100TH	-2.822655783	1.000
	150TH	-8.4636514*	*.000*
	200TH	-1.4096536	1.000
	300TH	2.1678732	1.000
	POST SEIZURE STATE	-0.507047103	1.000
300TH SEIZURE	PRE	5.5005875*	*.000*
	1ST	1.13740347	1.000
	50TH	-5.3140039*	*.001*
	100TH	-4.9905290*	*.007*
	150TH	-10.6315246*	*.000*
	200TH	-3.577526786	.389
	250TH	-2.1678732	1.000
	POST SEIZURE STATE	-2.67492029	1.000
POST SEIZURE STATE	PRE	8.1755078*	*.000*
	1ST	3.8123238*	*.006*
	50TH	-2.639083619	.282
	100TH	-2.31560868	1.000
	150TH	-7.9566043*	*.000*
	200TH	-0.902606496	1.000
	250TH	0.507047103	1.000
	300TH	2.67492029	1.000

	300TH	3.952593877	1.000
	POST SEIZURE STATE	10.8007898*	*.000*
200TH SEIZURE	PRE	6.8291644*	*.000*
	1ST	4.322421865	.150
	50TH	.3232854	1.000
	100TH	-.9856027	1.000
	150TH	-4.855295379	.446
	250TH	-1.162686802	1.000
	300TH	-0.902701502	1.000
	POST SEIZURE STATE	5.9454944*	*.002*
250TH SEIZURE	PRE	7.9918512*	*.001*
	1ST	5.485108667	.180
	50TH	1.485972169	1.000
	100TH	0.177084143	1.000
	150TH	-3.692608577	1.000
	200TH	1.162686802	1.000
	300TH	.2599853	1.000
	POST SEIZURE STATE	7.1081812*	*.008*
300TH SEIZURE	PRE	7.7318659*	*.000*
	1ST	5.2251234*	*.040*
	50TH	1.225986869	1.000
	100TH	-0.082901156	1.000
	150TH	-3.952593877	1.000
	200TH	0.902701502	1.000
	250TH	-.2599853	1.000
	POST SEIZURE STATE	6.8481959*	*.000*
POST SEIZURE STATE	PRE	0.883669984	1.000
	1ST	-1.6230725	1.000
	50TH	-5.6222090*	*.000*
	100TH	-6.9310971*	*.000*
	150TH	-10.8007898*	*.000*
	200TH	-5.9454944*	*.002*
	250TH	-7.1081812*	*.008*
	300TH	-6.8481959*	*.000*

ONE-WAY ANOVA WITH POST-HOC BONFERRONI COMPARISONS FOR THE NORMALISED WAVEFORM DATA

NORMALISED PR INTERVAL **NORMALISED QRS WIDTH**

Comparisons		Mean Difference	Significance	Comparisons		Mean Difference	Significance
Preinduction State	1st	-.0610782*	***.000***	Preinduction State	1st	-.0762632*	***.002***
	50th	-.0211325*	***.030***		50th	-.0702506*	***.005***
	100th	-.0196340	.162		100th	-.0128463	1.000
	150th	-.0865991*	***.000***		150th	-.1543570*	***.000***
	200th	-.0142420	1.000		200th	-.0532148	.553
	250th	.0409018*	***.001***		250th	-0.038463173	1.000
	300th	.0555736*	***.000***		300th	0.006807257	1.000
	Post Seizure State	-.0687808*	***.000***		Post Seizure State	-0.032158659	1.000
1st Seizure	Pre	.0610782*	***.000***	1st Seizure	Pre	.0762632*	***.002***
	50th	.0399457*	***.000***		50th	0.006012586	1.000
	100th	.0414442*	***.000***		100th	0.063416893	.102
	150th	-.0255209	.218		150th	-.0780938	.148
	200th	.0468363*	***.000***		200th	0.023048425	1.000
	250th	.1019800*	***.000***		250th	0.037800013	1.000
	300th	.1166518*	***.000***		300th	.0830704*	***.023***
	Post Seizure State	-.0077026	1.000		Post Seizure State	.0441045	.783
50th Seizure	Pre	.0211325*	***.030***	50th Seizure	Pre	.0702506*	***.005***
	1st	-.0399457*	***.000***		1st	-0.006012586	1.000
	100th	.0014985	1.000		100th	.0574043	.227
	150th	-.0654665*	***.000***		150th	-0.084106393	.068
	200th	.0068906	1.000		200th	.0170358	1.000
	250th	.0620343*	***.000***		250th	0.031787427	1.000
	300th	.0767061*	***.000***		300th	0.077057857	.051
	Post Seizure State	-.0476483*	***.000***		Post Seizure State	0.038091941	1.000
100th Seizure	Pre	.0196340	.162	100th Seizure	Pre	.0128463	1.000
	1st	-.0414442*	***.000***		1st	-0.063416893	.102
	50th	-.0014985	1.000		50th	-.0574043	.227
	150th	-.0669651*	***.000***		150th	-.1415107*	***.000***
	200th	.0053920	1.000		200th	-.0403685	1.000
	250th	.0605358*	***.000***		250th	-0.02561688	1.000
	300th	.0752076*	***.000***		300th	0.01965355	1.000
	Post Seizure State	-.0491468*	***.000***		Post Seizure State	-0.019312365	1.000
150th Seizure	Pre	.0865991*	***.000***	150th Seizure	Pre	.1543570*	***.000***
	1st	.0255209	.218		1st	.0780938	.148
	50th	.0654665*	***.000***		50th	0.084106393	.068
	100th	.0669651*	***.000***		100th	.1415107*	***.000***
	200th	.0723571*	***.000***		200th	.1011422*	***.023***

	250TH	.1275009*	*.000*
	300TH	.1421726*	*.000*
	POST SEIZURE STATE	.0178183	1.000
200TH SEIZURE	PRE	.0142420	1.000
	1ST	-.0468363*	*.000*
	50TH	-.0068906	1.000
	100TH	-.0053920	1.000
	150TH	-.0723571*	*.000*
	250TH	.0551437*	*.000*
	300TH	.0698155*	*.000*
	POST SEIZURE STATE	-.0545388*	*.000*
250TH SEIZURE	PRE	-.0409018*	*.001*
	1ST	-.1019800*	*.000*
	50TH	-.0620343*	*.000*
	100TH	-.0605358*	*.000*
	150TH	-.1275009*	*.000*
	200TH	-.0551437*	*.000*
	300TH	.0146718	1.000
	POST SEIZURE STATE	-.1096826*	*.000*
300TH SEIZURE	PRE	-.0555736*	*.000*
	1ST	-.1166518*	*.000*
	50TH	-.0767061*	*.000*
	100TH	-.0752076*	*.000*
	150TH	-.1421726*	*.000*
	200TH	-.0698155*	*.000*
	250TH	-.0146718	1.000
	POST SEIZURE STATE	-.1243543*	*.000*
POST SEIZURE STATE	PRE	.0687808*	*.000*
	1ST	.0077026	1.000
	50TH	.0476483*	*.000*
	100TH	.0491468*	*.000*
	150TH	-.0178183	1.000
	200TH	.0545388*	*.000*
	250TH	.1096826*	*.000*
	300TH	.1243543*	*.000*

	250TH	.1158938*	*.035*
	300TH	.1611642*	*.000*
	POST SEIZURE STATE	.1221983*	*.000*
200TH SEIZURE	PRE	.0532148	.553
	1ST	-0.023048425	1.000
	50TH	-.0170358	1.000
	100TH	.0403685	1.000
	150TH	-.1011422*	*.023*
	250TH	0.014751588	1.000
	300TH	0.060022018	.912
	POST SEIZURE STATE	0.021056102	1.000
250TH SEIZURE	PRE	0.038463173	1.000
	1ST	-0.037800013	1.000
	50TH	-0.031787427	1.000
	100TH	0.02561688	1.000
	150TH	-.1158938*	*.035*
	200TH	-0.014751588	1.000
	300TH	.0452704	1.000
	POST SEIZURE STATE	0.006304514	1.000
300TH SEIZURE	PRE	-0.006807257	1.000
	1ST	-.0830704*	*.023*
	50TH	-0.077057857	.051
	100TH	-0.01965355	1.000
	150TH	-.1611642*	*.000*
	200TH	-0.060022018	.912
	250TH	-.0452704	1.000
	POST SEIZURE STATE	-0.038965915	1.000
POST SEIZURE STATE	PRE	0.032158659	1.000
	1ST	-.0441045	.783
	50TH	-0.038091941	1.000
	100TH	0.019312365	1.000
	150TH	-.1221983*	*.000*
	200TH	-0.021056102	1.000
	250TH	-0.006304514	1.000
	300TH	0.038965915	1.000

NORMALISED QT INTERVAL

COMPARISONS	MEAN DIFFERENCE	SIGNIFICANCE

NORMALISED QTC INTERVAL

COMPARISONS	MEAN DIFFERENCE	SIGNIFICANCE

Preinduction State	1st	-.0712823*	***.000***	Preinduction State	1st	0	.170
	50th	-.1836655*	***.000***		50th	-.1289907*	***.000***
	100th	-.1512937*	***.000***		100th	-.0990729*	***.000***
	150th	-.2129313*	***.000***		150th	-.1405613*	***.000***
	200th	-.1850093*	***.000***		200th	-.1745752*	***.000***
	250th	-.1397765*	***.000***		250th	-.1390061*	***.000***
	300th	-.1131340*	***.000***		300th	-.1528796*	***.000***
	Post Seizure State	-.1162053*	***.000***		Post Seizure State	-0.009813399	1.000
1st Seizure	Pre	.0712823*	***.000***	1st Seizure	Pre	0.045423051	.170
	50th	-.1123832*	***.000***		50th	-.0835677*	***.000***
	100th	-.0800115*	***.000***		100th	-0.053649824	.116
	150th	-.1416490*	***.000***		150th	-.0951383*	***.002***
	200th	-.1137270*	***.000***		200th	-.1291522*	***.000***
	250th	-0.0684942	.104		250th	-.0935831*	***.009***
	300th	-0.0418516	.931		300th	-.1074566*	***.000***
	Post Seizure State	-.0449231	.092		Post Seizure State	.0356097	1.000
50th Seizure	Pre	.1836655*	***.000***	50th Seizure	Pre	.1289907*	***.000***
	1st	.1123832*	***.000***		1st	.0835677*	***.000***
	100th	.0323717	1.000		100th	.0299178	1.000
	150th	-0.0292685	1.000		150th	-0.011570627	1.000
	200th	-.0013438	1.000		200th	-.0455845	.689
	250th	0.043888	1.000		250th	-0.010015389	1.000
	300th	.0705315*	***.006***		300th	-0.023888921	1.000
	Post Seizure State	.0674601*	***.000***		Post Seizure State	.1191773*	***.000***
100th Seizure	Pre	.1512937*	***.000***	100th Seizure	Pre	.0990729*	***.000***
	1st	.0800115*	***.000***		1st	0.053649824	.116
	50th	-.0323717	1.000		50th	-.0299178	1.000
	150th	-0.061637	.172		150th	-0.04148847	1.000
	200th	-.0337155	1.000		200th	-.0755023*	***.010***
	250th	0.0115172	1.000		250th	-0.039933232	1.000
	300th	0.0381597	1.000		300th	-0.053806764	.491
	Post Seizure State	0.0350883	1.000		Post Seizure State	.0892595*	***.000***
150th Seizure	Pre	.2129313*	***.000***	150th Seizure	Pre	.1405613*	***.000***
	1st	.1416490*	***.000***		1st	.0951383*	***.002***
	50th	0.029265	1.000		50th	0.011570	1.000
	100th	0.061637	.172		100th	0.041488	1.000
	200th	0.027922	1.000		200th	-0.0340138	1.000
	250th	0.073154	.251		250th	0.001555	1.000
	300th	.0997974*	***.001***		300th	-0.012318	1.000

	Post Seizure State	.0967260*	***.000***
200th Seizure	Pre	.1850093*	***.000***
	1st	.1137270*	***.000***
	50th	.0013438	1.000
	100th	.0337155	1.000
	150th	-0.027922	1.000
	250th	0.045232	1.000
	300th	.0718753*	***.020***
	Post Seizure State	.0688039*	***.003***
250th Seizure	Pre	.1397765*	***.000***
	1st	0.068494	.104
	50th	-0.043888	1.000
	100th	-0.011517	1.000
	150th	-0.073154	.251
	200th	-0.0452327	1.000
	300th	.0266426	1.000
	Post Seizure State	0.0235711	1.000
300th Seizure	Pre	.1131340*	***.000***
	1st	0.041851	.931
	50th	-.0705315*	***.006***
	100th	-0.038159	1.000
	150th	-.0997974*	***.001***
	200th	-.0718753*	***.020***
	250th	-.0266426	1.000
	Post Seizure State	-0.003071	1.000
Post Seizure State	Pre	.1162053*	***.000***
	1st	.0449231	.092
	50th	-.0674601*	***.000***
	100th	-0.035088	1.000
	150th	-.0967260*	***.000***
	200th	-.0688039*	***.003***
	250th	-0.023571	1.000
	300th	0.003071	1.000

	Post Seizure State	.1307479*	***.000***
200th Seizure	Pre	.1745752*	***.000***
	1st	.1291522*	***.000***
	50th	.0455845	.689
	100th	.0755023*	***.010***
	150th	0.034013	1.000
	250th	0.035569	1.000
	300th	0.021695	1.000
	Post Seizure State	.1647618*	***.000***
250th Seizure	Pre	.1390061*	***.000***
	1st	.0935831*	***.009***
	50th	0.010015	1.000
	100th	0.039933	1.000
	150th	-0.001555	1.000
	200th	-0.035569	1.000
	300th	-.0138735	1.000
	Post Seizure State	.1291927*	***.000***
300th Seizure	Pre	.1528796*	***.000***
	1st	.1074566*	***.000***
	50th	0.023888	1.000
	100th	0.053806	.491
	150th	0.012318	1.000
	200th	-0.021695	1.000
	250th	.0138735	1.000
	Post Seizure State	.1430662*	***.000***
Post Seizure State	Pre	0.009813	1.000
	1st	-.0356097	1.000
	50th	-.1191773*	***.000***
	100th	-.0892595*	***.000***
	150th	-.1307479*	***.000***
	200th	-.1647618*	***.000***
	250th	-.1291927*	***.000***
	300th	-.1430662*	***.000***

Appendix B

SPIKE2 PAN-TOMPKINS R-WAVE DETECTION SCRIPT

```
'=========================================
'Pan Tompkins Algorithm
'=========================================
'OVERVIEW
'A modified Pan Tompkins Algorithm that will place a marker on each
'QRS complex and create a virtual channel of the heart rate.

var v18% := ViewFind("AAL150202_150301_001 [32-bit]");
var data%;                          'Data file
var wChan%;                         'Waveform channel
var pChan%;                         'Memory channel for imported events
var sTime,eTime;                    'Start and end time for import
var tChangeFlag%;                   'Flag to say time range has changed
var mode%;                          'Import mode
var minInt;                         'Min Interval
var timeMode% := 0;                 'Use whole file or between cursors
var mSaved%;                        'Memory channel to hold saved event in cursor specified sections
var savedMark%;                     'Marker channel holding times of imported events in cursor specified
sections
var showDup% := 0;                  'Flag for whether to display duplicate channel in different draw
mode
var ch1%;
var ch2%;
var ch3%;
var ch5%;
var ChanX%;
var ok%;

data% := FrontView();               'Bring data file to the front
if ViewKind(data%)<>0 then          'If no data file
   Message("Open a data file for analysis");    'prompt user
   data%:= FileOpen("",0,1);
   if data% < 0 then                'If unable to open file
      Message("Unable to open a data file!");   'Warn user and quit script
      Halt;endif;
```

```
endif;

Func Done%()
ToolbarClear(0);                        'Clear the toolbar
Halt;
return 1;
end;

Func ChooseChannel%();
DlgCreate("Channel Selection");
DlgChan(1,"Waveform channel for feature extraction",513);

ok% := DlgShow(ChanX%);                 'Set channel to use and method of detection
if ok% = 0 then
   Halt;                                'Halt script if user cancels
endif;
end;

Func End% ()                            'End script if user requests
ToolbarClear(0);
Halt;
return 1;
end

FrontView(v18%);                        'Make the file full screen
WindowVisible(3);
XRange(0, MaxTime());

ToolbarSet(9, "Run",ChooseChannel%);    'Set up toolbar
ToolbarSet(3, "Done", Done%);
ToolbarSet(7, "End", End%);
ToolbarEnable(3,0);
ToolbarEnable(5,0);
ToolbarEnable(7,1);
Toolbar("Pan Tompkins QRS Detection",1023);

HCursorDelete(-1);
FrontView(v18%);
ChanProcessAdd(ChanX%,2);
ChanProcessArg(ChanX%,1,1,0.05);
```

```
FiltCreate(-1, 4, 20, 42, 61);                    'FIR Band pass
ch1% := FiltApply(-1, 0,ChanX%, 0.000000, MaxTime(), 3);   'Apply created filter
ChanProcessAdd(ch1%, 3);
ChanProcessArg(ch1%, 1, 1, 0.004);                  'Add Slope to channel 401
ch2% := VirtualChan(0, "");                       'Create new virtual channel
VirtualChan(ch2%, "sqr(ch(401))", 0, 0.0005, 0);        'Edit virtual channel
ChanProcessAdd(ch2%, 1);                          'Add Smooth to channel 701
ChanProcessArg(ch2%, 1, 1, 0.025);                  'Set Smooth Time constant (s)
ChanSave(ch2%,12);
ChanDelete(ch2%);
ChanDelete(ch1%);
ChanShow(12);
ChanTitle$(12, "Sqr P-T");

var mean%;
var SD%;
var threshold%;
var logchan%;

logchan% := VirtualChan(0,"");
VirtualChan(logchan%, "Ln(Ch(12))", 0, 0.0005,0);
ChanSave(logchan%,13);
ChanShow(13);
ChanTitle$(13,"Log Sq");
Optimise(13);
ChanDelete(logchan%);

mean% := ChanMeasure(13,16,0,MaxTime());
SD% := ChanMeasure(13,12,0,MaxTime());
threshold% := mean%;

MeasureX(102, 1, "Cursor(0)", "0");                 'Peak detection of squared channel
MeasureY(100, 1, "Cursor(0)", "0");
ch1% := MeasureToChan(0, "Sqr EVENT", 3,4, 13, 0, threshold%, 0, 1, "", 0);
Process(0.0, 21600.1, 0, 1, ch1%);

FrontView(v18%);
WindowVisible(3);
XRange(0, MaxTime());
```

```
var T, peakpos;
var ch4%;
const pretime := 0.025;
const posttime := 0.025;
var peakAmp;
ch4% := memchan(3);
T := -1;

while 1 do
   T := NextTime(ch1%, T);
      peakAmp:=ChanMeasure(ChanX%,8,T - pretime, T + posttime);
   if T < 0 then
      break;
   endif

   peakpos := ChanSearch(ChanX%, 1, T - pretime, T + posttime, peakAmp);

   if peakpos > 0 then
      MemSetItem(ch4%, 0, peakpos);
endif
wend

ch3% := VirtualChan(0,"");
VirtualChan(ch3%, "IF(402,0.5)*60",0,0.1,0);
ChanShow(ch3%);
ChanShow(ch4%);
ChanTitle$(ch4%, "QRS EVENT");
YRange(701, 200, 600);
ChanTitle$(ch3%,"HeartRate");
ChanUnits$(ch3%, "bpm");
ChanSave(ch4%,16);
ChanShow(10);
ChanShow(16);
ChanDelete(13);
ChanDelete(12);
ChanDelete(ch1%);
ch5% := VirtualChan(0,"");
VirtualChan(ch5%,"(1/(Ch(701)/60))*1000",0,0.1,0);
ChanShow(ch5%);
ChanTitle$(ch5%, "RRinterval");
```

```
YRange(702,100,300);
ChanUnits$(ch5%,"ms");
ChanProcessClear(ChanX%);
HCursorNew(702,150);
HCursorNew(702,145);
HCursorNew(702,155);
HCursorNew(702,170);
HCursorNew(702,175);
HCursorNew(702,165);
HCursorNew(701,350);
HCursorNew(701,400);
HCursorNew(701,450);
HCursorLabel(4,7,"Min HR");
HCursorLabel(4,8,"Mean HR");
HCursorLabel(4,9,"Max HR");
XAxisStyle(3);
FrontView(v18%);
WindowVisible(3);
XRange(0, MaxTime());
Optimise(-2);
YRange(702,100,300);
YRange(701, 200, 600);
Speak("Pan Tompkins Complete");
```

Appendix C

MATLAB HEART RATE VARIABILITY SCRIPT

```
%=========================================================================
=%
 %            TIME-BASED HEART RATE VARIABILITY ANALYSIS
%=========================================================================
=%

%This script performs multiple types of analysis on data exported from
%Spike2. Specifically, the data must be a matrix of time points which
%correspond to the R-waves of an ECG signal. Once imported as a [matrix],
%the data is analysed to provide TIME-DOMAIN HRV measures (RMSSD, SDNN,
%SDSD, SD1 and SD2), the change in HEART RATE in the data set.

close all
clear variables
clc

% SETTING UP PARAMETERS

sheet = input('enter Animal ID here: ');% enter the animal ID here which
should be the name of the Excel sheet
Row   = 5; % enter the row that you wish the data to be copied into
End   = input('Type in the last column number here: ');

[filename,pathname]   =   uigetfile('*.xlsx','Select   Excel   File   to
Analyse');% Opens a user interface to select the Excel file containing
the data
file_name           = [pathname filename];% Sets file name where you want
to extract data from

[num,txt,raw] = xlsread(file_name, sheet, 'AB:End','basic');% set up 'R',
a matrix containing the R wave time points
R             = num;

%=========================================================================
=%
 %        CALCULATE TIME-BASED HEART RATE VARIABILITY VALUES
%=========================================================================
=%
```

```
% SET UP LOOP
rMSSD_all = [];
SDNN_all  = [];
SDSD_all  = [];
SD1_all   = [];
SD2_all   = [];
AvHR_all  = [];

for g  = 1:size(R,2)
column = R(:,g);
column = column(~isnan(column));        % removes NaN from each column

R1 = column;                            % Remove any NaN from 'R'
R1 = R1 - (min(R1));                    % Take the minimum value to set to
start at 0

   % Calculate RR interval
        D1          = diff(R1,1);% Calculate RR Intervals
   % Remove RR intervals greater than 0.5 sec
        index3        = find(D1>=0.5);% creates a list of all those RR
intervals greater than 0.5 sec
        index4       = [index3-2 index3-1 index3 index3+1 index3+2];   %
creates a [matrix] of the RR intervals exceding 0.5 sec, and the two RRs
immediately before and after as these may have been "contaminated"
        index4(index4<1)           = [];
        index4(index4>length(D1)) = [];
        D1(index4)                 = [];

      % Calculate rMSSD
        A1                 = diff(D1,1);        % Calculate diff between
neighbouring RRs
        B1           = A1.^2;              % Square to remove negatives
        C1           = sum(B1);            % Sum all
        average1     = C1/(length(R1)-1);  % divide by n-1
        rMSSD          = sqrt(average1);       % sqrt to remove previous
square
        rMSSD        = rMSSD*1000;         %converts from sec to msec
        rMSSD_all(g) = rMSSD;

       % Calculate Standard Deviation of the RR interval

        E1           = mean(D1);           % calculate mean RR interval
        F1             = D1-E1;     % Difference between each RR interval
and the mean
```

```
        G1            = sum(F1.^2);      % sum all differences squared
        H1            = G1/(length(R1)-1);   % divide by n-1
        SDNN          = sqrt(H1);        % sqrt to remove previous square
        SDNN          = SDNN*1000;     % converts from sec to msec
        SDNN_all(g)   = SDNN;

        % Standard Deviation of the Successive Differences

        SDSD                = std(A1);    % st dev of the diff between
neighbouring RRs
        SDSD          = SDSD*1000;  % converts from sec to msec
        SDSD_all(g)   = SDSD;

        % SD1

        SD1           = sqrt(0.5*(SDSD^2));    % Calcuates SD1
        SD1_all(g)  = SD1;

        % SD2
        SD2             = sqrt((2*(SDNN^2))-(0.5*(SDSD^2)));   % Calculates
SD2
        SD2_all(g)  = SD2;

       % POINCARE PLOT

        x = D1;
        y = x(2:length(x),:);
        figure (1);
        scatter(x(1:length(x)-1),y,'.','k')
            title('Poincaré Plot')
            xlabel('RR_n (s)')
            ylabel('RR_n_+_1 (s)')
            axis([min(x)-0.01 max(x)+0.01 min(y)-0.01 max(y)+0.01])
            m=1; x=0:0.01:10; intercept=0;
            hold on; identity = plot(x, m*x+intercept);
            set(identity, 'color', 'r', 'LineWidth',1)

       % Calculate Heart Rate for each epoch

        HR          = 60./D1;       % Calculate Heart Rate
        AvHR        = mean(HR);     % Mean Heart Rate
        AvHR_all(g) = AvHR;
```

```
%=========================================================================
=%
%                          WRITE TO EXCEL FILE
%=========================================================================
=%

%SET UP POINCARE PLOT AUTOSAVE

File         = txt(g);
File         = char(File);
PoincarePlot = ('_Poincare Plot');
image_name     = [sheet File PoincarePlot];%sets the image name to be
ANIMAL ID_FILE NAME_POINCARE PLOT
path_name     = [pathname 'Poincare Plots'];%Sets the directory where the
poincare plot is to be saved
path_name     = [path_name '\' sheet];
saveas(gcf,fullfile(path_name,image_name),'emf')%saves the poincare plot
as the image name to the correct directory

close all;
end

rMSSD_all = transpose(rMSSD_all);
SDNN_all  = transpose(SDNN_all);
SDSD_all  = transpose(SDSD_all);
SD1_all   = transpose(SD1_all);
SD2_all   = transpose(SD2_all);
AvHR_all  = transpose(AvHR_all);

h = waitbar(0,'0% copied...');%shows progress of the copying of the data
to the excel sheet

%rMSSD WRITE
xlrange1=['T' num2str(Row)];
xlswrite(file_name,rMSSD_all,sheet,xlrange1); %copies rMSSD data

%SDNN WRITE
xlrange2=['U' num2str(Row)];
waitbar(0.25,h,'25% copied...');
xlswrite(file_name,SDNN_all,sheet,xlrange2); % copies SDNN data

%SDSD WRITE
xlrange3=['V' num2str(Row)];
xlswrite(file_name,SDSD_all,sheet,xlrange3);  % copies SDSD data
```

```
waitbar(0.5,h,'50% copied...');

%SD1 WRITE
xlrange4=['W' num2str(Row)];
xlswrite(file_name,SD1_all,sheet,xlrange4);% copies SD1 data

%SD2 WRITE
xlrange5=['X' num2str(Row)];
xlswrite(file_name,SD2_all,sheet,xlrange5); % copies SD2 data

waitbar(0.75,h,'75% copied...');

%AvHR WRITE
xlrange6=['Y' num2str(Row)];
xlswrite(file_name,AvHR_all,sheet,xlrange6); % copies AVHR data

waitbar(1,h,'100% copied...');
close (h)


%=========================================================================
=%
%                                   FIN
%=========================================================================
=%
```

APPENDIX D

PHYSIOLOGY 2014 ABSTRACT

Cardiac effects of brief seizures in a chronic model of temporal lobe epilepsy

A. Ashby-Lumsden, W. Chang, T. Lovick, J. Jefferys

Sudden unexplained death in epilepsy (SUDEP), where the death of a patient cannot be attributed to any other cause, is a relatively poorly understood phenomenon. Sudden death is over 20 times more prevalent in people with epilepsy than in the general population and is of considerable concern to those at risk and their families. The mechanism of SUDEP is unknown, but ictal respiratory depression, autonomic dysfunction and fatal arrhythmia are all hypothesised to have a role. Using the Tetanus Neuro-Toxin (TeNT) model of temporal lobe epilepsy, we examined the affect of chronic epileptic seizures on the electrocardiogram (ECG) of freely moving rats. Adult male Wistar rats were injected with 2.5ng TeNT in 1µl phosphate buffered saline with bovine serum albumin at 200nl.min-1 (toxin omitted in controls) into the ventral hippocampus. Electrocorticogram and ECG were continuously recorded via dual-biopotential Telemetry Research radiotelemeters (Millar Instruments, US) implanted ~2 weeks before injection. Both surgeries were performed under isoflurane anaesthesia (5% induction, 2-3% maintenance). Animals were housed with naïve companion rats and video-recorded for seizure classification. Seizure-related changes in heart rate and the incidence of arrhythmias were analysed. Data are given as mean ± SEM. Seizures lasted 75.3±2.9 s. They induced dramatic changes in heart rate: ictal bradycardia occurred in 89% of seizures with the heart rate as low as 70 bpm, along with ictal tachycardia (447.5±4.7 bpm) that persisted 863.5±86.7s post-ictally. Seizure-induced arrhythmias occurred in 71% of seizures, with missed beats (59%), ventricular premature depolarisations (22%) and ventricular fibrillation (17%) seen both in isolation and in concert. The ECG waveform also changed, with the P-wave absent for many heartbeats in the majority of seizures. Our results demonstrate that repeated brief epileptic seizures have substantial effects on heart rate, with arrhythmias present during the majority of seizures. Similar cardiac consequences of seizures have been seen in human patients. We conclude that the TeNT model provides a valuable tool to investigate autonomic mechanisms implicated in SUDEP.

APPENDIX E

BNA FESTIVAL OF NEUROSCIENCE 2015

Autonomic consequences of spontaneous temporal lobe epileptic seizures

Alex Ashby-Lumsden, Thelma Lovick and John Jefferys

Sudden unexpected death in epilepsy (SUDEP) is a constant threat to people with epilepsy; the overall risk of dying unexpectedly is >20% higher than the general population and for people with chronic refractory epilepsy SUDEP has been reported to account for up to 50% of deaths (2). Epileptic seizures are accompanied by autonomic disturbances, including cardio-respiratory abnormalities (1). Little is known about the long-term effects of repeated episodes of autonomic dysfunction but it is possible that repeated seizure activity predisposes to the development of a fatal seizure-induced autonomic event.

In the present study, we carried out long term monitoring of the cardiac activity in a rat model of temporal lobe epilepsy (3) to investigate whether seizure-related cardiac changes were affected by seizure history. Focal microinjections of tetanus neurotoxin (TeNT) were made into the ventral hippocampus in male Wistar rats, instrumented to record cortical EEG and ECG (lead II) by radiotelemetry. TeNT induced repeated spontaneous brief (20-140 s) seizures, often in clusters, and recurring over weeks.

>95% of seizures were associated with prolonged tachycardia, lasting <53 min, long after each seizure had ended. Dysrhythmias and bradycardias occurred during ~90% of seizures: a minority had sinus bradycardia alone, while in most cases bradycardia included episodes of asystole, premature ventricular depolarisations and fibrillation. Episodes of disrupted heart activity could last 10-20 s. The incidence, intensity and duration of these seizure-related changes in cardiac activity varied considerably over the course of each rat's epileptic syndrome. Secondarily generalized seizures (4-5 on the "Racine Scale") and seizure clusters both were associated with increases in tachycardia and with more prominent dysrhythmias.

Understanding the cardiac and respiratory consequences of repeated epileptic seizures will provide rational approaches to predicting and reducing the risk of SUDEP.

APPENDIX F

AES 2014 ABSTRACT

Cardiac consequences of repeated brief seizures in chronic experimental temporal lobe epilepsy

John Jefferys, Alexander Ashby-Lumsden, Thelma Lovick, Kurt Qing, Steven Lee and Pedro Irazoqui

Rationale: Sudden unexplained death in epilepsy (SUDEP) accounts for ~15% of deaths of people with epilepsy. Sudden death is >20x more common than in the general population. By definition causes are not clear, but both cardiac and respiratory malfunctions have been implicated. We used the intrahippocampal Tetanus Neuro-Toxin (TeNT) chronic model of temporal lobe epilepsy to investigate the effects of repeated brief epileptic seizures on the electrocardiogram (ECG) of freely moving rats. Methods: We recorded ECoG and ECG using electrodes and Telemetry Research devices implanted under isofluorane general anaesthesia in 8 adult male Wistar rats. Two weeks later we performed intrahippocampal injection of 2.5ng tetanus neurotoxin (TeNT) in 1 µl PBS (toxin omitted in controls). Animals were housed with naïve companion rats and video-recorded for seizure classification. Results: Electrographic seizures (lasting 30-133s) developed after ~4 days with an average number per animal in the range of 7-18 per day. Every epileptic rat experienced dramatic changes in heart activity associated with seizures. In 76 analysed seizures an initial transient ictal bradycardia (lasting 38 ± 2s) occurred in 89% (lasting 38 ± 2s with heart rate falling to as low as 70 beats per minute). This was followed by late-ictal or postictal tachycardia in 93% of seizures, reaching 448±4 bpm, which persisted for 864±87s postictally. Arrhythmias occurred in 71% of seizures, with: missed beats (59%), ventricular premature depolarisations (22%) and ventricular fibrillation (17%) seen both in isolation and in concert. Typically, the P-wave transiently disappeared during seizures to be replaced with signs of atrial fibrillation. Conclusions: These preliminary data indicate that repeated brief epileptic seizures result in several cardiac pathophysiologies. Most seizures were associated with arrhythmias and with postictal tachycardia. More capable devices able to monitor a greater number of critical cardio-respiratory, cerebral and vagal and other autonomic variables are necessary to understand the underlying mechanisms and to develop potential therapies. Such devices are under joint development and evaluation with the Purdue team and will be presented.

APPENDIX G

AES 2015 ABSTRACT

Interictal and ictal ECG changes in a chronic experimental model of temporal lobe epilepsy

Alexander Ashby-Lumsden, Thelma Lovick, John Jefferys

Rationale: The risk of sudden unexpected death is a significant burden for people with epilepsy, particularly those who experience drug-resistant tonic clonic seizures. There is a pressing need to model the condition in animals in order to understand the mechanism that underlies the fatal episode, the predisposing factors and potential triggers. The tetanus neurotoxin (TeNT) model of epilepsy in rats develops clusters of randomly occurring seizures over periods of several weeks, without causing status epilepticus at any stage. Using this model we reported last year that seizures were associated with arrhythmias and long lasting postictal tachycardia. Here we present a more detailed analysis of the ECG.Methods: Rats were implanted under isoflurane anaesthesia with Telemetry Research dual biopotential radiotelemeters to record ECG and ECoG (Millar Inc, TX). 2-3 weeks after initial surgery TeNT (2.5 ng in 1 µl) was injected into right ventral hippocampus through a guide cannula. Controls received vehicle solution only. Continuous recordings were made for up to 6 weeks from rats co-housed with non-epileptic buddies. Data were recorded and analyzed using Spike2 software and a Power 1401 signal acquisition system (Cambridge Electronic Design, UK); some analyses also used Matlab routines. Results: Seizures started after 2-7 days, typically lasted 0.5-3.0 minutes and recurred at <15 per day (average incidence ranges from 1 to 11 per day in different rats). Seizures were characterized by periods of cardiac arrhythmia, which sometimes recurred during the postictal period, and also prolonged postictal tachycardias lasting up to 1 hour (typically 8-10 min). Ictal arrhythmias were more prevalent during secondarily generalized Racine 4 and 5 seizures. Ictal sinus bradycardias were more prevalent during non-convulsive seizures. Over the course of the seizure syndrome interictal QT interval increased to 78.5 ± 1.5 ms from 69.8 ± 1.1 ms measured in the same rats before induction of epilepsy. The increase often was associated with changes in the shape of the T component of the ECG waveform (e.g. increased amplitude, inversion and/or duration). During each seizure QT increased further, when the heart was in sinus rhythm between periods of arrhythmia, and this increase could persist for several minutes into the postictal period. Conclusions: The data suggest that the TeNT model undergoes progressive development of neurally-induced pathophysiological changes in the heart. The ictal and postictal increased QT and arrhythmias are consistent with previous reports of centrally-evoked sympathetically-mediated changes long recognized in the physiological literature. Cardiac repolarization dysfunction during progression of epilepsy may predispose to development of fatal arrhythmias.

APPENDIX H

SOCIETY FOR NEUROSCIENCE 2016 ABSTRACT

Cardiac and respiratory consequences of repeated epileptic seizures in rat

D. Pederson, A. Ashby-Lumsden, P. P. Irazoqui, J. G. Jefferys

Sudden death in epilepsy (SUDEP) is a significant and devastating risk in some kinds of epilepsy. The most likely explanations are respiratory or cardiac failure during or following a seizure. To determine the impact of recurrent seizures on cardiac and respiratory function we induced temporal lobe epileptic foci by injecting tetanus toxin (5-10 ng in 400 -1000 nl) into rat hippocampus. Spontaneous seizures started a few days later, each lasting <2 min. Status epilepticus did not occur at any stage. We implanted wireless telemetry devices (either a subcutaneous Bionode developed and manufactured at Purdue, or an intra-abdominal Millar TR50BB). Leads were tunnelled subcutaneously to ECG and ECoG electrodes and, in the case of the Bionode, to a thermocouple implanted in the nasal passage. Telemetry and video recordings were made for <6 weeks after injection, and in some cases for 1-2 weeks before injection. Heart rate increased during nearly all seizures and remained high for minutes to tens of minutes afterwards. This postictal tachycardia could occur when the rat was completely inactive and was exacerbated by postictal physical activity. Arrhythmias were common during secondarily generalised seizures and included missed beats, asystoles, premature ventricular depolarizations, torsades and fibrillation. Progressive changes occurred over the duration of the epileptic syndrome. Interictal QT interval, measured for 5-s epochs where heart rate was 350 per min, progressively lengthened from a baseline of ~60 ms, by ~15 ms after >50 seizures. Prolonged QT most likely reflects changes in cardiac ion channels and may increase the risk of arrhythmia. Respiration was affected by epileptiform activity, including interruptions of respiratory rhythm after ECoG spikes and hyperventilation >120 per min during postictal immobility. These seizure-related cardiac and respiratory dysfunctions should be considered as potential risk factors for SUDEP.